(2)

ESL-TR-89-55

LABORATORY INVESTIGATIONS OF CASCADE CROSSFLOW PACKED TOWERS FOR AIR STRIPPING OF VOLATILE ORGANICS FROM GROUNDWATER

D. P. HARRISON, K. T. VALSARAJ, L. J. THIBODEAUX

HAZARDOUS WASTE RESEARCH CENTER
DEPARTMENT OF CHEMICAL ENGINEERING
LOUISIANA STATE UNIVERSITY, 3418 CEBA
BATON ROUGE LA 70803

DECEMBER 1990

FINAL REPORT

APRIL 1986 - AUGUST 1989

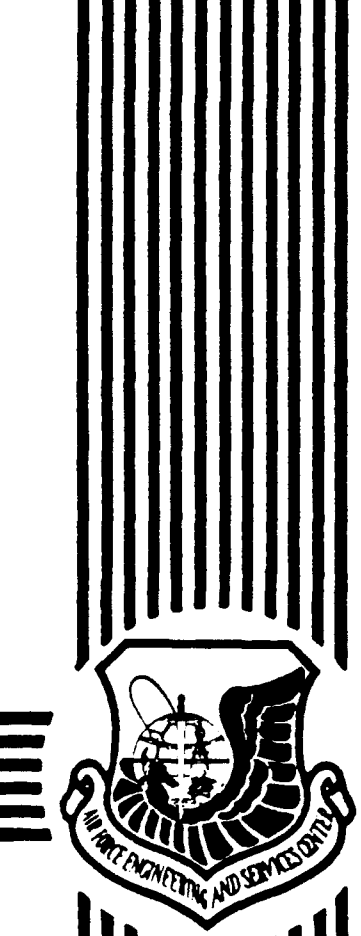

AIR FORCE ENGINEERING & SERVICES CENTER
ENGINEERING & SERVICES LABORATORY
TYNDALL AIR FORCE BASE, FLORIDA 32403

NOTICE

PLEASE DO NOT REQUEST COPIES OF THIS REPORT FROM HQ AFESC/RD (ENGINEERING AND SERVICES LABORATORY). ADDITIONAL COPIES MAY BE PURCHASED FROM:

NATIONAL TECHNICAL INFORMATION SERVICE
5285 PORT ROYAL ROAD
SPRINGFIELD, VIRGINIA 22161

FEDERAL GOVERNMENT AGENCIES AND THEIR CONTRACTORS REGISTERED WITH DEFENSE TECHNICAL INFORMATION CENTER SHOULD DIRECT REQUESTS FOR COPIES OF THIS REPORT TO:

DEFENSE TECHNICAL INFORMATION CENTER
CAMERON STATION
ALEXANDRIA, VIRGINIA 22314

REPORT DOCUMENTATION PAGE

Form Approved
OMB No 0704-0188

1a. REPORT SECURITY CLASSIFICATION Unclassified	1b RESTRICTIVE MARKINGS
2a. SECURITY CLASSIFICATION AUTHORITY N/A	3. DISTRIBUTION/AVAILABILITY OF REPORT Approved for Public Release Distribution Unlimited
2b. DECLASSIFICATION/DOWNGRADING SCHEDULE N/A	
4. PERFORMING ORGANIZATION REPORT NUMBER(S)	5 MONITORING ORGANIZATION REPORT NUMBER(S) ESL-TR-89-55
6a. NAME OF PERFORMING ORGANIZATION Hazardous Waste Res. Center & Dept. of Chemical Eng., LSU 6b OFFICE SYMBOL (If applicable)	7a. NAME OF MONITORING ORGANIZATION Air Force Engineering and Services Center
6c. ADDRESS (City, State, and ZIP Code) Louisiana State University, 3418 CEBA Baton Rouge, LA 70803	7b. ADDRESS (City, State, and ZIP Code) HQ AFESC/RDVW Tyndall AFB, FL 32403
8a. NAME OF FUNDING/SPONSORING ORGANIZATION HQ AFESC 8b OFFICE SYMBOL (If applicable) RDV	9 PROCUREMENT INSTRUMENT IDENTIFICATION NUMBER F-8635-86-C-0159
8c. ADDRESS (City, State, and ZIP Code) HQ AFESC/RDVW Tyndall AFB, FL 32403-6001	10 SOURCE OF FUNDING NUMBERS PROGRAM ELEMENT NO: 62206F; PROJECT NO: 1900; TASK NO: 70; WORK UNIT ACCESSION NO: 48

11. TITLE (Include Security Classification)
(U) Laboratory Investigations of Cascade Crossflow Packed Towers for Air Stripping of Volatile Organics from Groundwater

12 PERSONAL AUTHOR(S)
Harrison, Douglas P.; Valsaraj, Kalliat T.; Thibodeaux, Louis J.

13a. TYPE OF REPORT	13b TIME COVERED	14 DATE OF REPORT (Year, Month, Day)	15 PAGE COUNT
Final	FROM 4/21/86 TO 8/24/89	December 1990	

16. SUPPLEMENTARY NOTATION
Availability of this report is specified on the reverse of the front cover.

17. COSATI CODES			18 SUBJECT TERMS (Continue on reverse if necessary and identify by block number)
FIELD	GROUP	SUB-GROUP	Air Force, Contamination, Countercurrent, Groundwater, Pollution, Water, Crossflow, Treatment, Air Stripping

19 ABSTRACT (Continue on reverse if necessary and identify by block number)

This report evaluates the effectiveness of a cascade crossflow air stripper for the removal of Volatile Organic Compounds (VOCs) from simulated groundwater. Experimental tests were conducted on four VOCs - methylene chloride, chloroform, 1,2-dichloroethane and carbon tetrachloride - on both a 6-inch internal diameter laboratory scale column and a 12-inch internal diameter pilot-scale column. The additional variable, α, which is the ratio of gas to liquid flow areas was investigated. Experimental data on stripping efficiencies were used to obtain mass transfer coefficients in crossflow operation. These mass transfer coefficients were compared with literature correlations obtained for conventional countercurrent operation, but modified appropriately for crossflow. For liquid phase controlled chemicals, the modified Onda's correlation satisfactorily predicted the crossflow mass transfer coefficient. Additionally α had no significant effect on

(continued on reverse side)

20 DISTRIBUTION/AVAILABILITY OF ABSTRACT ☒ UNCLASSIFIED/UNLIMITED ☐ SAME AS RPT ☐ DTIC USERS	21 ABSTRACT SECURITY CLASSIFICATION Unclassified
22a NAME OF RESPONSIBLE INDIVIDUAL Capt. Ed Marchand	22b TELEPHONE (Include Area Code) (904) 283-2942 22c OFFICE SYMBOL RDVW

19. Abstract (continued)

efficiency and mass tranfer coefficients for liquid phase controlled chemicals. The 6-inch crossflow column was also converted into a 6-inch countercurrent column and experiments were conducted at identical conditions to obtain a direct comparison between the two modes of operation. The results showed that the efficiencies and mass transfer coefficients for liquid phase controlled chemicals were practically identical on the lab-scale columns. Extensive pressure drop data on both crossflow and countercurrent columns revealed that crossflow columns showed dramatic reductions in gas phase pressure drop. The crossflow columns were stable under conditions where conventional countercurrent columns would be inoperable. A preliminary economic comparison of both crossflow and countercurrent flow stripping is also reported.

EXECUTIVE SUMMARY

Laboratory Investigations of Crossflow Packed Towers for Air Stripping of Volatile Organics from Groundwater.

OBJECTIVE: The objective of this project was to investigate the effectiveness of cascade crossflow operation in packed towers for the removal of volatile organic compounds from groundwater.

BACKGROUND: Air stripping is one of several economic alternatives for the decontamination of groundwater contaminated with volatile organic compounds (VOCs). The traditional operation of packed air-stripping towers is in the "countercurrent" mode where the air is forced upward through the packing and liquid flows down by gravity. High pressure drops and low liquid and gas throughputs limit the applicability of this mode of operation. The present study seeks to avoid these limitations by conducting the same operation in a "crossflow cascade" mode. This involved changes in the internals of the tower to disconnect the air and liquid flow paths so that the two fluids flow perpendicular to each other inside the packing. This mode of operation results in reduced pressure drop and a greater range of stable operation without any serious loss in mass transfer efficiency.

SCOPE: This project was conducted in two phases. Phase I involved the design, construction, and testing of a 6-inch internal diameter crossflow device for the removal of four VOCs. Phase II involved (1) the direct comparison of crossflow and countercurrent results on a laboratory scale, (2) the design, construction and operation of a 12-inch pilot scale crossflow device and (3) an economic and cost comparison of typical countercurrent flow and crossflow devices.

METHODOLOGY AND TEST DESCRIPTION: A semibatch operation was used in all the experiments. Simulated groundwater was prepared by dissolving appropriate amount of VOCs in tap water. Gas and liquid flow rates were adjusted to required values and the VOC concentrations in the reservoir and the effluent were obtained as functions of time. Gas chromatography was used to analyze the samples. The stripping efficiency (E) was obtained from the exit and inlet concentrations. The stripping efficiency was then used to obtain the experimental mass transfer coefficients. Experiments were conducted at various liquid and gas flow rates and various values of α, the new variable in crossflow α is the ratio of gas to liquid flow areas in crossflow.

The experiments were done on 6-inch inside diameter, 8-foot tall crossflow column, 6-inch i.d., 8-foot tall countercurrent column and a 12-inch i.d., 11-foot tall crossflow column. Liquid flow rates were measured using rotometers and gas flow rates were obtained from pressure drops across standard orifice plates. Pressure drop per unit height of packing in both crossflow and countercurrent columns were obtained using pressure taps near the top and bottom of the packing which were connected to a manometer.

Experimental mass transfer coefficients were compared with predicted values using four different mass transfer correlations modified from those for conventional countercurrent operations.

Conceptual design calculations for both countercurrent and crossflow modes of operation were performed to estimate process equipment specifications required for 99 percent removal of three contaminants of varying volatility at two flow rates. Comparative economic studies were then made to determine the conditions under which crossflow stripping would exhibit favorable economics.

RESULTS: The stripping efficiencies and mass transfer coefficients for liquid phase controlled chemicals in crossflow operation were similar to those in countercurrent operation at equivalent liquid loading rates. However, pressure drops in crossflow operation were as much as an order of magnitude smaller than in countercurrent flow. The permissable ranges of gas and liquid flow rates were also larger in crossflow with several experiments conducted under conditions that would result in flooding in countercurrent columns.

The evaluation of mass transfer correlations showed that the frequently cited Onda correlation for liquid phase controlled chemicals could be easily modified for crossflow operation and that it predicted experimental values satisfactorily within ±30 percent.

Higher capital costs associated with the more complex column internals required for crossflow operation tend to be offset by reduced operating costs associated with the lower gas-phase pressure drop. For compounds with relatively high Henry's constants such as trichloroethylene (TCE), high stripping efficiency can be achieved at relatively low gas rates. In such cases, the increased capital costs appear to be more important than the reduced operating costs, and traditional countercurrent stripping should be less costly. However, for compounds with low Henry's constants where high gas rates are required for high efficiency stripping, operating costs are relatively more important and crossflow stripping shows a potential for significant cost savings. The attractiveness of crossflow stripping also increases as the scale (liquid treatment rate) of the process increases, since operating costs are directly proportional to treatment rate while capital costs show a less than proportional dependence.

CONCLUSIONS: Laboratory-scale crossflow cascade systems are efficient mass transfer devices and can be used to strip VOCs from groundwater with efficiencies similar to those of countercurrent flow devices. However the crossflow systems have the added advantages of very low pressure drop and greater range of stable operation. Mass transfer correlations obtained from conventional countercurrent operation can be modified to predict crossflow mass transfer coefficients as well.

The low pressure drop associated with crossflow operation becomes more important as the required volume of air increases. Hence, the potential economic attractiveness of crossflow relative to countercurrent flow increases as the Henry's constant of the contaminating organic decreases. This factor may make air-stripping applicable to

compounds which previously have been thought to be strippable only using steam.

RECOMMENDATIONS:

Cascade crossflow air stripping is an attractive alternative to conventional countercurrent air stripping from the point of view of reduced pressure drop and greater range of stable operating conditions. The efficiency of crossflow air stripping for the removal of compounds of moderate volatility, i.e., those with Henry's constants less than 0.06 (1,2-dichloroethane, the least volatile in the present study), should be investigated since the advantages of reduced pressure drop and stable operation at high air loading should be of greater economic significance in these cases. It is also recommended that studies be undertaken to elucidate the effect of total packed cross-sectional area in crossflow.

(The reverse of this page is blank)

PREFACE

This report was prepared by the Hazardous Waste Research Center of Louisiana State University, Baton Rouge, Louisiana 70803, under contract number FO8635-86-C-0159, for the Air Force Engineering and Services Center, Engineering and Services Laboratory (HQ AFESC/RDVW), Tyndall Air Force Base, Florida 32403-6001. The project officers were Captains Michael G. Elliot and Edward G. Marchand.

This report describes laboratory tests of an innovative air stripping technique for removal of volatile organic compounds from groundwater. This technique, referred to as crossflow air stripping, involves changing the internals of a conventional countercurrent packed air stripping tower. These changes result in dramatic reductions in operating pressure drop and increases in gas loading rates without a significatn reduction in the strippng efficency. The report describes laboratory tests on 6- and 12-inch crossflow towers and, for comparison purposes, a 6-inch countercurrent tower. The tests were performed between 21 Apr 1986 and 24 Aug 1989. Mention of trademarks and trade names of material and equipment does not constitute endorsement or recommendation for use by the Air Force, nor can the report be used for advertising the product.

The report has been reviewed by the Public Affairs Office (PA) and is relasable to the National Technical Information Service (NTIS). At NTIS, it will be avaliable to the general public, including foreign nationals.

The technical report has been reviewed and approved for publication.

Edward G. Marchand

EDWARD G. MARCHAND, Captain, USAF
Project Officer

MICHAEL L. SHELLEY, Major, USAF
Chief, Environics Division

Robert G. LaPoe

ROBERT G. LaPOE, Major, USAF
Chief, Restoration R&D

FRANK P. GALLAGHER III, Colonel, USAF
Director, Engineering and
Services Laboratory

(The reverse of this page is blank)

TABLE OF CONTENTS

TABLE OF CONTENTS (Continued)

LIST OF FIGURES

LIST OF FIGURES (Continued)

LIST OF FIGURES (Continued)

LIST OF FIGURES (Continued)

LIST OF FIGURES (Continued)

LIST OF TABLES

SECTION I

INTRODUCTION

A. OBJECTIVE

Contamination of groundwater and soil with hazardous and toxic organic pollutants has been identified at numerous Air Force bases. Most of these contaminants are organic solvents, fuel components and/or degreasers which were inadvertently released to the soil. Remedial actions to prevent or reduce these contamination problems are being considered. Most available technologies are unable to remove the contaminants in a efficient and cost-effective manner. Hence the Air Force has been looking into a variety of innovative techniques that are capable of achieving the above tasks.

B. BACKGROUND

Of the presently available technologies for groundwater remediation, the two most promising are packed tower air stripping and granular activated carbon adsorption. Several investigators (References 1-3) have shown that air stripping is more economical for a long-term remediation process. Air stripping is traditionally conducted in a "countercurrent" mode with the liquid flowing down through the packing by gravity and gas being forced upward. However it suffers from a major disadvantage - "flooding" - the point where the gas cannot be forced upward through the packing and mass transfer ceases. Our research study seeks to avoid this constraint by adopting a "crisscross flow" mode of operation. This involves changes in the internals of conventional packed towers that have the potential of achieving dramatic reduction in operating pressure drop and increases in liquid and gas loading rates without significant reduction in the stripping efficiency. The key factor of this innovation is the disconnection of the areas through which air and water move within the packing. In the case of a crossflow cascade, baffles placed at strategic locations cause the air to crisscross the liquid several times at approximately 90° before exiting. Figure 1 shows a comparison of a conventional countercurrent column and a crisscross flow column.

The potential advantages of this mode of operation are (1) very low operating pressure drop in the gas phase and (2) stable operation at very high gas to liquid ratios (G/L). These advantages are possible because the gas flow area is disconnected from the liquid flow area. The low operating pressure drop may result in lower operating cost for crossflow, as compared to countercurrent flow. Operating cost is directly proportional to the energy delivered to the air in overcoming the pressure drop for flow through the packing. High G/L ratios are necessary to remove many components having moderate Henry's law constants. The crisscross flow mode will allow G/L ratios that would amount to inoperable (flooding) conditions in conventional countercurrent operation. In addition the crossflow operation has the potential of a greater range of turn-down ratio (i.e., range of stable operation, both high and low flows). The advantage is that a single unit design has a range of operating conditions and general versatility

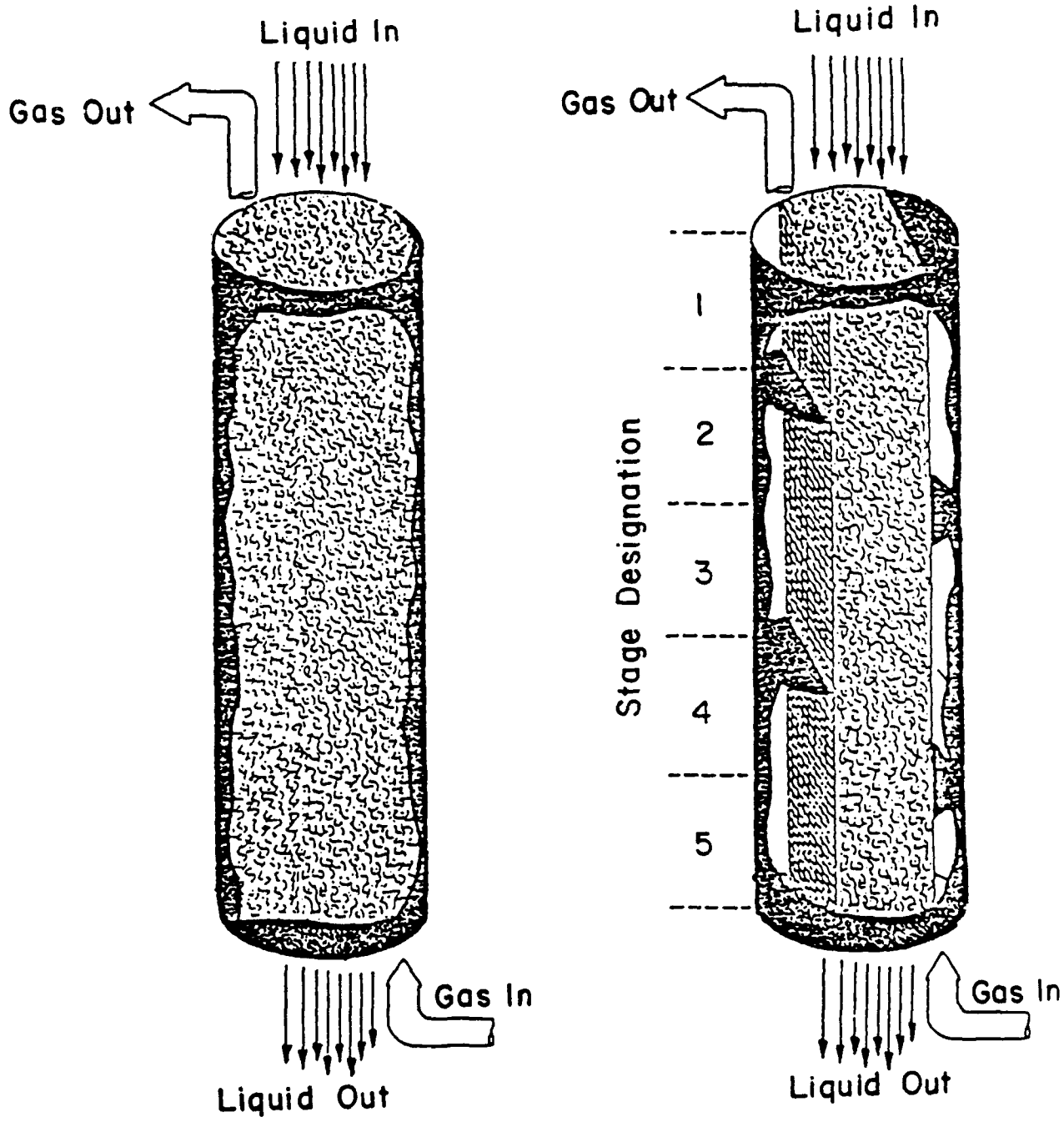

Figure 1. Schematic Diagram of Countercurrent and Cascade Crossflow Contacting Devices.

that makes it suitable for organics with both high and medium Henry's constants.

C. SCOPE

The work described in this report pertains to the use of this innovative mass-transfer device for air stripping volatile organic compounds (VOCs) from water, both on a laboratory scale 6-inch internal diameter unit and a larger pilot scale 12-inch internal diameter unit. An economic comparison of a crossflow unit with that of a conventional countercurrent device is also presented.

SECTION II

LITERATURE REVIEW OF CROSSFLOW MASS TRANSFER

The concept of crossflow was first utilized in water cooling towers (Reference 4). These single-cell devices proved to be more economical for certain applications. Some characteristics of crossflow and countercurrent towers are listed in Table 1. Conceptual design procedures for single-cell, general-purpose, crossflow mass transfer devices were presented by Thibodeaux (Reference 5). An example calculation involving the air-stripping of methanol was also presented. Roesler et al., (Reference 6) performed design calculations for stripping ammonia based on the numerical algorithm proposed by Thibodeaux (Reference 5) and predicted ammonia removals of up to 95 percent for a G/L ratio of 4 in a 20-foot tall tower. Another application of single cell crossflow cooling towers was the air-stripping of VOCs from water of a contaminated aquifer (Reference 7). Two crossflow towers were used in series. From an inlet concentration of 6200 µg/ℓ (1,1,1-trichloroethane), the concentration was reduced to 186 µg/ℓ after the first tower and to 10 µg/ℓ after the second tower with an overall removal efficiency of 99.8 percent.

McCarty (Reference 8) performed a detailed technical analysis of a large single-cell crossflow stripping tower for the removal of ammonia from reclaimed wastewater. He used the number of transfer units technique developed by Thibodeaux et al. (Reference 9) to analyze the operation. The overall removal efficiency of ammonia was used to calculate an overall mass transfer coefficient in the tower from which it was possible to calculate the removal efficiencies of other chemicals as a function of G/L ratios and Henry's Constant. Upon completion of the evaluation, McCarty (Reference 8) concluded that:

1. Adequate data were not available to evaluate the removal of compounds other than those with high H values, and so the true potential of crossflow tower was not measured,

2. Natural draft crossflow towers may have a potential of stripping relatively volatile compounds at low energy consumption,

3. Crossflow stripping has good potential for removal of compounds with intermediate water solubility and Henry's constants.

4. To achieve very high G/L ratios, crossflow towers have a decided advantage over countercurrent towers.

5. The most appropriate system for a given situation depends upon economics plus a variety of other considerations with the major trade-off being between construction costs and power costs.

Pittaway and Thibodeaux (Reference 9) studied the stripping of oxygen from supersaturated water using a single-cell crossflow device. The crossflow mass transfer coefficients were slightly less than

TABLE 1: COMPARISON OF CROSSFLOW AND COUNTERCURRENT TOWERS BY DESIGN CONSIDERATIONS (Reference 5)

Design Consideration	Crossflow	Countercurrent
Unit complexity	Complex	Simpler
Gas-liquid ratio	High	Lower
Large potential driving force	Efficient	Efficient
Small potential driving force	Less efficient	Efficient
Gas-phase pressure drop	Small	Large
Gas-phase power requirement	Small	Large
Tower size and area	Small	Smaller
Liquid phase power requirement	Same	Same
Tower fill	Moderate	Small

countercurrent flow but greater than cocurrent flow. The crossflow device was operated at conditions that would flood a normal countercurrent system. Another significant aspect of this work was the introduction of the batch-stripping mode of operation which did not require a steady-state condition to be achieved. This resulted in significant reduction in tankage requirement and a faster experiment turnaround.

Hayashi and Hirai (Reference 10) obtained mass transfer coefficients for packed crossflow devices with carbon dioxide-water and ammonia-water systems. Hayashi and Hirai (Reference 11) also demonstrated that the interphase mass transport concepts would predict the two-dimensional concentration profiles within a single-stage device.

Thibodeaux et al. (Reference 12) showed that more efficient crossflow units can be created by interconnecting single-cell crossflow units to create a cascade. In each stage of this "crisscross flow" device air flows horizontally and the water flows downward. Partial baffles within the air plenum deflect the air flow into the packing. Thibodeaux (Reference 13) reported the fluid dynamic characteristics and gas-liquid patterns in a cascade crisscross flow device. Qualitative observations, over the entire range of G/L ratio, indicated that the phases cross at approximately 90 degrees on each stage. Other important findings were:

1. Pressure drop for 1/2-inch Raschig rings and 5/8-inch pall rings were at least an order of magnitude smaller than for the equivalent countercurrent operation,

2. Stable operating conditions were achieved at conditions that would have flooded the equivalent countercurrent device,

3. Good liquid agitation and distribution was observed in the packing on each stage,

4. Liquid holdup in the crossflow device was slightly larger than in the equivalent countercurrent device, with the baffles being the chief points of increased liquid hold-up,

5. Dry zones were noted opposite the baffles.

Thibodeaux and Moncada (Reference 14) compared the performance of a crossflow cascade and a conventional countercurrent packed tower for air stripping methanol from water. The two towers were of identical exterior dimensions and both were operated in a semi-batch mode. The crossflow tower proved to be the more efficient stripper based on unit volume of packing, unit of pressure drop, and unit of expended work. Hayashi et al. (Reference 15) performed experiments with a cascade crossflow tower for water cooling with air. A degree of cooling equivalent to the countercurrent arrangement was achieved. Velaga et al. (Reference 16) showed that mass transfer coefficient correlations for conventional countercurrent columns can be used with success in predicting mass transfer efficiencies in cascade crossflow towers in the case of both stripping and distillation. Bayan (Reference 17) performed

absorption experiments with a crossflow cascade. Buchelli (Reference 18), Eldridge (Reference 19) and Velaga (Reference 20) performed distillation experiments using a crossflow cascade.

This literature review demonstrates that laboratory crossflow units can be a versatile mass transfer device.

SECTION III

EQUIPMENT DESCRIPTION AND EXPERIMENTAL PROCEDURES

A. 6-INCH COLUMN

1. Overview

Initial experiments were conducted using a 6-inch stripping column designed and constructed at Louisiana State University. The unit operated in a semibatch mode with liquid recycle and once-through air flow, which reduced the quantity of organic contaminant handled and eliminated the continuous discharge of contaminated water during experimental runs.

The equipment consisted of a packed crossflow tower having variable packed height and baffle spacing, a liquid distribution and storage system, an air distribution system, and temperature and flow monitors as shown in Figure 2. Liquid from the reservoir was pumped to the distributor where it flowed downward by gravity through the packing and back into the reservoir. A liquid recycle loop was included in the pumping system to ensure that liquid within the reservoir was thoroughly mixed at all times. Liquid flow rate was monitored by a rotameter and controlled by a hand-operated valve. Air from the variable speed blower entered the system at the bottom of the column, flowed upward through the packing, and exited from the top where it was discharged through the laboratory vent. Air flow was monitored by an orifice meter connected to a U-tube manometer.

The plexiglass packed tower was constructed in five sections to permit operation with varying packed heights. Each section contained internal stainless steel screens to restrict the packing to the center section of the column, and adjustable baffles to direct the air in the desired cascade crossflow pattern.

The stripping capability of the system was determined by simultaneously taking liquid samples from the sample ports located in the liquid reservoir and just below the packing. The concentration of organics in each sample was then determined using gas chromatography. A minimum of three samples from each port taken at nominal 10-minute intervals was used to insure that pseudo steady-state operation was achieved and to determine stripping efficiency. Pressure drop data was obtained using an air-water system (no organics) with column pressure taps located 4.1 meters apart.

2. Detailed Equipment Description

This portion of the report provides specifications of each of the major equipment items.

a. Packed Column Modules

Five column modules were constructed from plexiglass cylinders having 15.24 cm (6-inch) inside diameter and 0.635 cm (1/4-

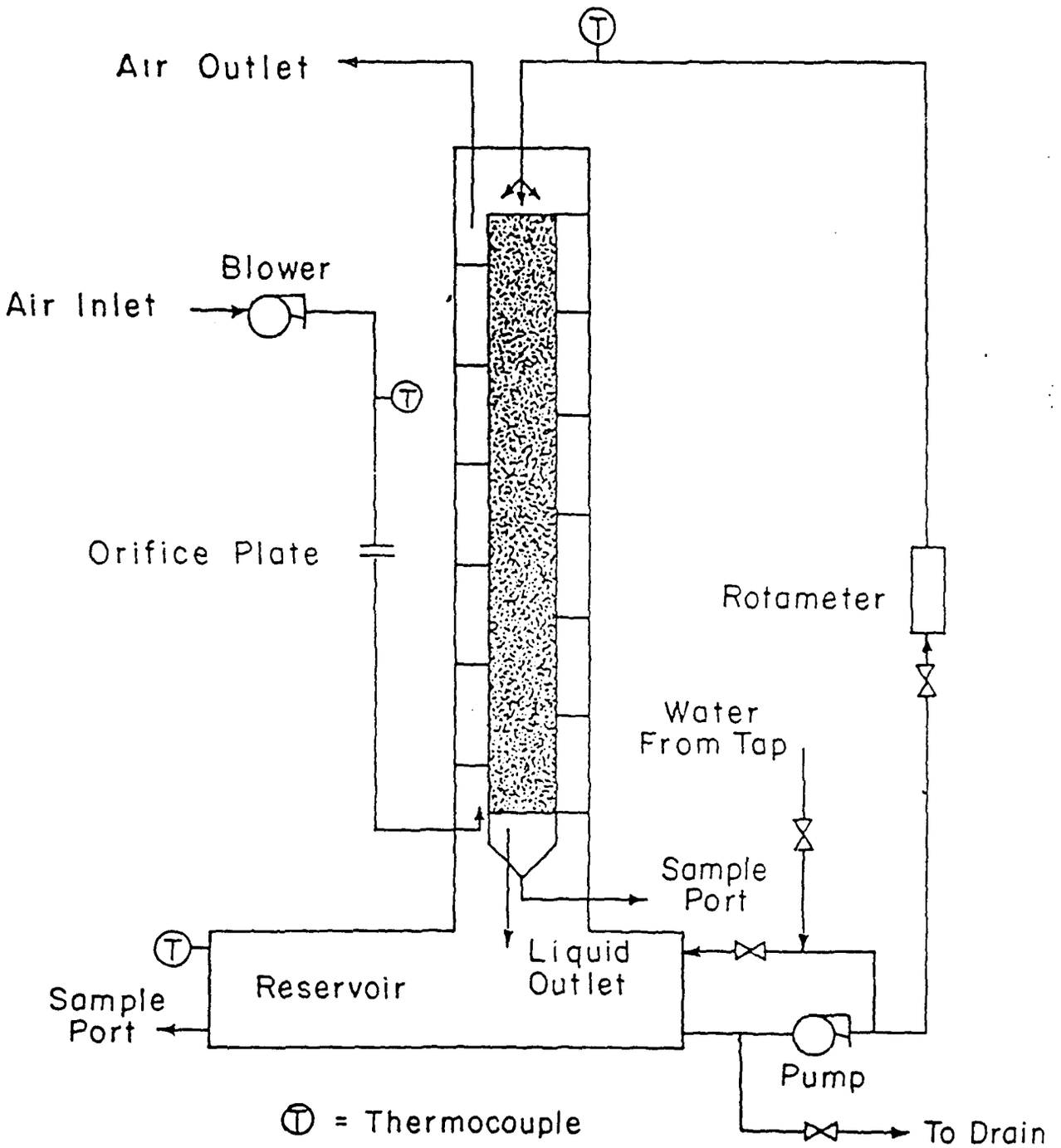

Figure 2. Schematic Diagram of the Semibatch Cascade Crossflow Air Stripper

inch) wall thicknesses. Four of the modules were 1.22 meters (4 feet) high and the fifth was 1.52 meters (5 feet) high. The additional length of the 1.52-meter cylinder housed the liquid distributor, and this module was always used at the top of the column. The modules were connected by bolted flanges thereby permitting operation at packing heights of 1.22, 2.44, 3.66, 4.88 or 6.10 meters (4, 8, 12, 16, or 20 feet).

The removable stainless steel internal structure shown in Figure 3 separated the packing from the open air plenum and supported the adjustable baffles which produced the overall cascade crossflow pattern. Top and bottom stainless steel rings were attached to each end of four 0.635 cm (1/4-inch) stainless steel rods. The bottom ring and two sides of the support were covered with stainless steel welded wire fabric (2x2 mesh per inch with wire diameter 0.063-inch and width of opening 0.437-inch) having a porosity of 82 percent. The wire fabric holds the packing in place and the dimensions of the support result in 65 percent of the column cross-section being packed, leaving 35 percent open for air flow. The overall support structure fits within the plexiglass cylinder by friction.

Baffles were attached to the wire mesh at selected intervals to divert the air and force it to flow across the packing at 90 degrees to the liquid. Each baffle was constructed from two semicircular stainless steel plates bolted together with a piece of butyl rubber between each plate. The rubber insured an air- and water-tight fit against the plexiglass column. The baffles were placed on alternating sides of the stainless steel mesh as shown in Figure 3, and the vertical position of the baffles could be adjusted to provide for variable gas flow area.

Polypropylene pall rings having a nominal diameter of 5/8 inch were used as packing. The packing was dumped into the column module and wetted to facilitate settling. A tamping rod was used to increase the packing density.

b. Liquid Distributor

The liquid was distributed over the packing using a distributor constructed of lexan® in the form of a rectangular box having dimensions of 13 cm x 8.2 cm x 9.5 cm (5 1/8 inches x 3 1/4 inches x 3 3/4 inches). Forty-five holes having diameters of 0.3175 cm (1/8-inch) were drilled through the bottom of the box to provide uniform liquid distribution. V-shaped weirs were cut along the tops of the four sides of the distributor to provide for possible overflow at high liquid rates. The distributor was suspended approximately 1 cm (3/8-inch) above the top of the packing.

c. Liquid Sampler

A specially designed sampler was placed at the bottom of the column to collect a liquid sample as it exited the packing. The funnel-shaped sampler was equipped with a trap door which could be manipulated by the operator from outside the column. Normally the trap door was open, permitting the liquid to flow freely from the packing

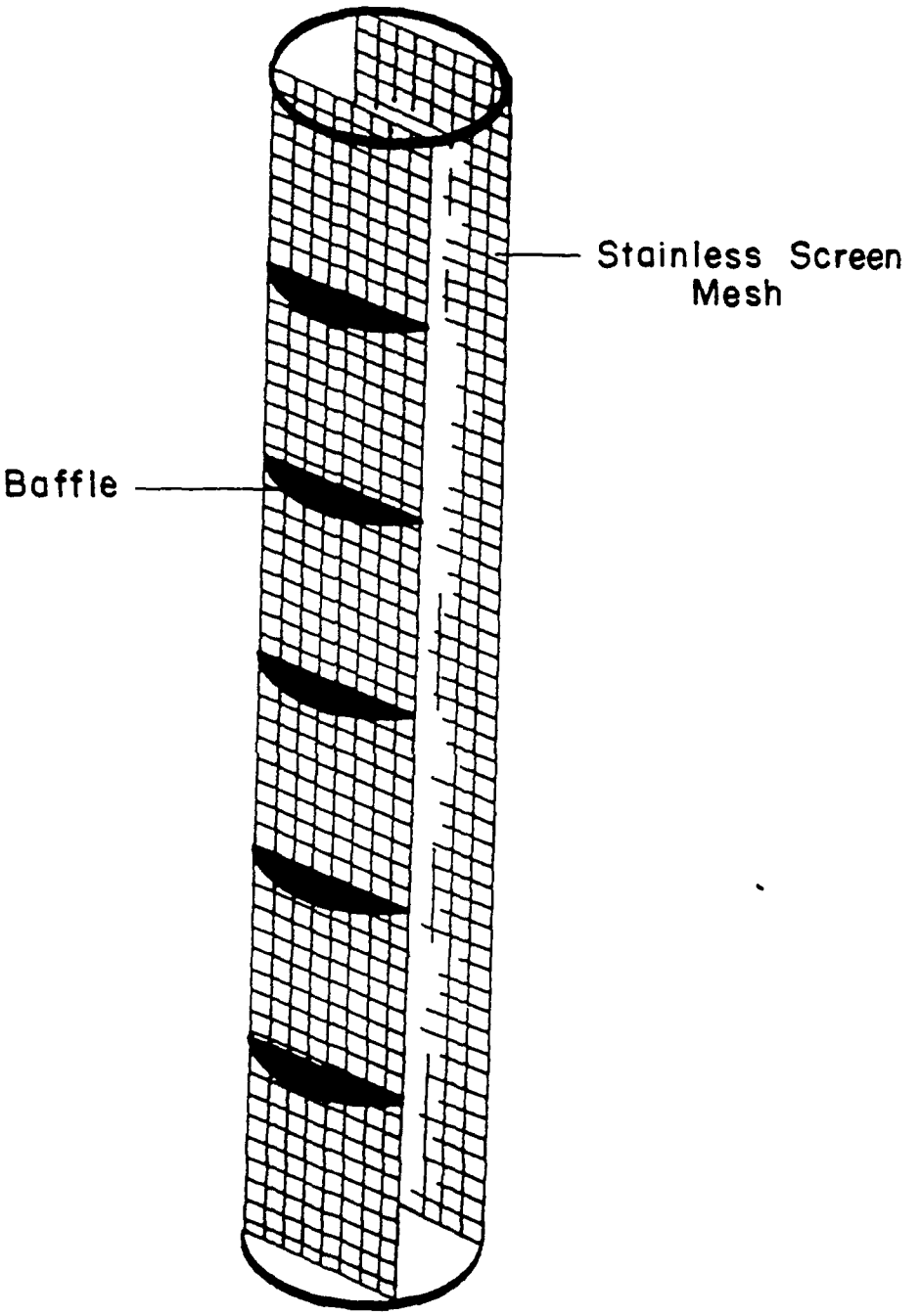

Figure 3. Schematic of Internals for Crossflow Column.

back into the reservoir. When a sample was desired, the trap door was closed and liquid flowed through a sample tube past a sample port equipped with a septum, from which samples were collected using a hypodermic syringe. After the sample was acquired the trap door was opened and water flowed directly back into the reservoir.

Additional sampling ports were installed at various positions in the liquid reservoir. In initial studies, samples were taken simultaneously from a number of positions to determine if the liquid in the reservoir was well mixed. In normal operation, samples were taken simultaneously from a position in the liquid reservoir and from the liquid sampler at the bottom of the column. Following chemical analysis of these samples, the overall stripping efficiency can be directly calculated. The equations for the calculation of the stripping efficiency are described in Section IV.

d. Liquid Reservoir

The stripping column sits atop a 395-liter (14-ft^3) aluminum tank which serves as the liquid reservoir. Liquid is pumped directly from the reservoir to the liquid distributor at the top of the column where it flows vertically downward through the packed column by gravity back into the reservoir. Sampling ports were placed around the perimeter of the tank and a sight glass was installed to monitor liquid depth. Numerous sampling ports through the tank walls were provided for water addition, drainage, solution recirculation and to provide access for cleaning.

e. Liquid Pump

A 0.75-hp centrifugal pump having a maximum capacity of 1.89 L/s at 1700 N/m^2 (30 gpm at 55 feet of water) delivers liquid to the distributor. The pump operates at full capacity at all times with all liquid in excess of the desired column feed recycled to the liquid reservoir to promote mixing.

Two rotameters connected in parallel are used to measure liquid feed to the column. The larger rotameter (Omega Model 710-b) which has an operating range of 0.06 to 0.64 L/s (1 to 10 gpm) was used in most tests. The smaller rotameter (Omega Model 1502-2) with a range of 0.01 to 0.07 L/s (0.1 to 1.1 gpm) was used only for tests requiring very low liquid feed rates. Liquid flow is controlled with a 3.8 cm (1.5-inch) gate valve at the rotameter inlet

f. Air Blower

A 1.5-hp Powerbloc blower (model E120751) with a Westinghouse Accutrol variable speed controller delivers air to the column. The blower has a maximum capacity of 22.7 m^3/min (800 ft^3/min). Air flow is measured using an orifice with flange taps connected to a U-tube manometer filled with n-hexane (specific gravity = 0.659).

g. Thermocouples

Temperature is monitored using three Maverick type T stainless steel thermocouples connected to a Eurotherm Model 840 digital indicator. Thermocouples are located in the liquid reservoir, at the liquid inlet to the column, and at the blower outlet.

3. Design Changes

Two significant design changes were made in our experimental tower. In our initial design, air was fed directly into the liquid reservoir so that it was in contact with the liquid before entering the packing. Significant mass transfer was found to occur within the reservoir so that the air entering the packing was not free of organics. To alleviate this problem the inlet air line was rerouted so that air was fed directly into the column at the bottom of the packing, thereby eliminating mass transfer within the reservoir which occurred with the original design. Also, the original design only permitted liquid sampling from the liquid reservoir. In principle, the stripping efficiency at a given set of operating conditions can be calculated by material balance if the concentration within the tank is known as a function of time; however, this method of analyzing performance lacked the necessary precision and provided no means of checking the material balance closure. As a result, a liquid sampler at the bottom of the column was installed to permit simultaneous sampling of the liquid entering and leaving the packed section.

4. Operating Procedure

The liquid reservoir was originally charged to about two-thirds capacity with water spiked with the volatile organic compounds of interest. Saturated aqueous solutions prepared previously were diluted with tap water to obtain nominal concentrations of 100 to 400 mg/L of organic. An exact initial concentration was not required; only relative concentrations were needed for the mass transfer analysis.

The solution was mixed for 30 to 60 minutes by pumping through the reservoir recycle loop to ensure uniform concentration. Liquid flow was then directed through the appropriate rotameter and into the column. Once liquid circulation was established, the blower was started and both air and liquid flow rates were adjusted to desired conditions.

The first set of liquid samples was collected approximately 10 minutes later and a minimum of three sets of samples were taken at nominal 10-minute intervals for each run. The samples were collected in 5 ml Pierce glass vials sealed with Teflon®-lined rubber septa and screw caps. Care was taken to see that each vial was completely filled to prevent vapor headspace. Vials were stored in a refrigerator until analysis.

QA/QC procedures as specified in the Standard Operating Procedures of the Hazardous Waste Research Center (Reference 42) were followed. Sample collection was as described in the previous paragraph. These samples were labelled according to the experiment number and date of

experiment. The identity of these samples was also noted in a laboratory notebook.

For pressure drop experiments, the procedures described above were used to establish water and air flow rates; however, no organics were added and liquid samples were not required. Pressure drop was measured directly by connecting the U-tube manometer containing hexane to pressure taps near the top and bottom of the column. The total pressure drop was divided by the vertical distance between pressure taps so that results are reported on a unit packed height basis.

5. Analytical Procedure

Chemical analysis was carried out using a Hewlett-Packard 5890 A gas chromatograph with a flame ionization detector. A 1.83-meter stainless steel column having a 0.32-cm internal diameter and packed with 80/120 Carbopak® B coated with 3 percent SP-1500 was used. The chromatograph was operated isothermally at the following conditions: oven temperature, 110°C; detector temperature, 220°C; injector temperature, 220°C; column head pressure, 40 psi.

The "solvent-push" technique was used to inject samples (Reference 44). One microliter of water was pulled into the syringe, followed by two microliters of sample. A minimum of two samples from each sample vial were analyzed. Additional samples were analyzed if the peak areas from the first two differed by more than 5 percent. Samples were injected using Hamilton 10-microliter syringes. Peak area was determined using a Hewlett-Packard 3390A integrator.

Calibration curves for the individuals organics tested may be found in Appendix A. Since the peak area was found to be directly proportional to the mass of organic injected, these calibration curves were used only when absolute concentrations were needed. Relative concentrations were determined simply by ratioing the peak areas.

The calibration curves were checked before and after each series of analyses to make sure that the response of the flame ionization detector was uniform. If detector response drifts were observed the entire analysis was repeated after a new calibration was carried out. Fresh samples were prepared for each calibration curve to avoid losses due to volatilization and/or degradation. The stability of the gas chromatography column was determined by the constancy in the retention times of the compounds and the reproducibility in the peak areas of the standard samples. We observed very little change in these factors even after 500 or more aqueous sample injections in agreement with the manufacturer's (Supelco Inc.) information (Reference 43). The columns were changed only if a serious loss in efficiency was observed. During the course of the entire experimental program, we have had to change the column only five times.

As mentioned earlier, two or more injections were made for each sample analysis so that the peak areas were reproducible within ±5 percent. Peak areas outside of one standard deviation were rejected. In most cases reproducibility of peak areas was ensured in three or four

injections. In some cases analysis of the same sample was carried out by two different analysts to check for reproducibility of results.

6. Countercurrent Packed Column

The internals for the crossflow column were removed and two sections of total height 2.74 meters (9 feet) were packed with polypropylene Pall rings to a height of 2.43 meters (8 feet). The liquid distributor at the top and the sampler at the bottom were redesigned to cover the entire cross section of the column. The experimental procedures and all other aspects were the same as described in the previous sections on crossflow.

B. 12-INCH COLUMN

1. Overview

Favorable results from the experimental program using the small 6-inch column provided the necessary incentive to scale-up the stripping studies to 12-inch diameter. The flexibility associated with adjustable baffle spacing was sacrificed because of the desire to minimize flow distribution problems attributed to the removable stainless steel internals.

It seemed desirable to involve a commercial firm presently active in the design, construction, and operation of packed column air stripping systems for groundwater remediation. Discussions were held with several firms, some of whom had neither the interest nor the capabilities for pursuing the crossflow concept. One firm, ORS Environmental Equipment, a division of Groundwater Technology Inc., was interested, and after a visit to their manufacturing and laboratory facilities, a decision was made to have ORS fabricate the column.

The convenience of the semibatch operation mode for laboratory studies was maintained but other changes made the new unit more closely resemble the type of unit which would be expected in field operation. For example, the column and liquid reservoir were fabricated from fiberglass-reinforced plastic (FRP). Therefore, visual observation of the gas and liquid contact was no longer possible. All column internals were permanently fixed in place, thereby sacrificing the flexibility of adjustable baffle spacing.

Original plans were to acquire a turnkey system, skid-mounted and complete with blower, pump, piping, and all required instrumentation. Unexpectedly high costs made this impossible, so that only the column and liquid reservoir were acquired from ORS; LSU supplied the pumps, blower, piping, packing, liquid distributor, liquid sampler, and all instrumentation.

An engineering drawing of the components fabricated by ORS is shown in Figure 4. The schematic for the pump and blower connections for the 12-inch crossflow column were identical to those of the 6-inch crossflow column shown in Figure 2. The operation and sampling procedure and the method of chemical analysis were identical to those used for the smaller 6-inch unit.

2. Detailed Equipment Description

a. Packed Column Modules

The 12-inch inside diameter fiberglass-reinforced plastic column, having an overall height of 3.94 meters (155 inches) and a packed height of 3.43 meters (135 inches), is attached to the liquid reservoir via a standard flange. Two vertical stainless steel screens which are permanently bonded to the baffles and the walls of the column keep the packing in place and provide the open plenum for air flow. The position of the screens is such that 65 percent of the cross-sectional area is packed leaving 35 percent open for air flow.

A total of nine fiberglass reinforced partial baffles, five on one side and four on the other side, divert the gas to create the cascade crossflow pattern. As shown in Figure 4, the vertical spacing between opposite baffles is 0.49 meters (19.3 inches). These dimensions result in an α, the ratio of gas to liquid flow area, of 2.6, and produce a total of seven crossflow stages.

Nominal 5/8-inch polypropylene pall rings were used as packing, the same as used in the smaller column. A fiberglass-reinforced grating across the bottom of the column supports the packing. The 6-inch threaded coupling near the bottom of the column provides direct access for packing removal.

b. Liquid Distribution

A liquid distributor similar in design to the distributor used with the 6-inch column was fabricated at LSU. Even liquid distribution was achieved by virtue of the numerous small holes in the bottom of the distributor which was located approximately one inch above the top of the packing. V-shaped weirs were cut along the tops of each side of the distributor to provide for possible overflow at high liquid rates.

c. Liquid Sampler

A liquid sampler similar to that used with the 6-inch column was fabricated at LSU and positioned in the 12-inch high section between the bottom of the packing and the liquid reservoir. Additional sampling ports in the reservoir provided the ability to obtain simultaneous samples of liquid entering and leaving the packed section.

d. Liquid Reservoir

The liquid reservoir was fabricated from fiberglass reinforced plastic in the form of a cylinder 1.22 meters (48 inches) in diameter and 1.01 meters (40 inches) high. The capacity of the reservoir was 1140 liters (300 gallons). 1-inch by 4-inch fiberglass-reinforced plastic I-beams were bonded across the top of the reservoir to provide structural support for the column and packing. Numerous openings through the walls (1-inch and 3-inch PVC fittings) were used for liquid addition, sample removal, and liquid circulation. A 12-inch diameter flanged port provided access to the reservoir for cleaning.

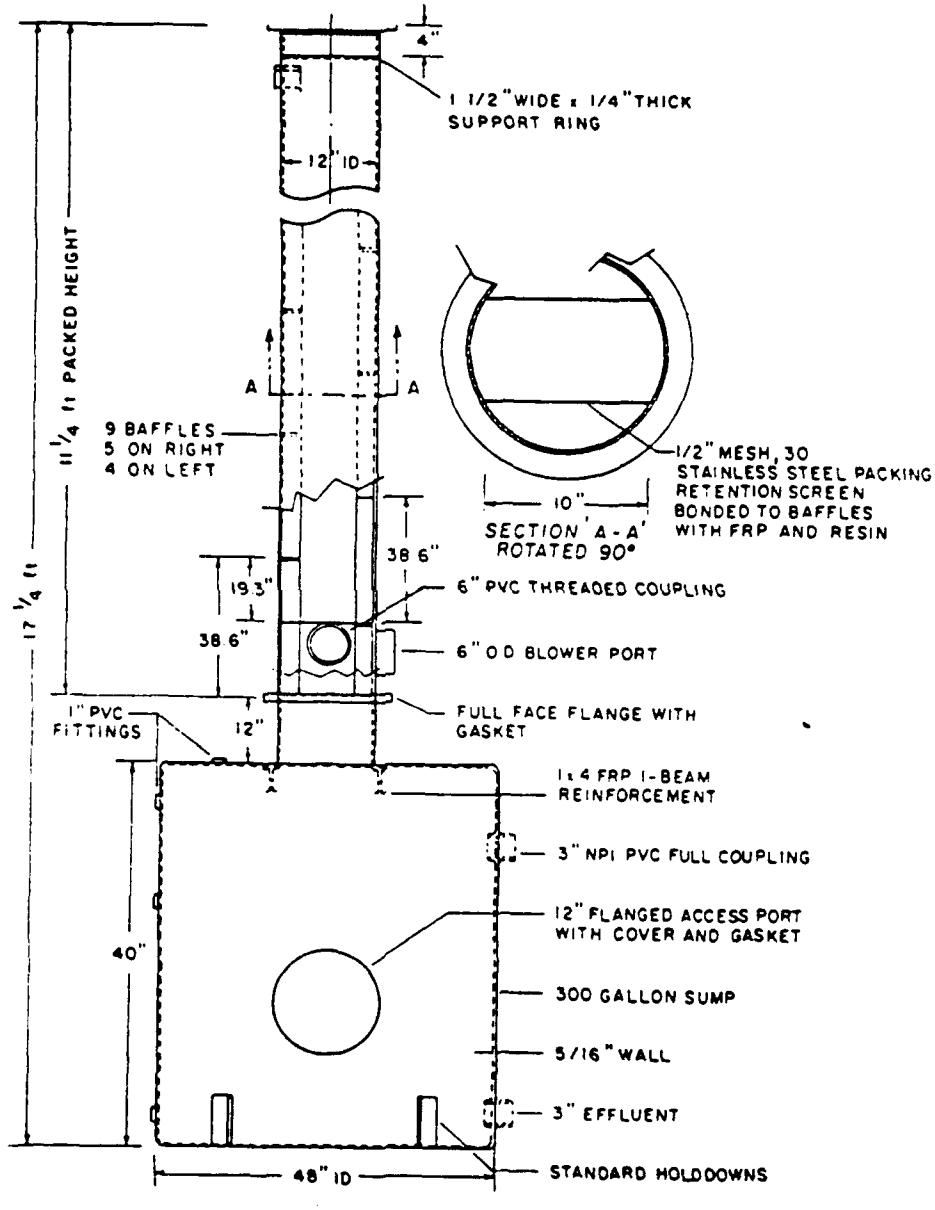

Figure 4. Engineering Drawing of 12-inch Pilot Scale Column

e. Liquid Pumps

The 0.75-hp pump was used to deliver liquid to the distributor at the top of the column. This pump did not have sufficient capacity for simultaneous liquid recirculation and feed; therefore a second 0.50-hp centrifugal pump was added for recirculation. This pump simply removed liquid from one access port on the reservoir and returned that liquid to an opposite access port.

Liquid feed rate was monitored using a King Industries Co., rotameter (Model K72-10/2 Series) having a capacity of 40 gpm. No effort was made to monitor the flow rate of recirculating liquid.

f. Air Blower

The 1.5-hp Powerbloc blower with Westinghouse Accutrol variable speed controller was used to deliver air to the column. Air flow was monitored using an orifice meter with pressure difference measured using a U-tube manometer filled with n-hexane.

g. Thermocouples

Temperature was measured using three Maverick type T, stainless steel thermocouples connected to a Eurotherm Model 840 digital indicator. The thermocouples were located in the liquid reservoir, at the liquid inlet to the column, and at the blower outlet.

3. Analytical Procedures

The analytical procedures were the same as described for the 6-inch column.

SECTION IV

RESULTS AND DISCUSSION

A. BACKGROUND

The flow paths of gas and liquid phases in a crossflow column are disconnected from one another, unlike in a countercurrent device where the two phases compete for the same area. This is achieved by packing only a portion of the total column cross-sectional area and using baffles to deflect air in the open plenum. The crossflow device thus introduces a new design parameter, α, which is the ratio of gas flow area to liquid flow area. Figure 5 shows the details of how α is obtained. The parameter α is adjustable in the 6-inch column whereas it is fixed at 2.6 in the 12-inch column. Increasing the baffle spacing increases the gas flow area and hence α. Since this is the key variable in crossflow and since this effects both mass transfer and pressure drop, the primary aim of the 6-inch column experiments was to study the effect of α on stripping efficiency and pressure drop. Experiments on the 12-inch column were used to check the 6-inch column results to determine the suitability for scale-up.

B. PERFORMANCE EQUATIONS

The overall operation of a cascade crossflow tower is still countercurrent. Hence the performance equations used in conventional countercurrent operations must also be applicable to the crossflow system. The following derivation is identical to that for a countercurrent device (References 21, 22). The key assumptions are (1) the amount of VOC in either phase is small with respect to the total phase volume and hence the volumes of the air and water streams remain unchanged during flow through the column, (2) the influent air stream does not contain the VOC being stripped, and (3) the stripped compound obeys Henry's law:

$$C_g = H_c\, C_\ell \qquad (1)$$

where C_g, C_ℓ = gas and liquid phase VOC concentrations, respectively ($mole/m^3$).

H_c = Henry's constant (dimensionless).

We also assume no species interactions in multicomponent systems (References 21 and 22).

With reference to Figure 6, we can write the following equation for the rate of mass transfer

$$dN = K_\ell a\, (C_\ell - C_\ell^*)\, A\, dZ \qquad (2)$$

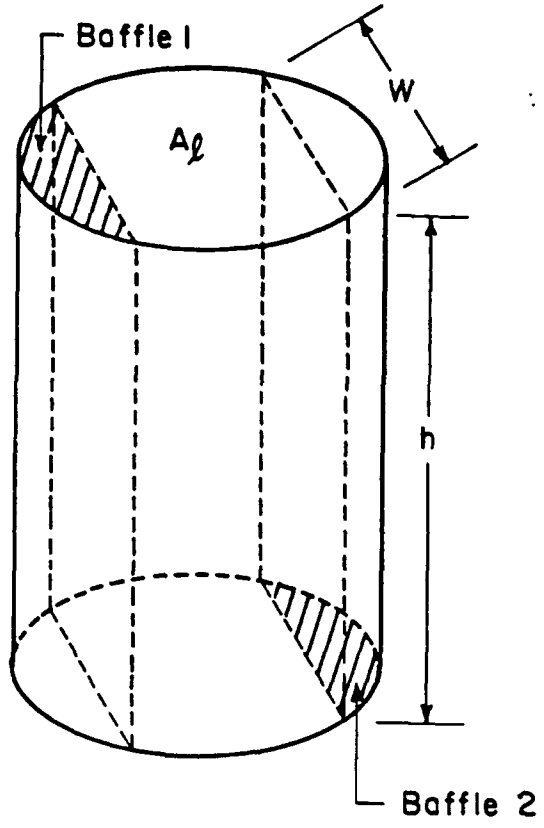

$$\alpha = \frac{Ag}{A_\ell} = \frac{Wh}{0.65 A_t}$$

Figure 5. Calculation of Alpha; A_t is the Total Cylindrical Column Cross-sectional Area.

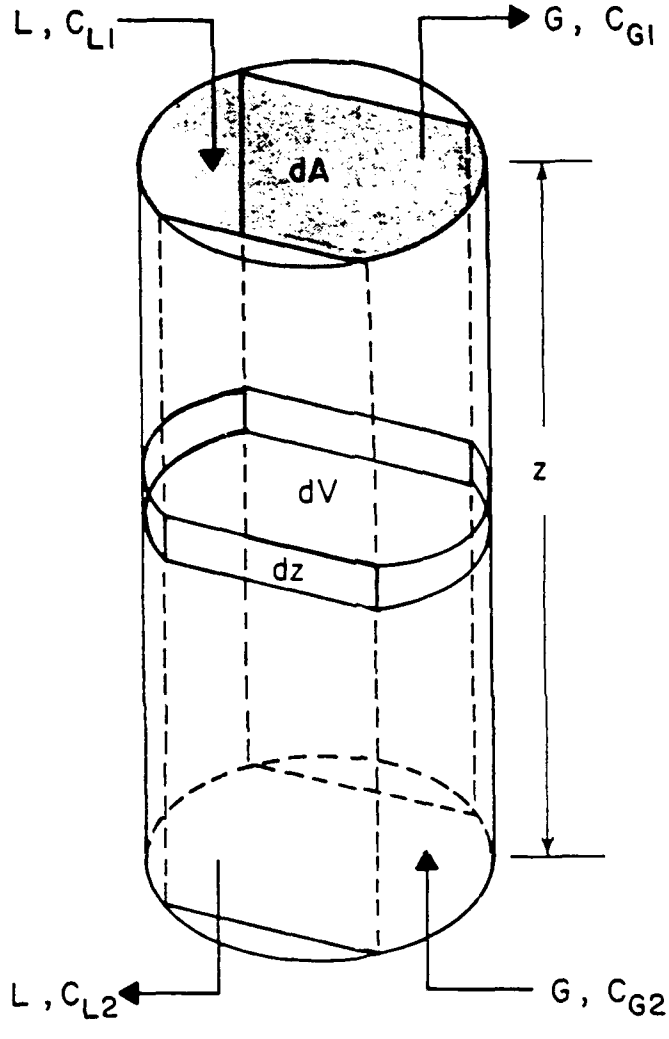

Figure 6. Overall Schematic of Cascade Crossflow Column.

where dN = rate of solute mass transfer $[d(LC_\ell)]$ (mol/min).

L = liquid flow rate (m^3/min)

C_ℓ = aqueous solute concentration (mol/m^3).

C_ℓ^* = solute concentration in the aqueous phase in equilibrium with the gas (= C_g/H_c), (mol/m^3).

K_ℓ = overall liquid phase transfer coefficient (m/min).

A = cross sectional area (m^2).

a = specific interfacial area per unit packed volume (m^2/m^3).

Z = height of the packing, (m).

Equation (2) may be rearranged to give

$$\frac{L\ dC_\ell}{(C_\ell - C_\ell^*)} = K_\ell a\ A\ dZ \qquad (3)$$

Since the operating and equilibrium lines for the system of interest are linear, the difference in the ordinates of the two lines must vary linearly in composition. If the ordinate $(C_\ell - C_\ell^*)$ is represented by Δ and the end points of the system represented by 1 and 2, i.e., $\Delta = \Delta_1$, at $Z = Z_T$ and $\Delta = \Delta_2$ at $Z = 0$ we have

$$\frac{d\ \Delta}{d\ C_\ell} = \frac{(\Delta_1 - \Delta_2)}{C_{\ell 1} - C_{\ell 2}} \qquad (4)$$

Thus

$$\frac{L(C_{\ell 1} - C_{\ell 2})}{(\Delta_1 - \Delta_2)}\ \frac{d\Delta}{\Delta} = K_\ell a\ A\ dZ \qquad (5)$$

Integrating Equation (5) provides

$$L(C_{\ell 1} - C_{\ell 2}) = K_\ell a\ A\ (C_\ell - C_\ell^*)_{\ell n}\ \ell n\ Z_T \qquad (6)$$

where

$$(C_\ell - C_\ell^*)_{\ell n} = (\Delta_1 - \Delta_2)\ \ell n\ \left(\frac{\Delta_2}{\Delta_1}\right) \qquad (7)$$

Using Henry's law we have

$$C^*_{\ell 1} = C_{g1}/H_c \quad , \quad C^*_{\ell 2} = C_{g2}/H_c = 0 \text{ since } C_{g2} = 0$$

Hence we have

$$\frac{K_\ell a\ A\ Z_T}{L} = \frac{\ell n[\frac{C_{\ell 1}}{C_{\ell 2}} - \frac{C_{g1}}{C_{\ell 2}\ H_c}]}{1 - \frac{C_{g1}}{(C_{\ell 1} - C_{\ell 2})H_c}} \tag{8}$$

A solute mass balance around the column gives

$$C_{g1} = (\frac{L}{G})\ (C_{\ell 1} - C_{\ell 2}) \tag{9}$$

where G = gas flow rate (m^3/min)

Denoting the efficiency of stripping as

$$E = 1 - \frac{C_{\ell 2}}{C_{\ell 1}} \tag{10}$$

and substituting (9) and (10) in (8) we have

$$K_\ell a = (\frac{L}{A\ Z_T})\ \frac{\ell n[\frac{1}{1-E} - (\frac{E}{1-E})\ \frac{L}{G\ H_c}]}{1 - \frac{L}{G\ H_c}} \tag{11}$$

The above equation explicitly gives the performance of a packed column as a function of column size (AZ_T), operating conditions (L and G), and solute characteristics (H_c and $K_\ell a$). Equations (10) and (11) are the two key equations in our experiments. The latter gives the mass transfer coefficient when the stripping efficiency, E is known from Equation (10). As described in Section III, E is determined in all experiments by directly measuring the exit ($C_{\ell 2}$) and inlet ($C_{\ell 1}$) concentration of solute in the aqueous stream.

C. MASS TRANSFER MODELS FOR PACKED COLUMNS

The overall mass transfer coefficients in air-stripping operations are defined in terms of individual liquid and gas phase coefficients (k_ℓ and k_g) and the Henry's constant (H_c) for a particular solute. The

detailed development of this principle is available in the literature (Reference 23). The overall liquid-phase mass transfer coefficient is defined by

$$\frac{1}{K_\ell a} = \frac{1}{k_\ell a} + \frac{1}{H_c\, k_g a} \qquad (12)$$

Each term in the above equation gives individual resistances in each phase. For most volatile organics, $[1/(H_c\, k_g a)] << (1/k_\ell a)$ and hence

$$\frac{1}{K_\ell a} \simeq \frac{1}{k_\ell a} \qquad (13)$$

Such compounds are said to be liquid-phase controlled in their mass transfer behavior.

Two types of correlations are generally used for estimating $K_\ell a$ values - single resistance and two resistance models. We have investigated the applicability of three often quoted correlations in the realm of air stripping of VOCs. These are given below:

1. Sherwood and Holloway (Reference 24) correlation: This is a single resistance model which assumes that $K_\ell a \simeq k_\ell a$ as in Equation (13). The liquid phase mass transfer coefficient $k_\ell a$ is given by

$$\frac{k_\ell a}{D_L} = 10.764\ \alpha \left[\frac{0.3048\ L_m}{\mu_L}\right]^{1-n} \left[\frac{\mu_L}{\rho_L\, D_L}\right]^{0.5} \qquad (14)$$

where D_L = solute diffusivity, $m^2/sec.$

L_m = liquid mass loading rate, $kg/m^2 \cdot sec.$

μ_L = liquid viscosity, $kg/m \cdot sec.$

ρ_L = liquid density, kg/m^3

α, n = constants which are functions of packing type and size.

The above correlation was developed using results from the air stripping of gases such as CO_2, O_2 and H_2 from water in a column packed with Raschig rings and Berl saddles. The valid flow parameters were 0.26 - 1.4 $kg/m^2 s$ gas loading rates. However α and n are available only for Rasching rings, Berl saddles and tiles. Cornell et al. (Reference 39) modified this relation for other types of packing.

$$k_\ell a = \left(\frac{3.28\ L_m}{\varphi\ \rho_L}\right)^{-0.5} \left(\frac{Z}{3.05}\right)^{-0.15} \qquad (15)$$

where φ = constant for a given packing, m

Z = total height of packing, m

Bolles and Fair (References 25 and 26) obtained good values of φ for various packing types using improved fit of a large body of data covering a variety of packings.

2. Shulman et al. (Reference 27) proposed a two resistance model with the following individual correlations for k_ℓ and k_g.

$$\frac{k_\ell\ d_s}{D_L} = 25.1 \left(\frac{d_s\ L_m}{\mu_L}\right)^{0.45} \left(\frac{\mu_L}{\rho_L\ D_L}\right)^{0.5} \qquad (16)$$

$$\frac{\rho_g\ k_g}{G_m} = 1.195 \left(\frac{d_s\ G_m}{\mu_g(1-\varepsilon)}\right)^{-0.36} \left(\frac{\mu_g}{\rho_g\ D_g}\right)^{-0.667} \qquad (17)$$

where d_s = diameter of a sphere having the same surface area as a unit of packing, m

ε = dry void fraction of packed column.

D_g = diffusivity of the solute in the gas phase, m^2/s.

G_m = gas mass loading rate, $kg/m^2 \cdot s$.

μ_g = gas viscosity, $kg/m \cdot s$.

ρ_g = gas density, kg/m^3.

Equation (16) was obtained via reinterpretation of the Sherwood and Holloway data and is valid for L_m in the range 0.65 - 9.7 $kg/m^2 \cdot s$. Equation (17) was obtained from data on the vaporization of naphthalene rings and is valid for G_m in the range 0.24 - 1.4 $kg/m^2 \cdot s$ and for volumetric G/L ratios of 1 to 100.

In order to obtain volumetric mass transfer coefficients from Equations (16) and (17), Shulman et al. (Reference 27) defined an effective interfacial area, a_ℓ to account for the liquid caught in pools that is unavailable for mass transfer. a_ℓ is smaller than the total wetted area of the packing and is a function of both G and L. In the original work of Shulman et al. (References 27 and 28) an extensive series of graphs for a_ℓ for Berl saddles and Raschig rings are

available. For packings such as Pall rings and Flexisaddles, the recent correlation of Bravo and Fair (Reference 29) should suffice.

$$\frac{a_\ell}{a_t} = 0.498 \left[\frac{\sigma^{0.5}}{z^{0.4}}\right] (Ca_L \; Re_g)^{0.392} \qquad (18)$$

where z = total height of packed bed, ft

σ = surface tension of the liquid, dyne/cm

Ca_L = liquid capillary number $\left(= \frac{\mu_L \; L_m}{\rho_L \; \sigma}\right)$

Re_g = gas Reynolds number $\left(= \frac{6 \; G_m}{a_t \; \mu_g}\right)$

a_t = total dry packing area/unit bed volume, m^{-1}.

Bravo and Fair (Reference 29) tested Equation (18) against a large amount of data and found it to predict a_ℓ values within ±20 percent of the observed values.

3. The most frequently used correlation for VOC air stripping is the one proposed by Onda et al. (Reference 30). This is also a two-resistance model in which the authors assumed that the effective area, a_ℓ is equal to the wetted surface area, a_w, and calculated k_ℓ and k_g by dividing measured values of $k_\ell a$ and $k_g a$ by a_w.

$$k_\ell \left(\frac{\rho_\ell}{g\mu_\ell}\right)^{0.333} = 0.0051 \left(\frac{L_m}{\mu\ell \; a_w}\right)^{0.667} \left(\frac{\mu_\ell}{\rho_\ell D_\ell}\right)^{-0.5} (a_t \; d_s) \qquad (19)$$

$$\frac{k_g}{a_t \; D_g} = 5.23 \left(\frac{G_m}{\mu_g \; a_t}\right)^{0.7} \left(\frac{\mu_g}{\rho_g \; D_g}\right)^{0.333} (a_t \; d_s)^{-2.0} \qquad (20)$$

where g = acceleration due to gravity, 9.8 m^2/sec.

a_w = wetted interfacial area/unit packed volume, m^{-1}

d_s = nominal packing diameter, m

a_w is given by

$$\frac{a_w}{a_t} = 1 - \exp\{-1.45 \left(\frac{\sigma_c}{\sigma}\right)^{0.75} Re^{0.1} Fr^{-0.05} We^{0.2}\} \qquad (21)$$

where σ_c = critical surface tension with respect to the packing material, kg/sec^2.

σ = surface tension of liquid, kg/sec^2.

Re = Reynolds number, $L_m/a_t \mu_\ell$

Fr = Froude number, $L_m^2 a_t/\rho_\ell^2 g$.

We = Weber number, $L_m^2/\rho_\ell G_m a_t$.

Onda et al. (Reference 30) reported that Equation (19) is valid within ±25 percent for Raschig rings, Berl Saddles, spheres, and rods for L_m values of 1 to 15 kg/m²·s while Equation (20) correlates to within ±30 percent for G_m values of 0.02 to 1.7 kg/m²·s. Both Gossett et al. (Reference 21) and Munz (Reference 22) have shown the utility of this correlation to predict mass transfer coefficients for VOCs that are liquid phase controlled. However for those compounds that have a large transfer resistance in the gas phase, this correlation has been observed to be only marginally acceptable (Reference 22).

For the crossflow mode of operation Hayashi and co-workers (Reference 11) have proposed a modified correlation for wetted area

$$\frac{a_w}{a_t} = 0.251\ Re^{0.2}\ We^{0.52}\ Fr^{-0.45}\ \left[\frac{0.025}{d_s}\right] \qquad (22)$$

This was developed using Raschig rings and eliminator type packings. This modified Onda correlation was tested in combination with Equations (19) and (20) to obtain crossflow mass transfer coefficients in our work.

D. STRIPPING EFFICIENCIES AND MASS TRANSFER COEFFICIENTS

Experiments on the removal of four compounds, viz., methylene chloride, chloroform, carbon tetrachloride and 1,2-dichloroethane were conducted at α values of 1, 2.0, 3.3, 6.0 and 8.0 on the 6-inch crossflow column. The relevant properties of the four compounds studied are given in Table 2. All experiments were performed at 22 ± 1°C and a packed height of 2.4 meters. Unless otherwise stated gas and liquid loading rates reported in this section are based on the cross sectional area for liquid flow through the packing. Experiments were also performed under the same loading rates and volumetric flow rates by converting the 6-inch crossflow column into a countercurrent column in

TABLE 2. PROPERTIES OF VOCs USED IN THE STUDY

Property	Methylene Chloride	Chloroform	Carbon tetra-chloride	1,2-dichloro-ethane
Molecular Weight	85.0	119.5	154.0	98.9
Density (g/cm^3)	1.32	1.48	1.59	1.23
Vapor Pressure[a,c] (mm·Hg)	426.0	158.1	91.2	109.3
Aqueous Solubility[a,c] (mg/ℓ)	16,700	8,200	803	8,700
Henry's Constant[b] (dimensionless)	0.104	0.147	1.076	0.060
log K_{ow}[a]	1.3	1.9	2.8	1.5

All properties are at 298K.

(a) Reference 35.

(b) Henry's constants are from Reference 36.
These are dimensionless ratios of molar concentrations.

(c) Reference 37

order to obtain a direct comparison between countercurrent and crossflow operation.

The last series of experiments was conducted on the large scale 12-inch crossflow column. Three compounds, namely, chloroform, carbon tetrachloride and 1,2-dichloethane were investigated. The α value was fixed at 2.6.

In the studies on the crossflow column, the effects of both gas phase flow variation and liquid flow variation were investigated. For the effects of gas flow variation, the liquid mass loading rate, L_m was held constant while G_m varied from 0.1 to 1.0 kg/m²·s. This was done at two L_m values of 17.6 and 32.0 kg/m²·s. The volumetric G/L ratio varied from 7.5 to 32. In order to study the effects of liquid flow variation, G_m was held at 0.43 kg/m²·s and L_m was varied from 10.7 to 42.7 kg/m²·s which corresponded to volumetric G/L ratios of 8.4 to 33.8.

Chloroform and methylene chloride were studied under all of the conditions mentioned above. Carbon tetrachloride and 1,2-dichloroethane were used only in selected experiments as described in the following pages.

The removal efficiencies in each case were obtained using the following equation

$$E = 1 - \frac{C_{\ell 2}}{C_{\ell 1}} \qquad (23)$$

where $C_{\ell 2}$ = exit concentration (at the sampler)

$C_{\ell 1}$ = inlet concentration (in the tank).

Since the experiments were all conducted in a semibatch mode with liquid recirculation (see Figure 2) it was imperative to obtain at least three values of E at different time intervals for each experiment so that a steady state value of E was confirmed. It should be noted that in these experiments both $C_{\ell 2}$ and $C_{\ell 1}$ will decrease with time, but they do so at the same rate so as to maintain a constant E value. A typical behavior of E with respect to time is shown in Figure 7. The values of E obtained from these experiments are the same values which would be obtained from a conventional steady-state operation. This mode of operation provides the advantage of dealing with only a relatively small volume of aqueous solution and obtaining data for several operating conditions in a limited amount of time.

Since the gas chromatographic calibration curves of the four compounds (See Appendix A) showed the concentration to be directly proportional to peak area over the concentration ranges encountered in our experiments, one can replace concentrations with their respective peak areas in Equation (23).

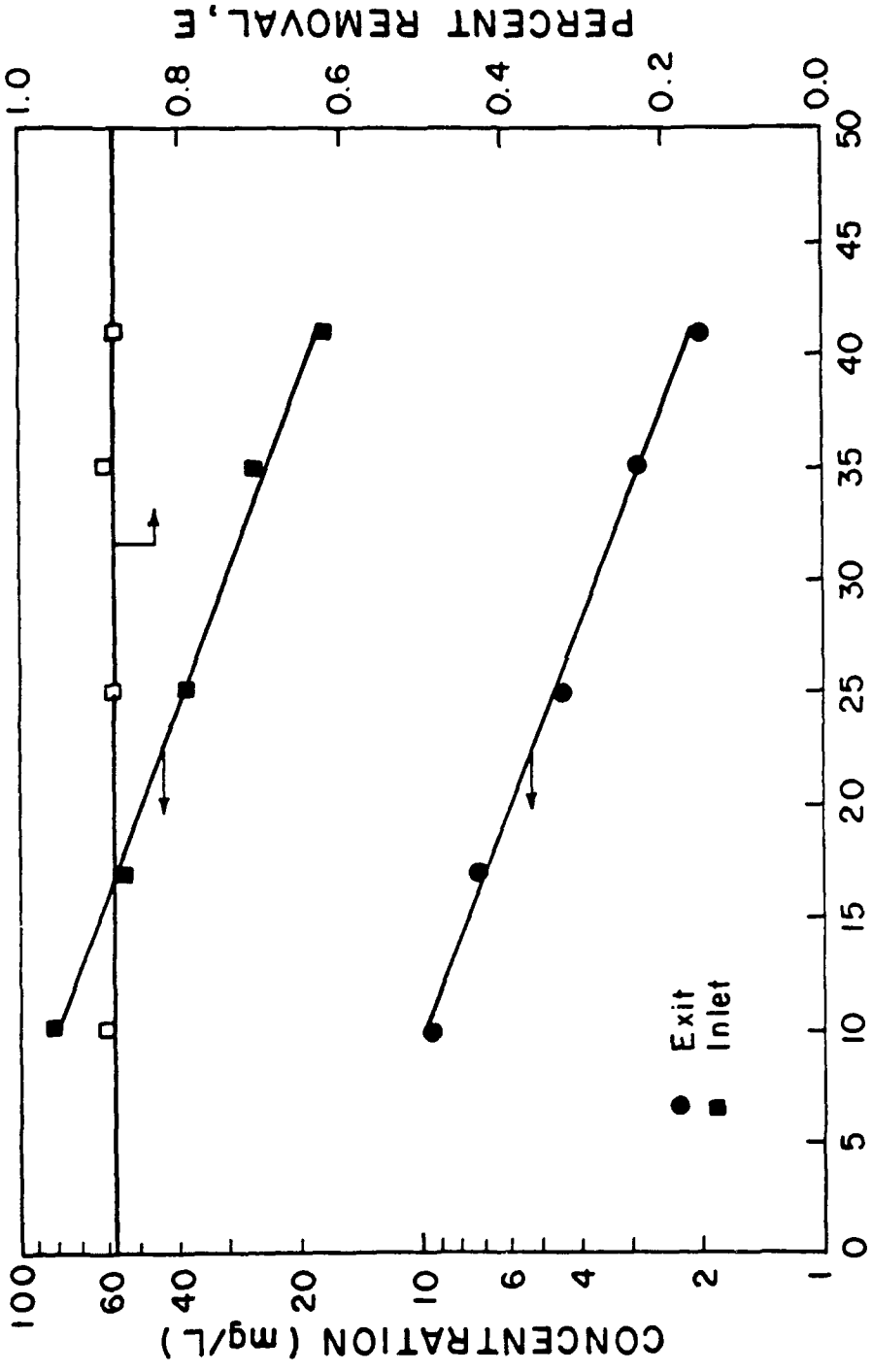

Figure 7. Example of (a) Inlet and Outlet Concentration Change with Time and (b) Percentage Removal with Time.

Figures 8, 9, 10 and 11 give the stripping efficiencies of the four compounds studied at L_m = 17.6 kg/m²·sec for various G/L ratios and α values. Figures 12 and 13 represent the E values for a constant liquid loading rate L_m of 32.0 kg/m²·sec for methylene chloride and chloroform, respectively.

In general, we observed that the removal efficiency approached an asymptotic value at high G/L ratios. A comparison of the removal efficiency of all four compounds at a constant L_m of 17.6 kg/m²·s and a constant α value of 2.0 is shown in Figure 14. The trend was as expected and as observed by other researchers (Reference 22). It was noted that the higher the Henry's constant for a compound the greater the percent removal at a given G/L. Thus over 95 percent removal was observed for carbon tetrachloride with the largest Henry's constant (1.076). At low G/L ratios, the stripping efficiencies for the four compounds differed considerably. These differences became less noticeable as G/L ratio increased and at G/L = 32 the efficiencies between three of the four VOCs differed by less than 4 percent. Even at a G/L of 32, the removal of 1,2-DCA was only 76.5 percent and was clearly the hardest to strip. However, it may be feasible to achieve a higher stripping efficiency at a higher G/L ratio for 1,2-DCA. This will be especially true for crossflow since the range of operability is greater for crossflow as compared to countercurrent flow.

Figures 8-11 clearly show that increasing gas flow rate at a constant liquid loading will increase the removal efficiency up to a certain G/L beyond which the stripping efficiency approaches an asymptotic value. The results at a constant gas loading as shown in Figure 15 for methylene chloride and Figure 16 for chloroform show that increased liquid flow rate decreased removal efficiency.

One of the main objectives of our work on the 6-inch column was to study the effects of the variation of α, the new variable in crossflow. Figures 8-10 show very little effect of α on the removal efficiencies of three of the four VOCs studied. Generally, it was observed that the efficiencies were slightly higher for α = 1 than for α = 2, 3.3, 6 and 8. The differences between the E values for all α values were indistinguishable at high G/L values. However at low G/L values these differences were more pronounced, as, for example, in the case of methylene chloride below a G/L of 7.5 at L_m = 17.6 kg/m²·s (Figure 9). The efficiencies for α of 2, 3.3, 6 and 8 were definitely lower than for α = 1 at the low G/L values. As α is increased, the gas velocity through the packing is decreased and hence those compounds that have a significant degree of gas phase resistance to mass transfer will show decreased rate of mass transfer. This effect was, however, not observed at a higher liquid loading rate (32 kg/m²·s). The α value probably affects the mass transfer rate only at low G_m values and only for compounds that have low Henry's constants. This explanation, however, does not seem to be general, since, as shown in Figure 10, the apparent effects on 1,2-DCA stripping are no larger than those for methylene chloride. A liquid phase controlled chemical will not show a significant increase in efficiency as G_m is increased beyond a certain value at constant L_m. However dramatic improvements may be observed for those compounds that have large gas phase resistance. Thus carbon

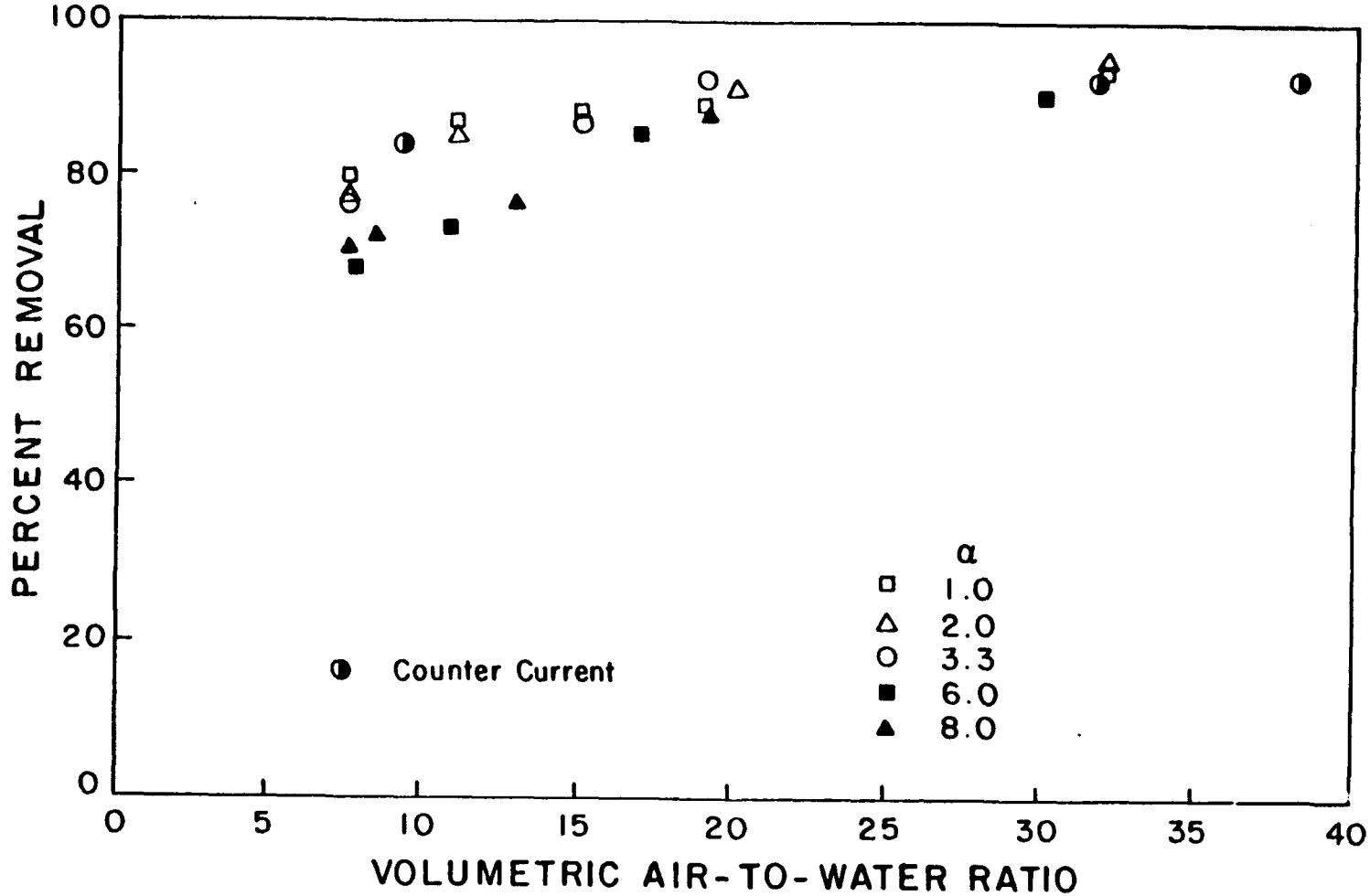

Figure 8. Percent Removal of Chloroform Versus Volumetric Air-to-Water Ratio; L_m = 17.6 kg/m^2.s.

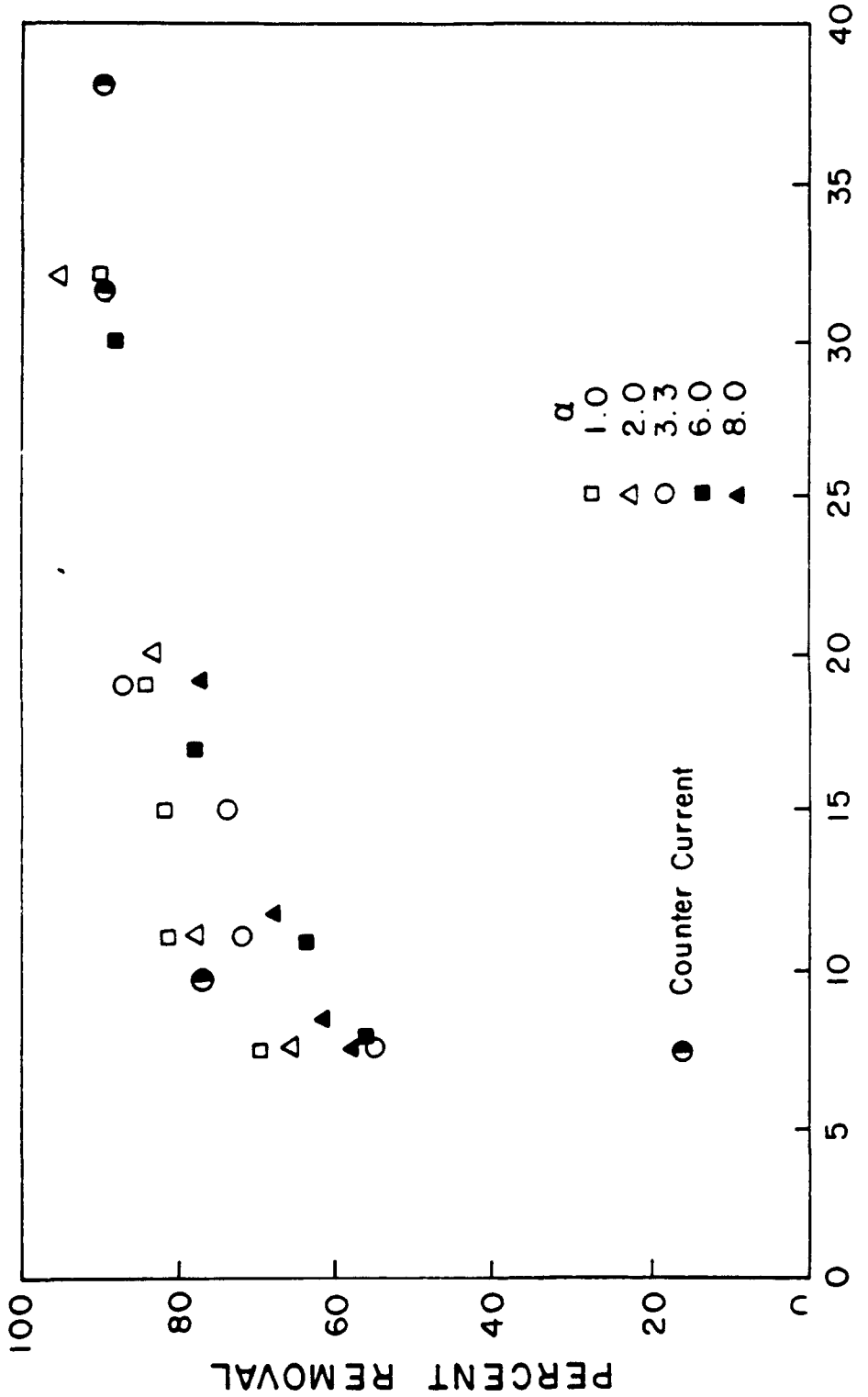

Figure 9. Percent Removal of Methylene Chloride versus Volumetric Air-to-Water Ratio; liquid loading = 17.6 kg/m^{2}s. (Crossflow 3.3 gpm; Countercurrent 5.1 gpm).

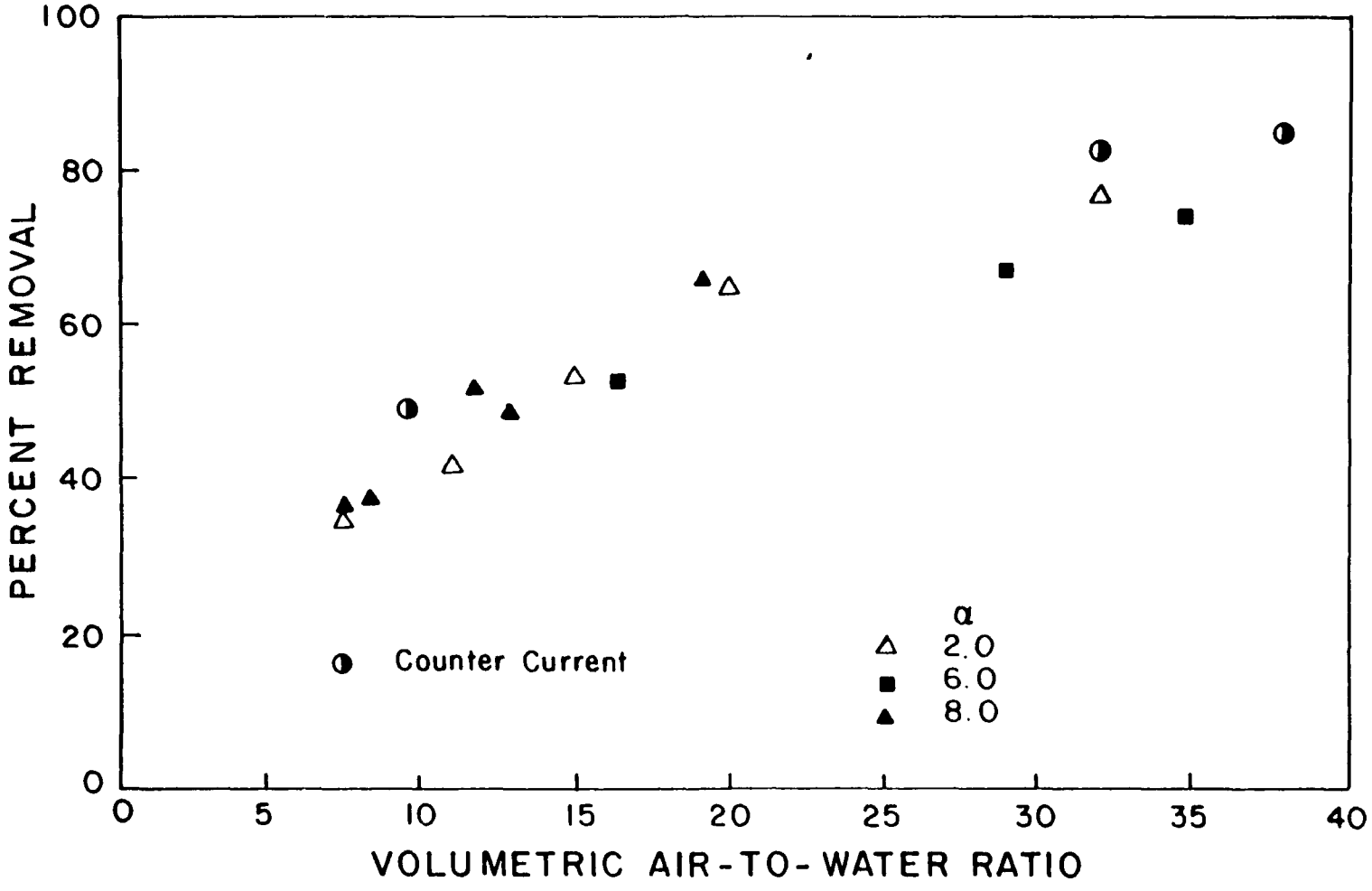

Figure 10. Percent Removal of 1,2-Dichloroethane versus Volumetric Air-to-Water Ratio; Liquid Loading = 17.6 kg/m^{2}s. (Crossflow 3.3 gpm; Countercurrent 5.1 gpm).

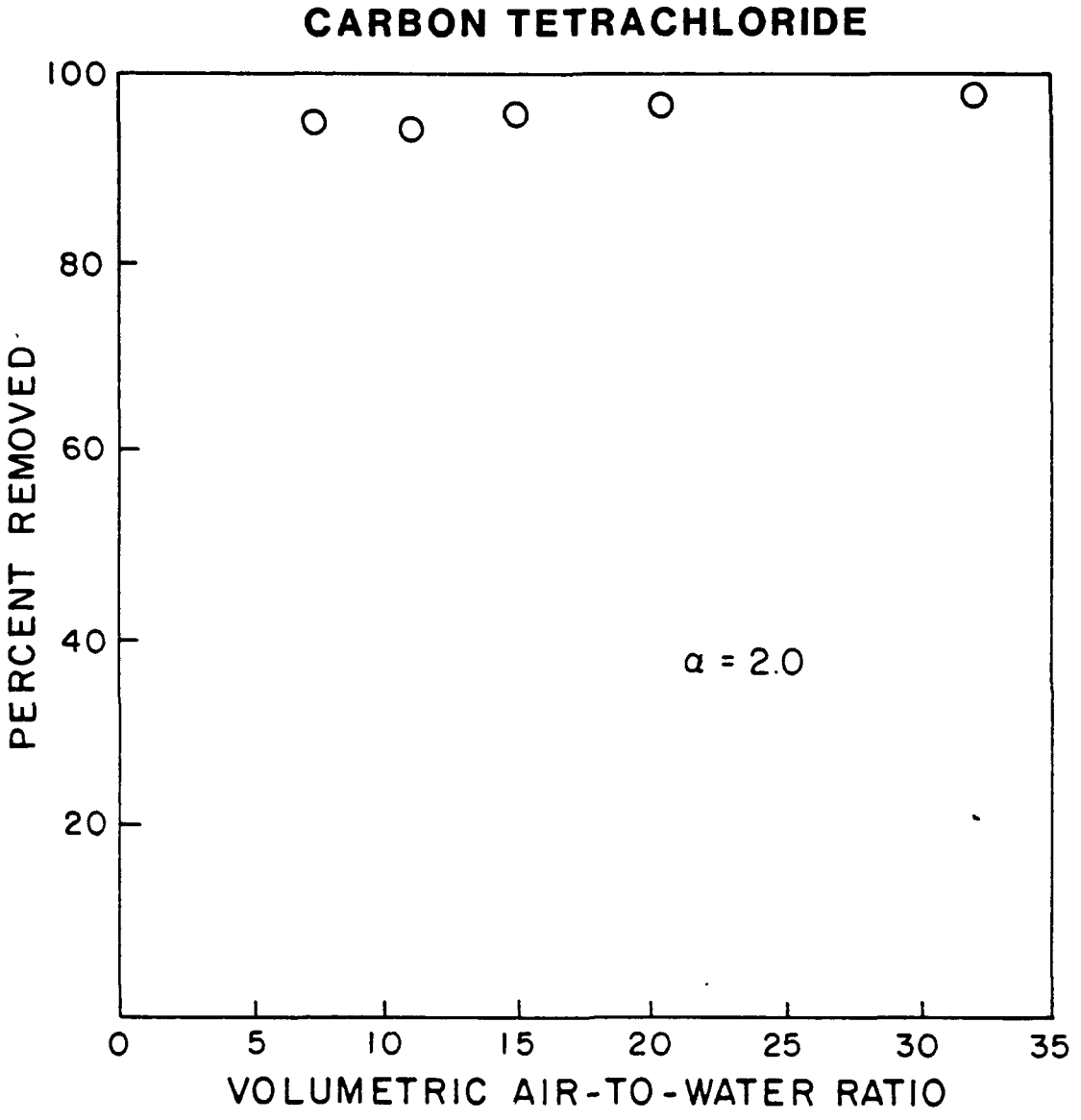

Figure 11. Percent Removal of Carbon Tetrachloride versus Volumetric Air-to-Water Ratio; L_m = 17.6 kg/m^{2}s.

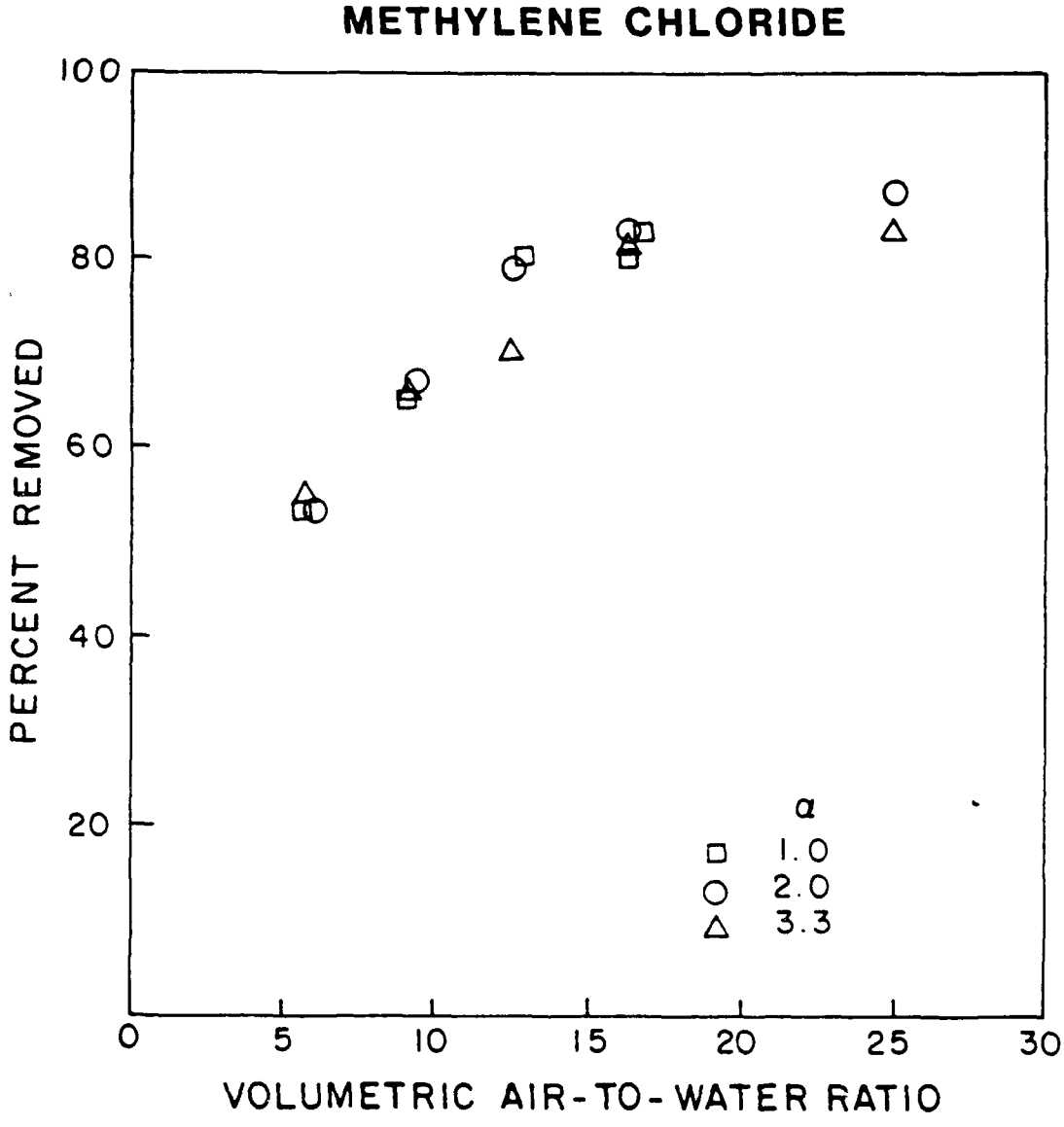

Figure 12. Percent Removal of Methylene Chloride versus Volumetric Air-to-Water Ratio; L_m = 32.0 kg/m^{2}s.

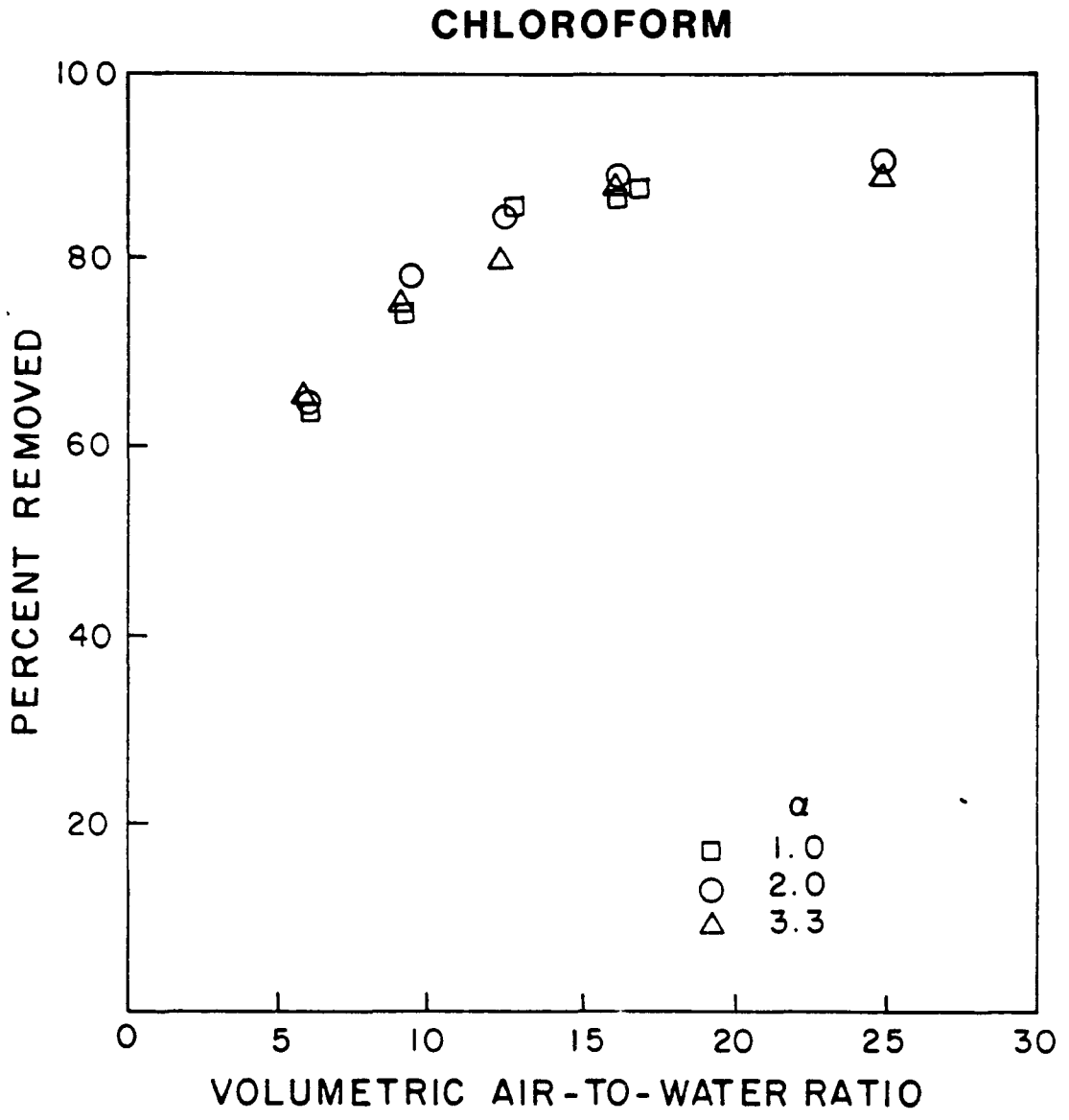

Figure 13. Percent Removal of Chloroform versus Volumetric Air-to-Water Ratio; L_m = 32.0 kg/m^{2}s.

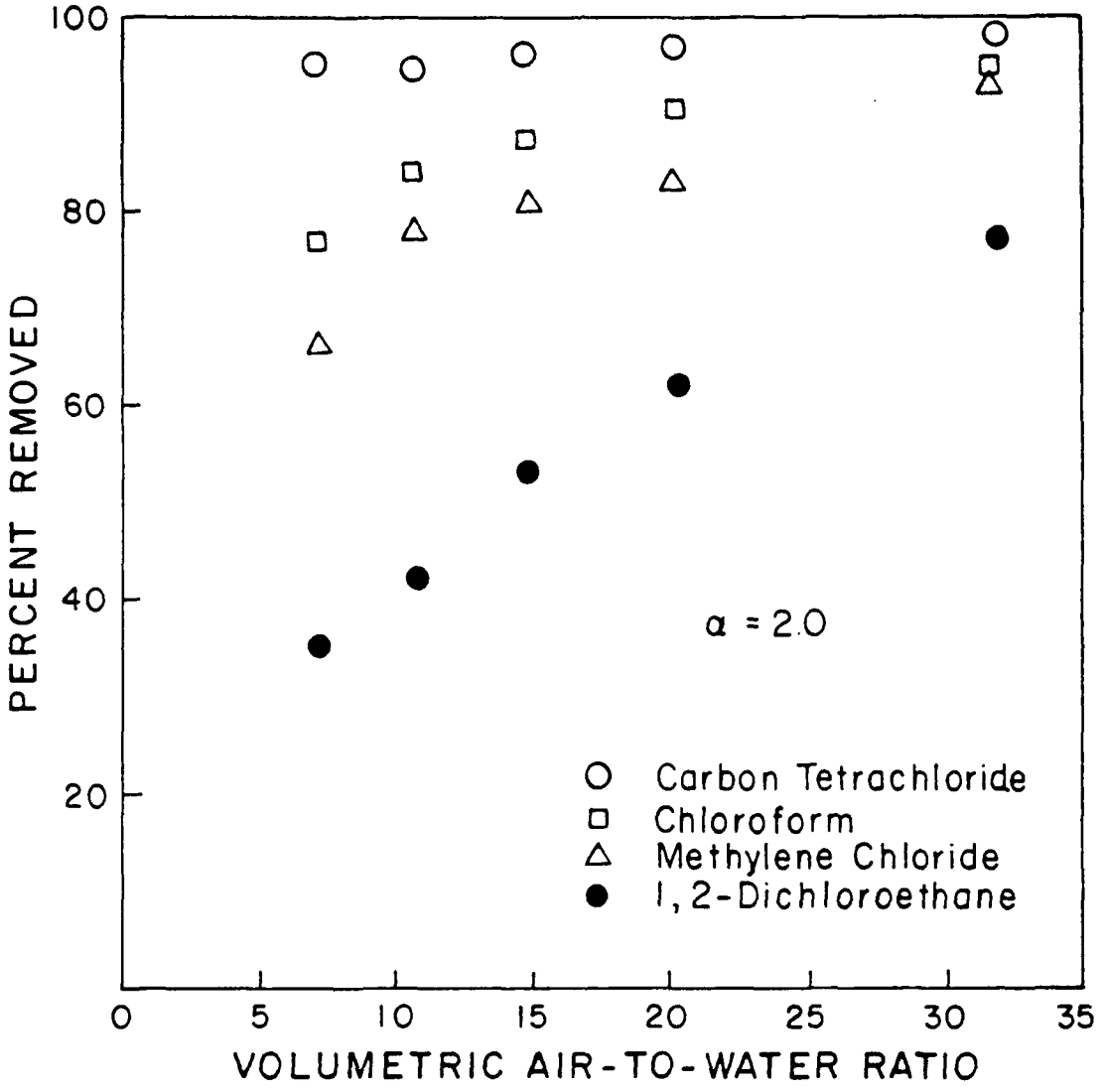

Figure 14. Percent Removal versus Volumetric Air-to-Water Ratio; L_m = 17.6 kg/m^{2}s.

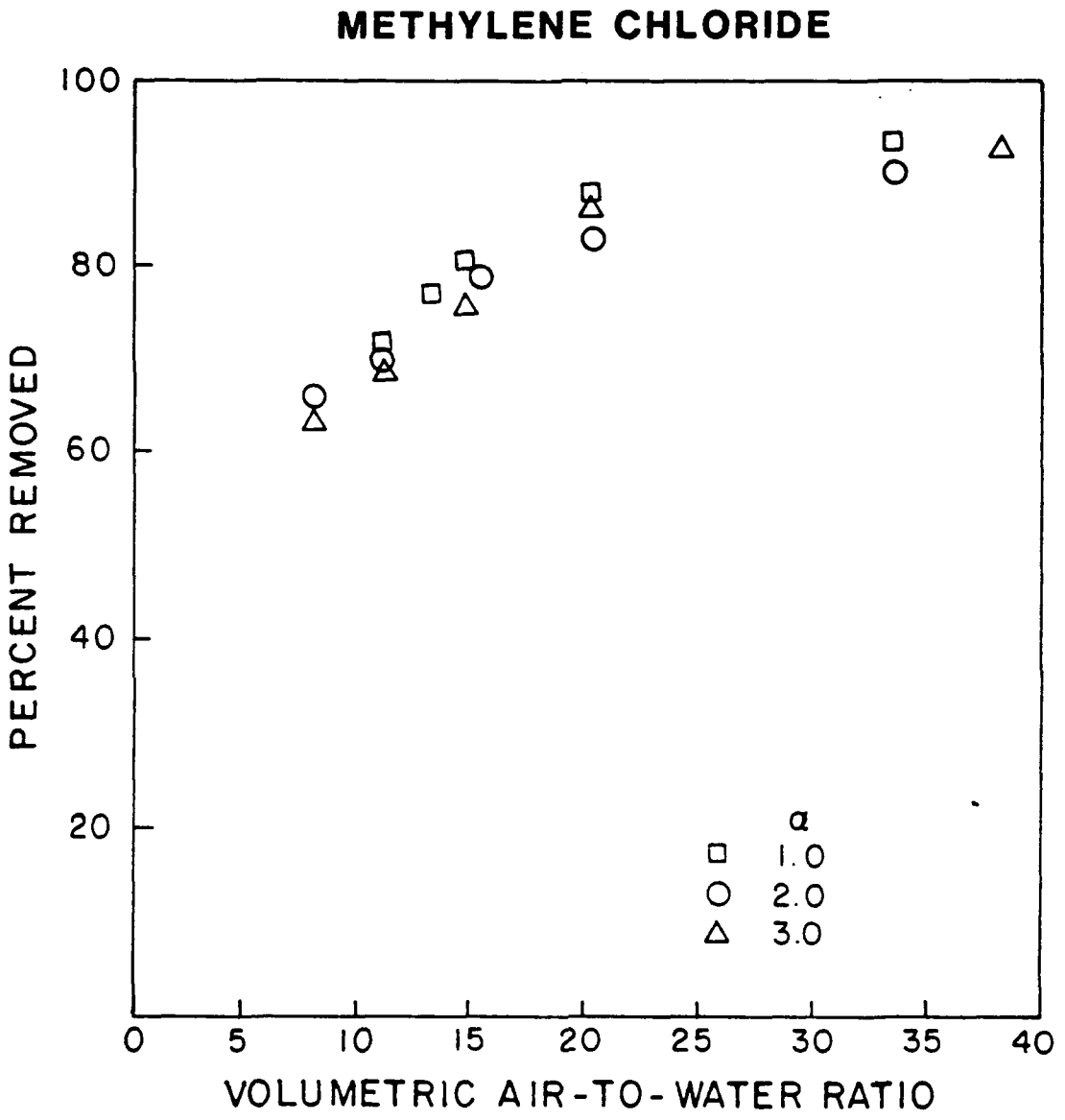

Figure 15. Percent Removal of Methylene Chloride versus Volumetric Air-to-Water Ratio; G_m = 0.43 kg/m^{2}s.

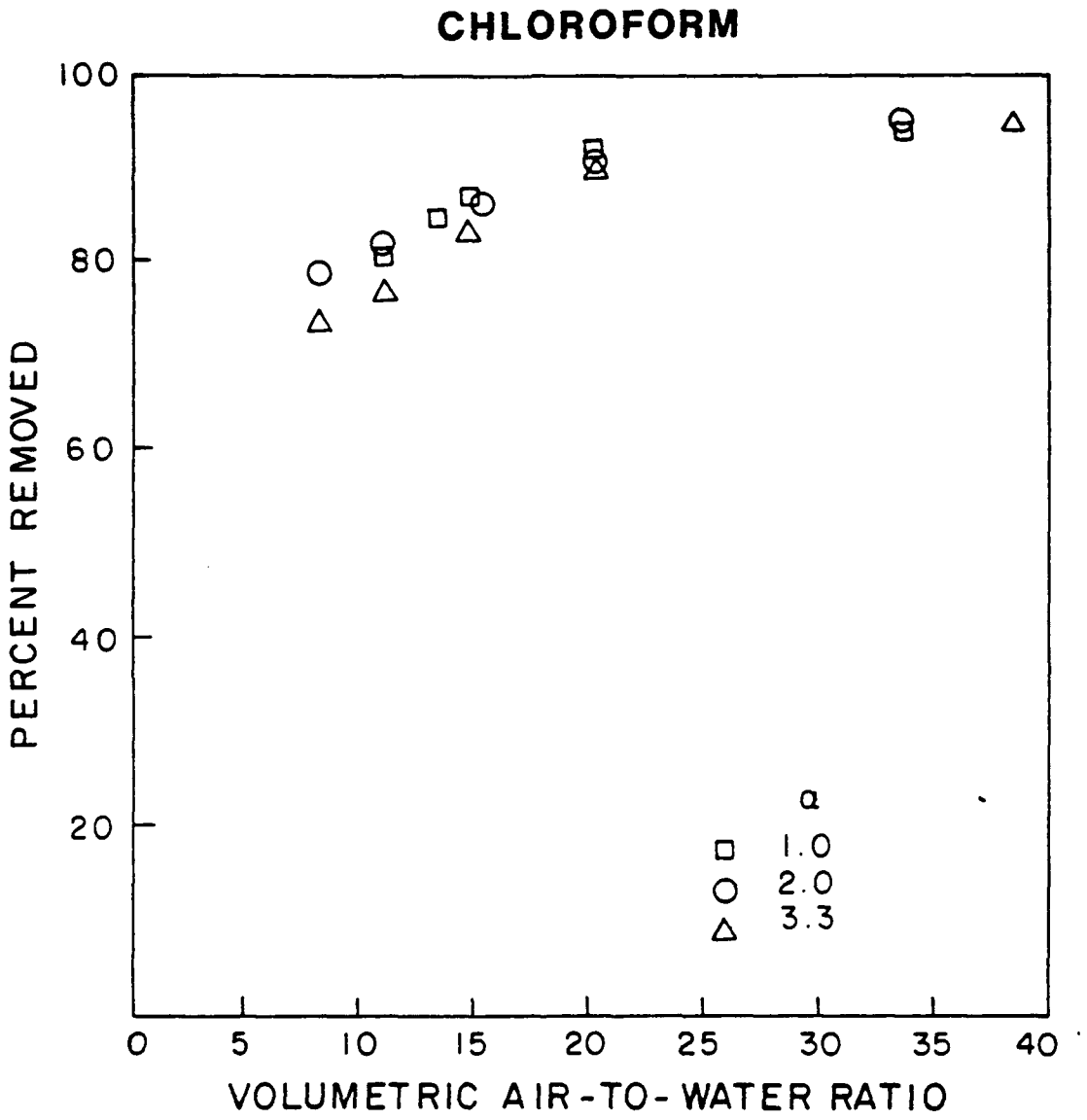

Figure 16. Percent Removal of Chloroform versus Volumetric Air-to-Water Ratio; G_m = 0.43 kg/m^{2}s.

tetrachloride with the largest liquid-phase resistance showed little improvement in efficiency at high G_m values (Figure 11) while DCA with the largest gas-phase resistance showed a large increase in E with increasing G_m values (Figure 10).

Figures 8-10 also show the countercurrent efficiencies for the three VOCs - chloroform, methylene chloride and 1,2-dichloroethane - under conditions of equal liquid loading rates as in the crossflow column. The total liquid flow rate in countercurrent operations was 5 gpm (0.018 m^3/min) as compared to 3.3 gpm (0.012 m^3/min) in the crossflow experiments, because the area for liquid flow in crossflow was only 65 percent of the countercurrent area. The total packed volume was kept the same in both cases by reducing the packed height. The results in Figures 8-10 show that the efficiencies were generally the same as those for the crossflow experiments. Countercurrent values were slightly larger than the crossflow values in certain cases, the differences being seldom larger than 1 or 2 percent. The effects of G/L at a constant L_m = 17.6 kg/m²·s were practically identical in both cases. These results show that for the 6-inch column, there was no loss of efficiency for crossflow compared to countercurrent operation. However, as will be discussed later, pressure drop considerations will allow the crossflow column to be operated over a much larger range of G/L as compared to countercurrent operation.

Figures 17-19 show the stripping efficiency for the 12-inch crossflow column at a liquid loading rate of L_m = 17.6 kg/m²·s. Though the L_m values were the same as for the 6-inch crossflow column, the liquid flow rate was four times higher since the area of the 12-inch column is 4 times larger. The efficiency values for methylene chloride, chloroform and carbon tetrachloride show the same response with increasing G/L as was observed for the smaller scale crossflow and countercurrent columns. In addition, the efficiency values for the 12-inch crossflow column were more or less similar to those for the other two cases. Since the amount of packing in the 12-inch case was more than 4 times larger than the 6-inch case, a slight improvement in stripping efficiency for the 12-inch crossflow column would be expected. Figure 20 shows the E values for the three VOCs at a L_m = 32 kg/m²·s in the 12-inch column. Once again the efficiencies were similar to those for the equivalent liquid loading rate in the 6-inch column. The G/L values at a constant L_m = 32 kg/m^2·s were all at conditions that would be expected to flood a 12-inch countercurrent column. In constrast, the crossflow column operated under such conditions without serious loss of stripping efficiency.

The experimental values of mass transfer coefficient, $K_\ell a$, calculated using the E values obtained on the 6-inch column and using Equation (11) are shown in Figures 21-24 for L_m = 17.6 kg/m²·s and varying G_m values. Figures 25 and 26 show $K_\ell a$ versus G_m at L_m = 32 kg/m²·s for chloroform and methylene chloride. The effect of changing L_m values at constant G_m = 0.43 kg/m²·s on the mass transfer coefficient for chloroform is shown in Figure 27. A comparison of $K_\ell a$ values for the four VOCs at an α value of 2.0 for the 6-inch column is shown in Figure 28.

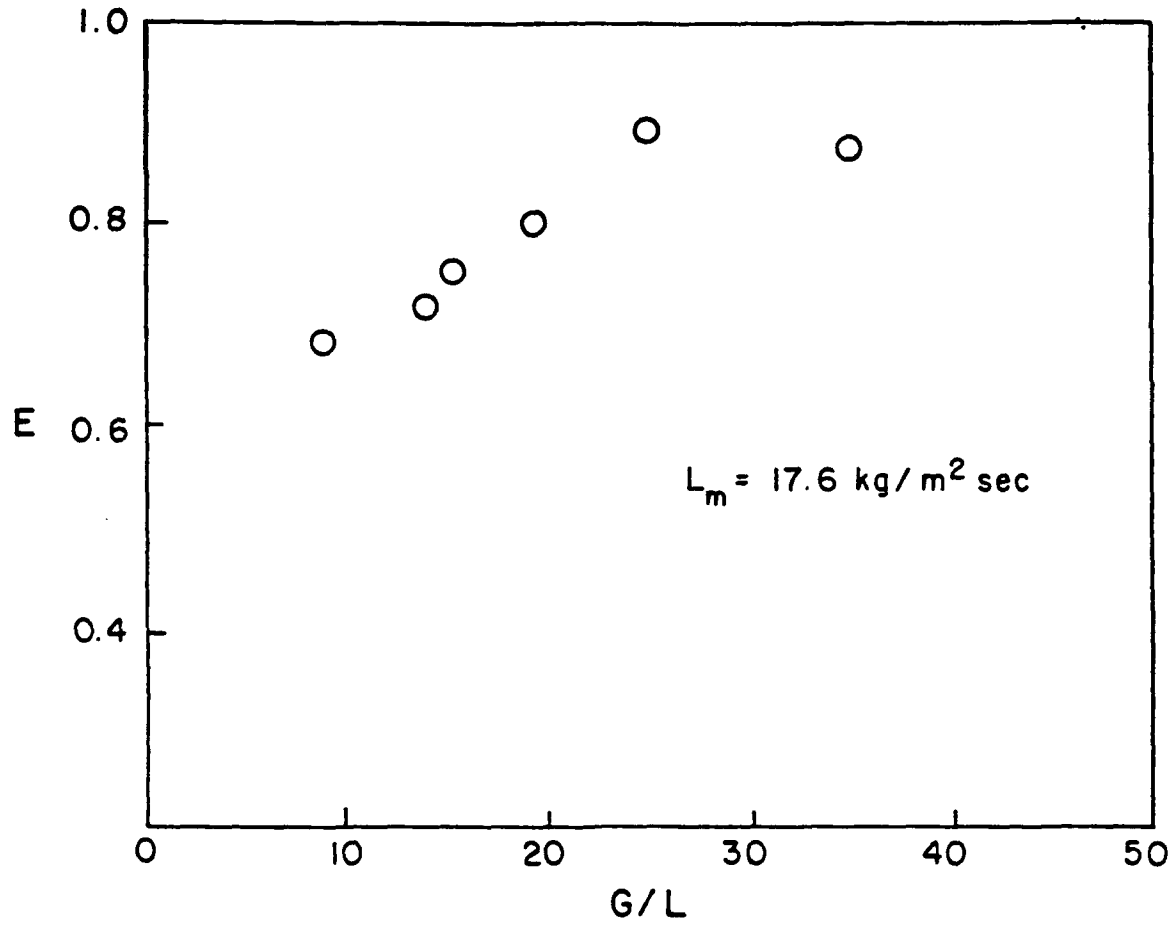

Figure 17. Percent Removal of Methylene Chloride at L_m = 17.6 $kg/m^2.s$ on the 12-Inch Pilot-Scale Column.

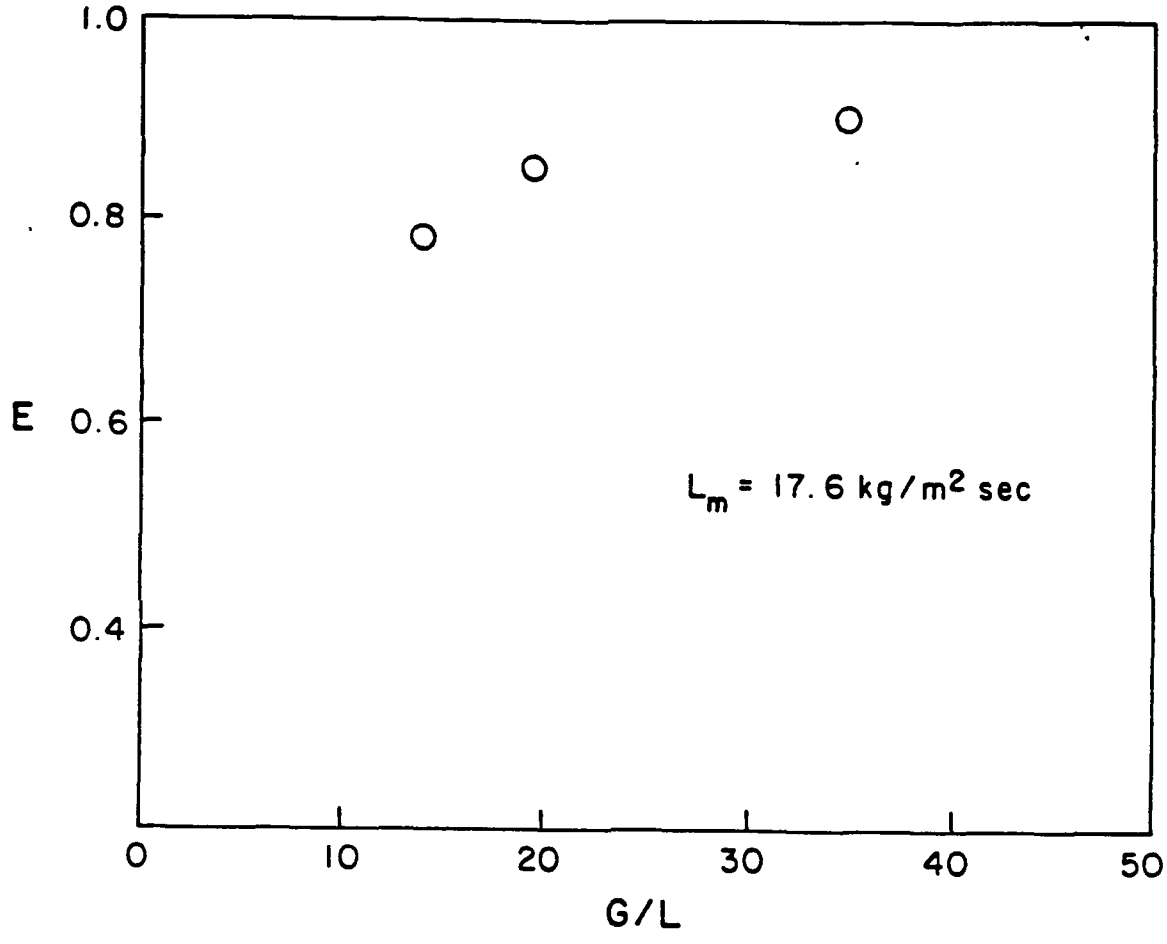

Figure 18. Percent Removal of Chloroform at L_m = 17.6 kg/m^2·s on the 12-Inch Pilot-Scale Column.

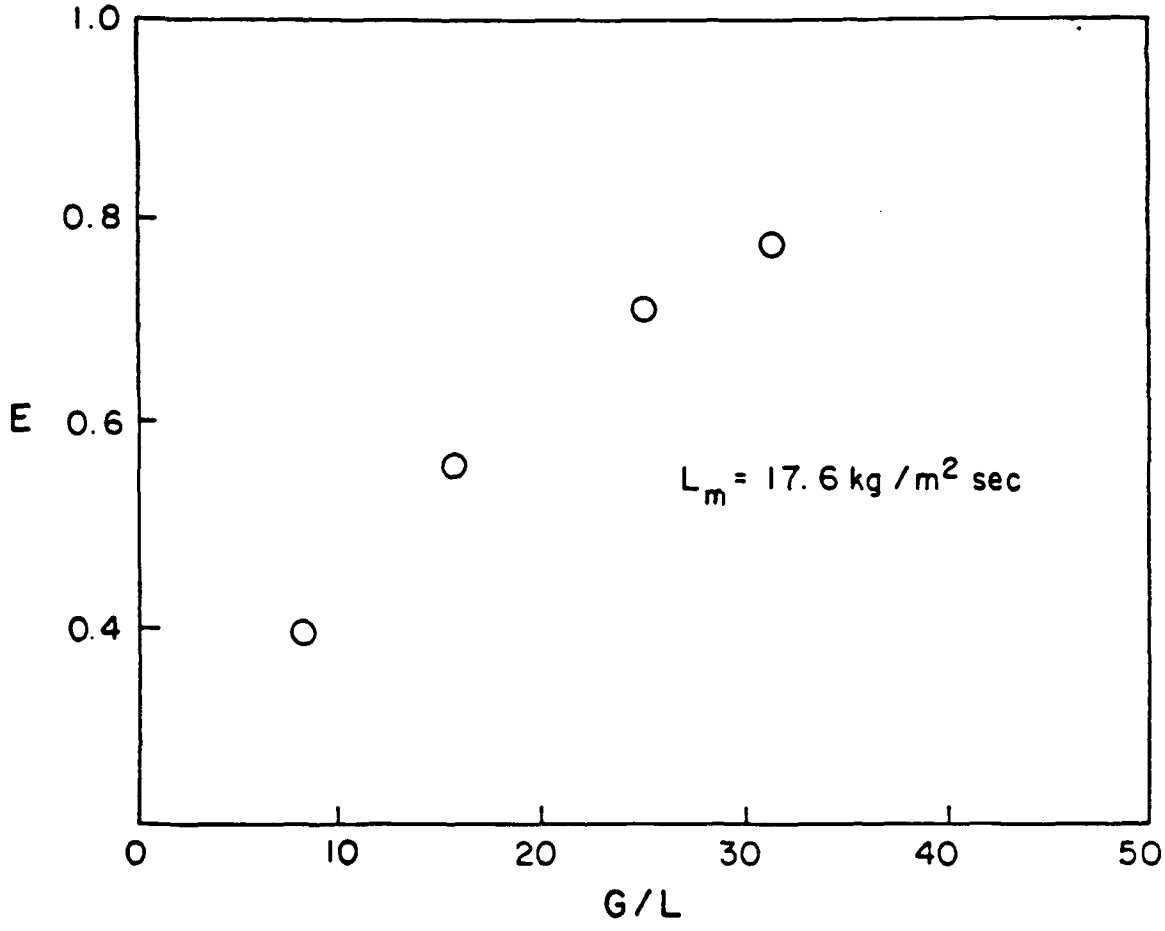

Figure 19. Percent Removal of 1,2-Dicholorethane at L_m = 17.6 $kg/m^2 \cdot s$ on the 12-Inch Pilot-Scale Column.

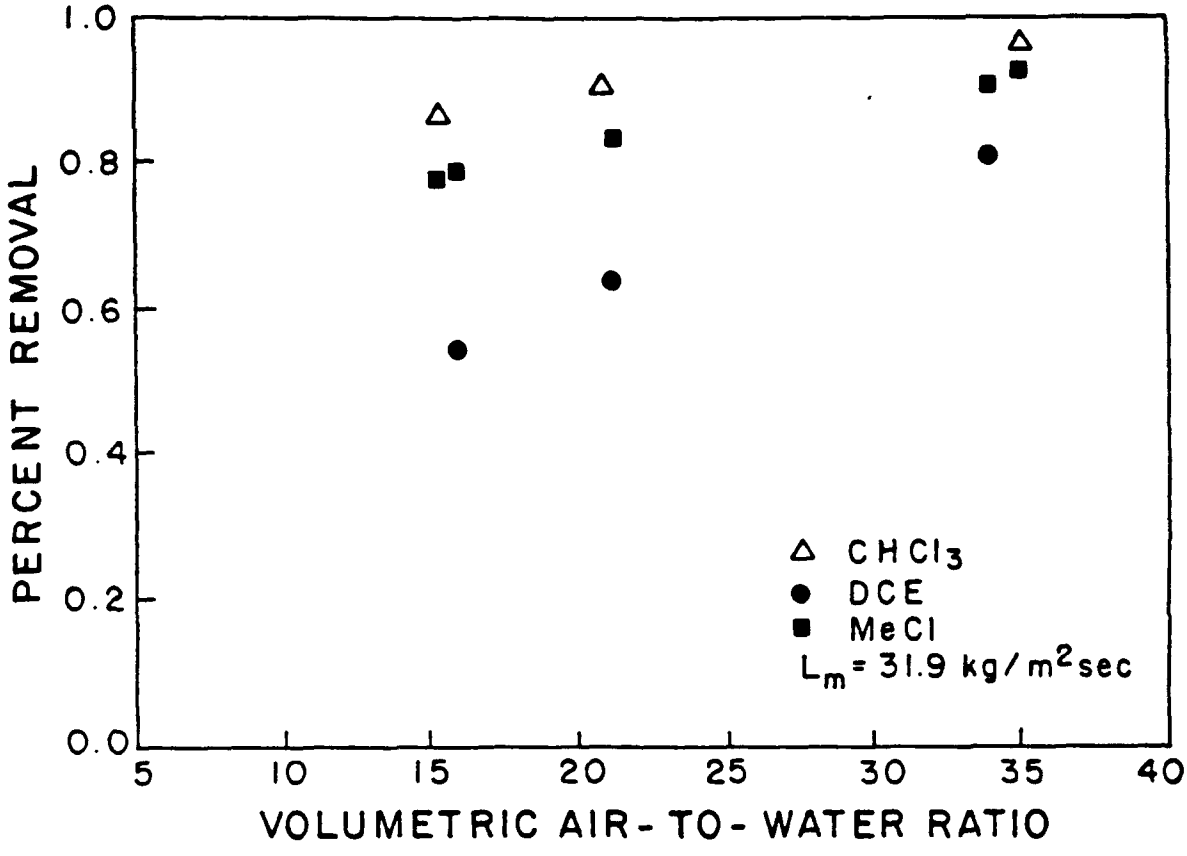

Figure 20. Percent Removal of Chloroform, Methylene Chloride and 1,2-Dichloroethane at L_m = 31.9 kg/m^2·s on the 12-Inch Pilot-Scale Column.

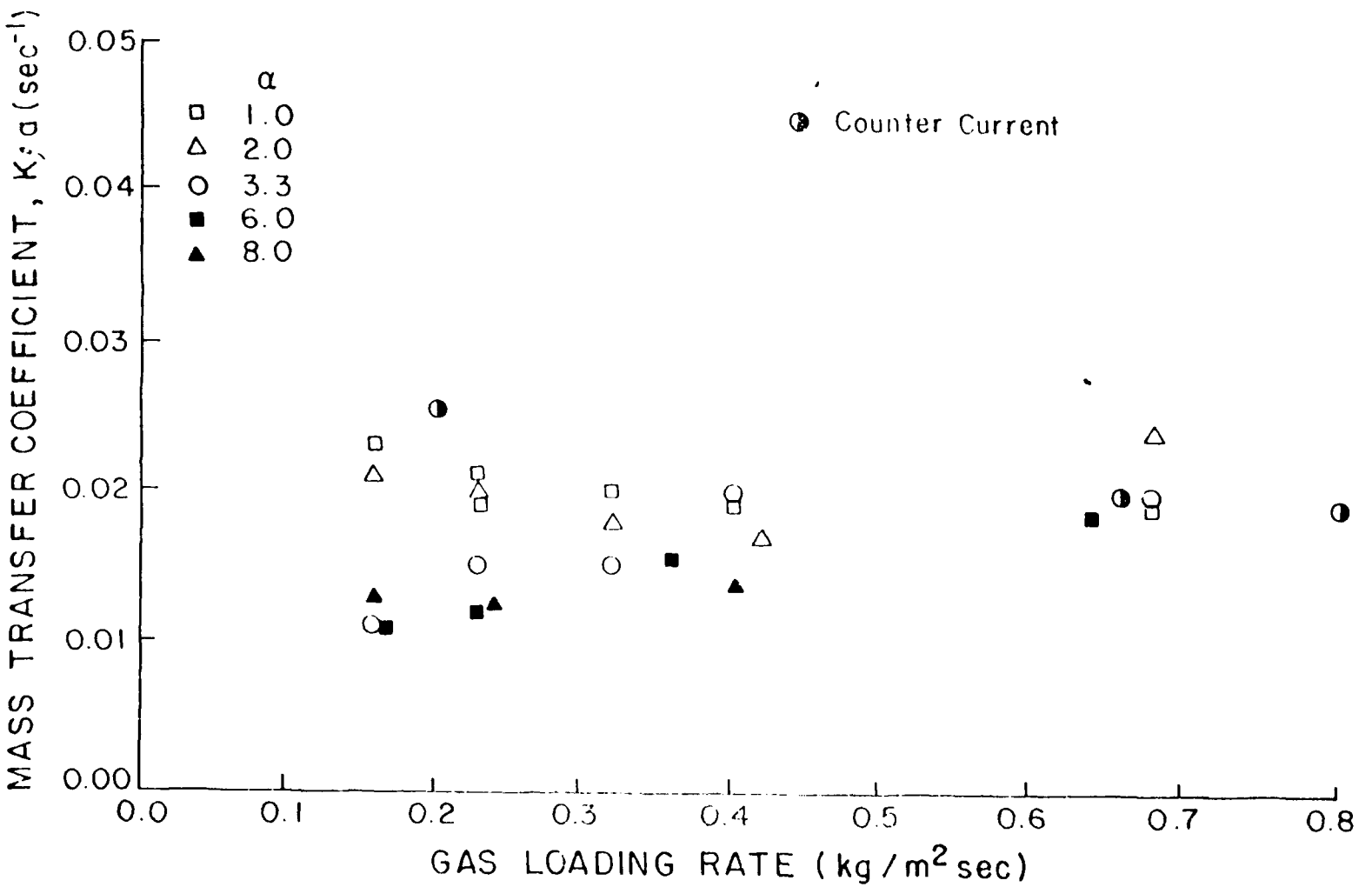

Figure 21. Methylene Chloride Mass Transfer Coefficient versus Gas Loading; Liquid Loading = 17.6 kg/m^{2}s.

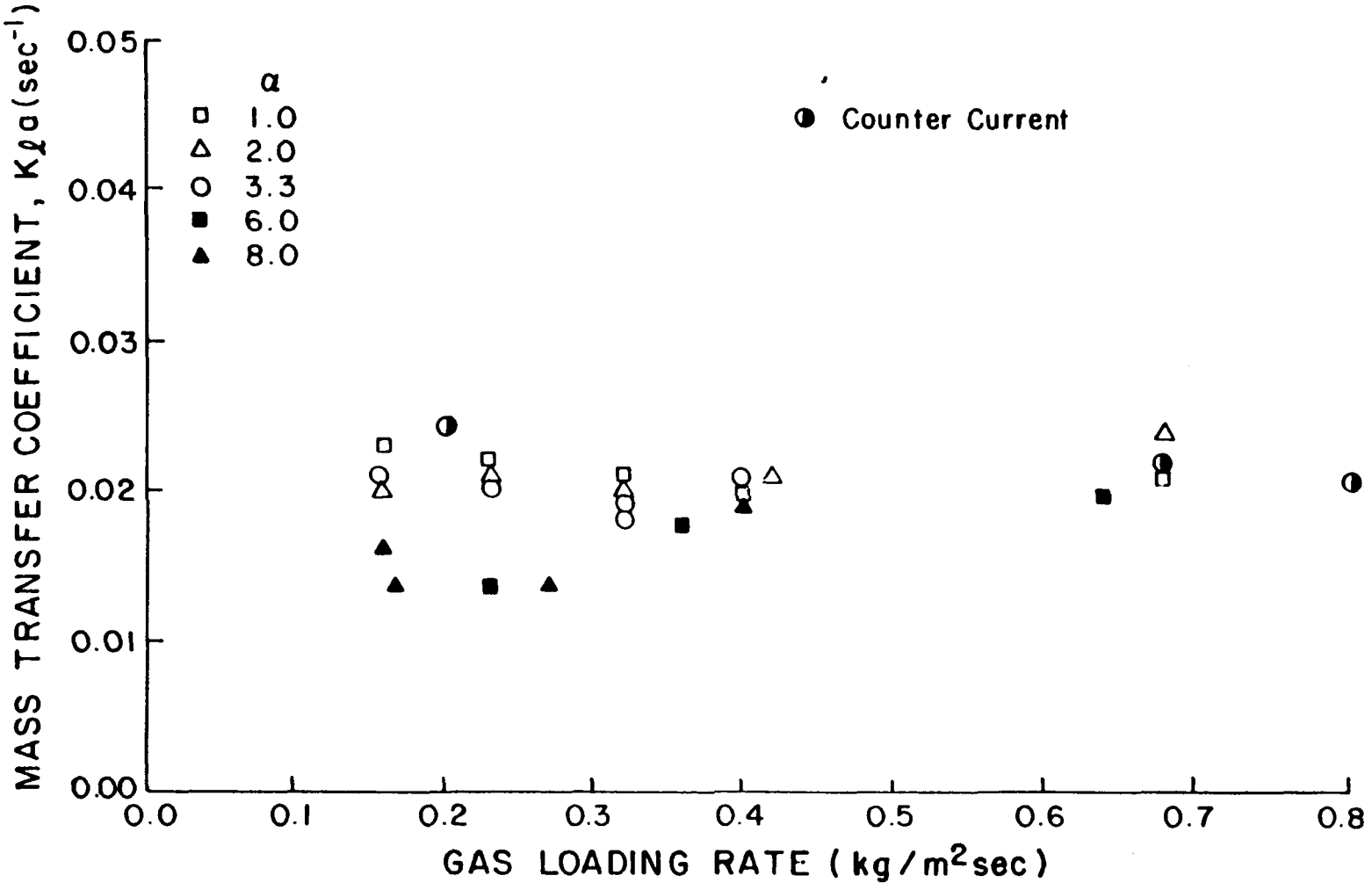

Figure 22. Chloroform Mass Transfer Coefficient versus Gas Loading; Liquid Loading = 17.6 kg/m^2s.

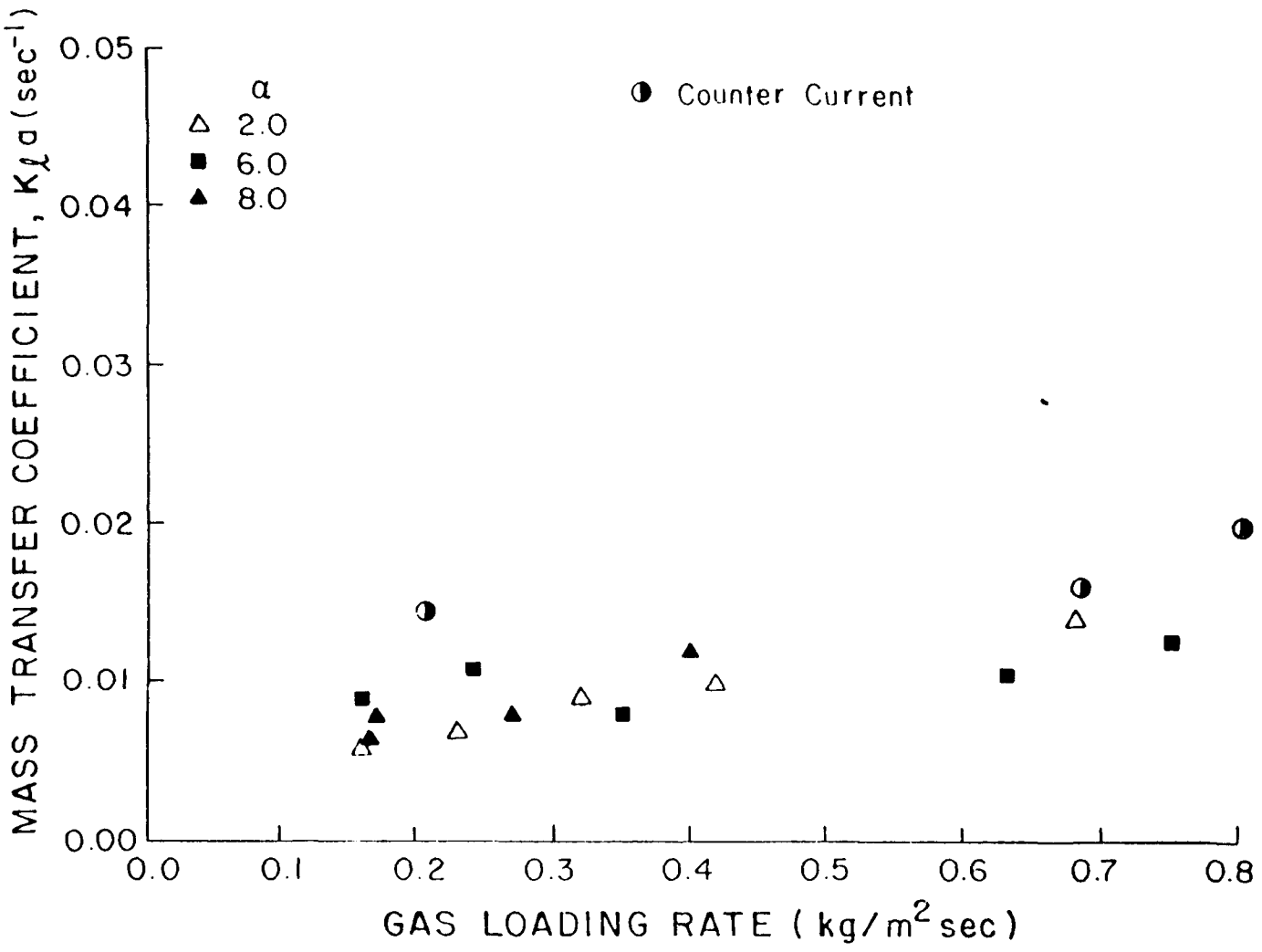

Figure 23. 1,2-Dichloroethane Mass Transfer Coefficient versus Gas Loading; Liquid Loading = 17.6 kg/m² s.

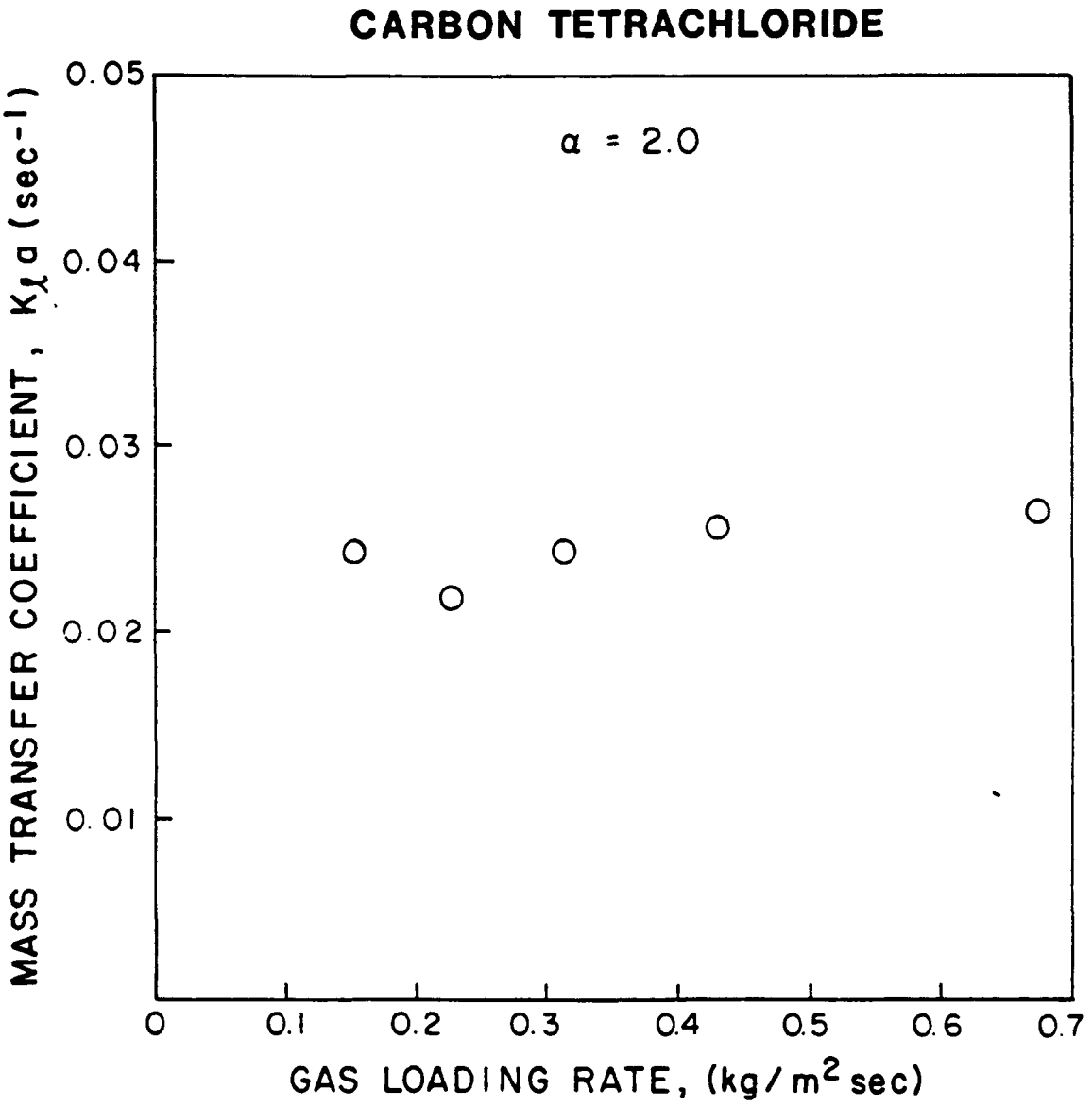

Figure 24. Carbon Tetrachloride Mass Transfer Coefficient versus Gas Loading; L_m = 17.6 kg/m^{2}s.

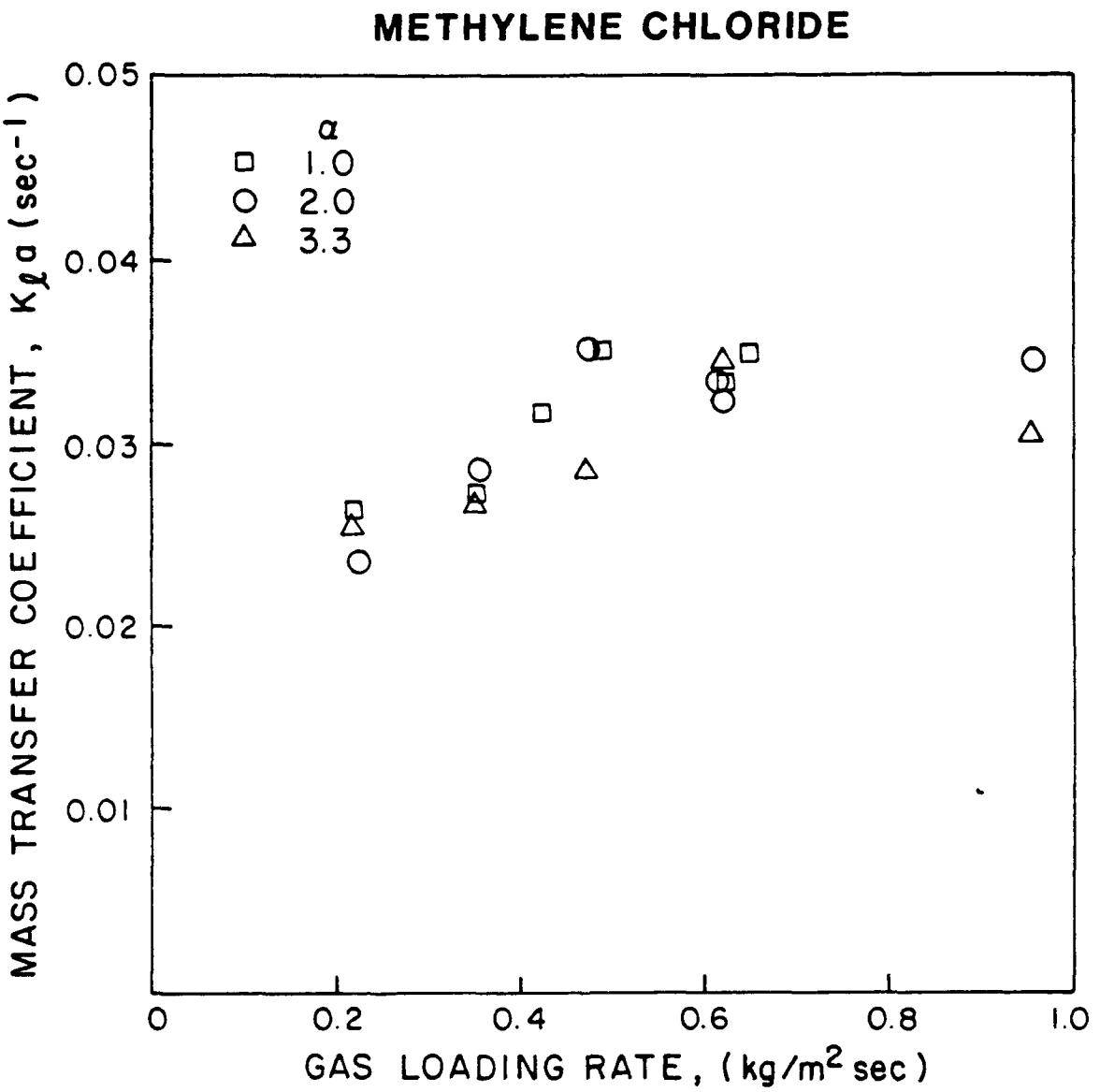

Figure 25. Methylene Chloride Mass Transfer Coefficient versus Gas Loading Rate; L_m = 32.0 $kg/m^2 s$.

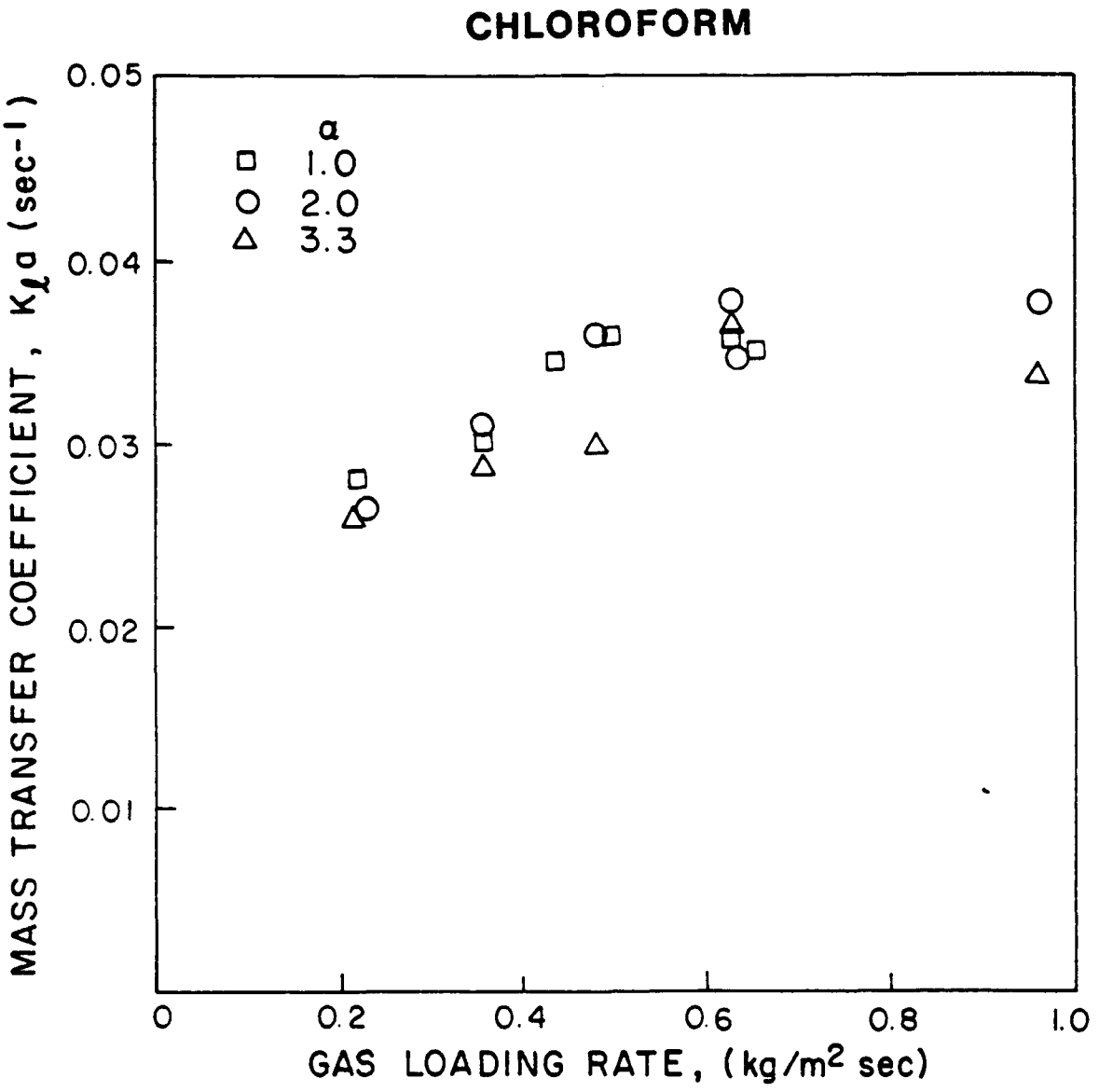

Figure 26. Chloroform Mass Transfer Coefficient versus Gas Loading Rate; L_m = 32.0 $kg/m^2 s$.

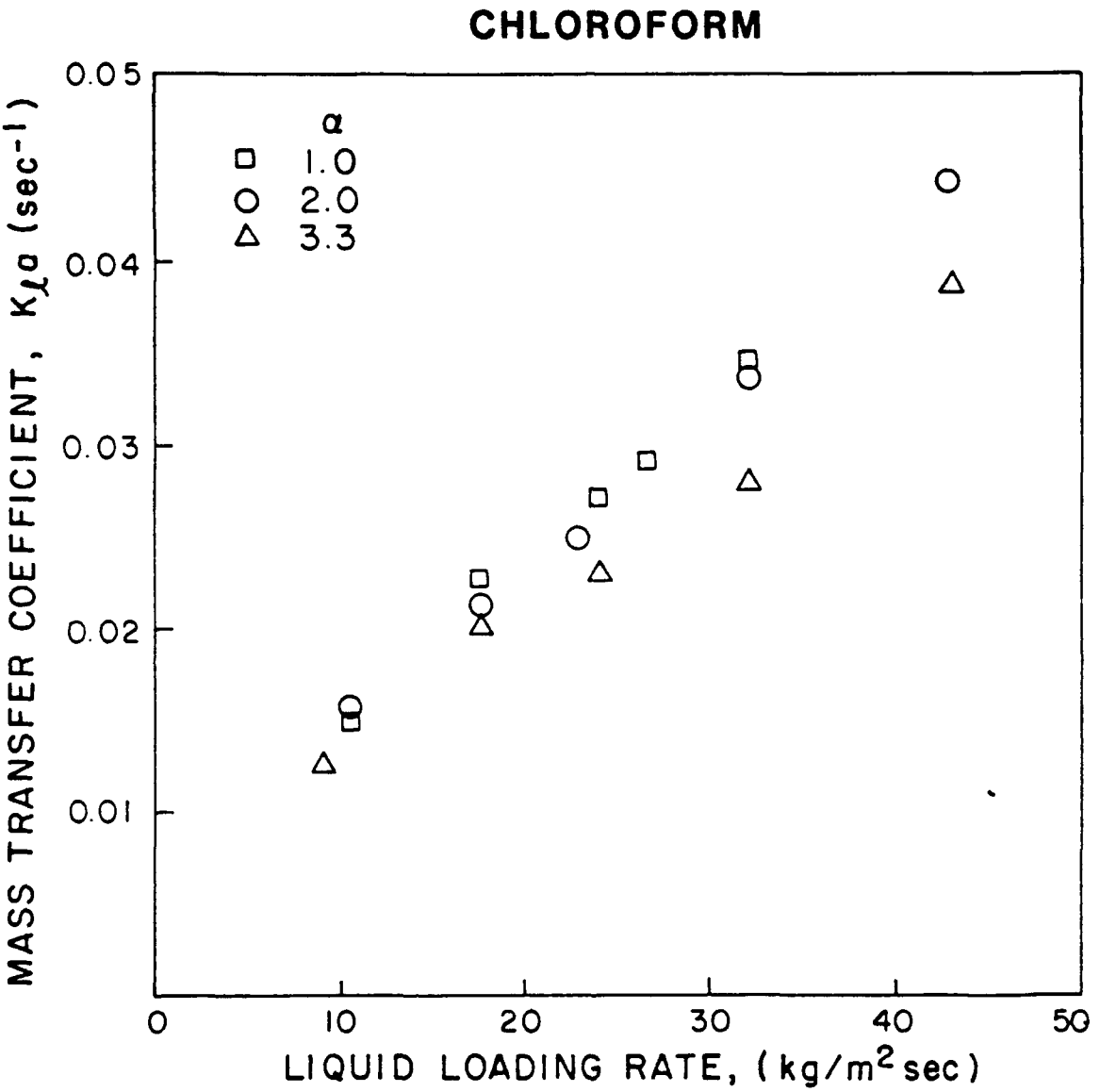

Figure 27. Chloroform Mass Transfer Coefficient versus Liquid Loading Rate; G_m = 0.43 kg/m^{2}s.

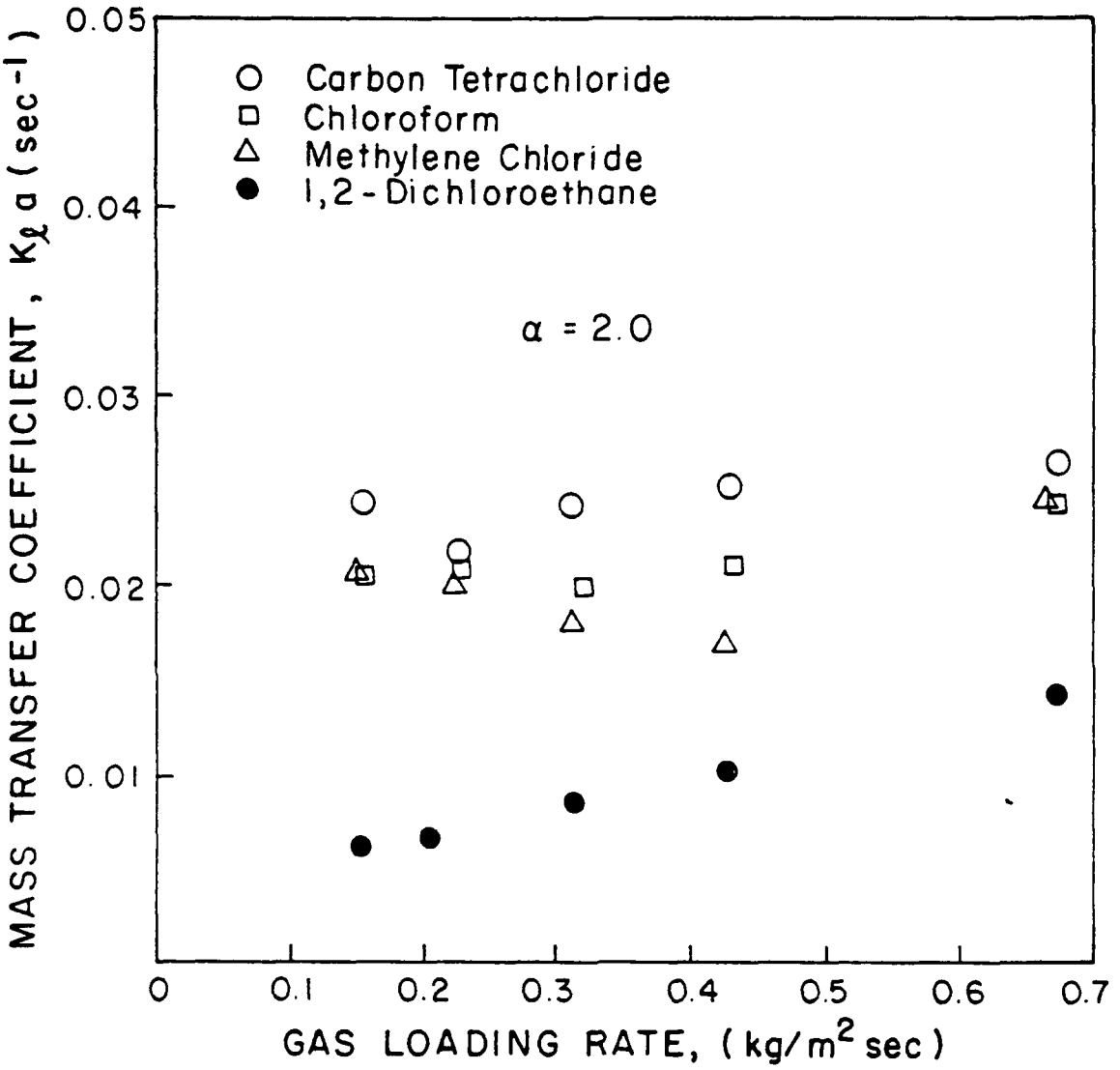

Figure 28. Mass Transfer Coefficients versus Gas Loading Rate; L_m = 17.6 $kg/m^2 s$.

The effect of gas flow rate on mass transfer coefficient varied among the four VOCs studied. As shown in Figure 28, the $K_\ell a$ values for carbon tetrachloride, chloroform and methylene chloride were nearly independent of gas loading rate. The least volatile compound 1,2-DCA showed a significant dependence on gas loading. These findings are consistent with the two resistance model, which predicts increased gas phase resistance (increased dependence on G_m) as H_c values decrease (at constant G_m and L_m).

The dependence of $K_\ell a$ on G_m for methylene chloride and chloroform were different at L_m = 32 kg/m²·s (Figures 25 and 26) as compared to L_m = 17.6 kg/m²·s (Figures 21 and 22). The $K_\ell a$ values were constant over most of the range of gas loadings studied at L_m = 17.6 kg/m²·s, while at L_m = 32 kg/m²·s, $K_\ell a$ values were constant at high gas loadings but decreased at low G_m. Increasing the liquid loading rate should increase the liquid phase mass transfer coefficient, k_ℓ, according to Onda's model. According to the two resistance theory of mass transfer, increasing k_ℓ reduces the liquid phase resistance (R_ℓ) while the gas phase resistance (R_g) remains unchanged. Thus R_g contributes more to the overall resistance, in agreement with the experimental observation.

The effect of α on the mass transfer coefficients was small at high G_m values. Generally we observed slightly lower $K_\ell a$ values at higher α values. However these differences were less than 5 percent and should be considered within the experimental error in the estimation of $K_\ell a$. At the low values of G_m, $K_\ell a$ decreased with increased baffle spacing (α) which may be due to decreased gas velocity through the packing. This effect is more important at low G_m values and is insignificant at high G_m, especially for those compounds which have their predominant resistance to mass transfer in the liquid phase. The dependence of $K_\ell a$ on L_m at constant G_m was nearly linear (Figure 27) as was observed by other workers (Reference 21) using conventional countercurrent columns.

The mass transfer coefficients calculated from the 6-inch countercurrent column are shown in Figures 21-23 for an equivalent L_m = 17.6 kg/m²·s. These values were within the range of values observed for various α values in the 6-inch crossflow column. The same general dependence on G_m was observed in the countercurrent operation as was seen for the crossflow column. The $K_\ell a$ values were higher for chloroform than for methylene chloride and 1,2-dichloroethane in the countercurrent tower, in agreement with the extensive work on countercurrent mass transfer coefficients by other groups of researchers (References 21 and 22). We conclude from these results that crossflow operation even at large α maintains the mass transfer efficiency of a countercurrent operation but with the added advantages of reduced pressure drop and greater ranges of gas to liquid ratio resulting in stable operation.

The mass transfer coefficients for the 12-inch crossflow column are shown in Figures 29 and 30 for two liquid loading rates of 17.6 and 32 kg/m²·s. These values also were constant at high G_m values for a particular L_m value and showed a slight decrease at low G_m. The values were higher for the more volatile compound. Although baffle spacing was fixed at α = 2.6 for the 12-inch column, we would assume that just as

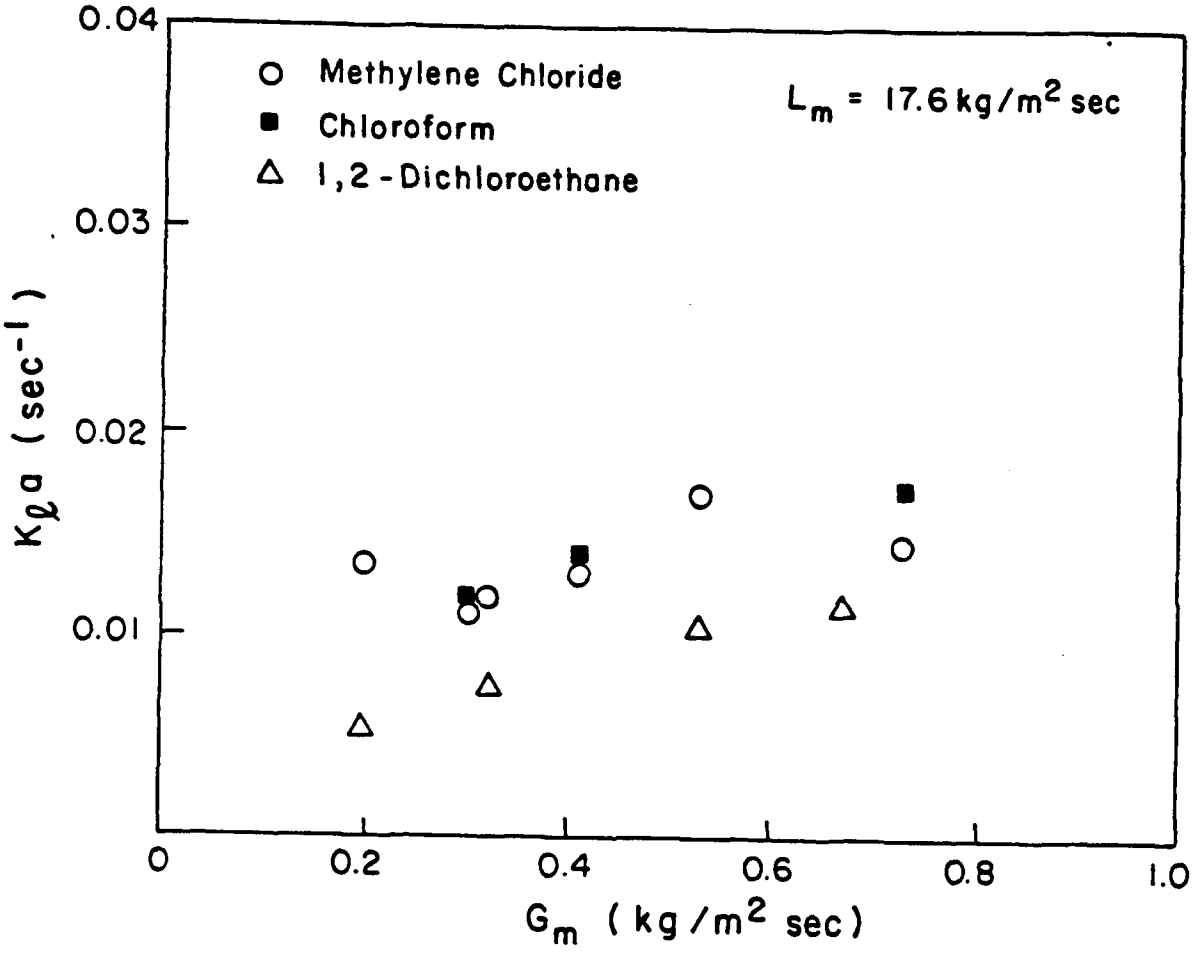

Figure 29. Mass Transfer Coefficients Versus Gas Loading Rates at L_m = 17.6 kg/m^2·s on the 12-Inch Pilot-Scale Column.

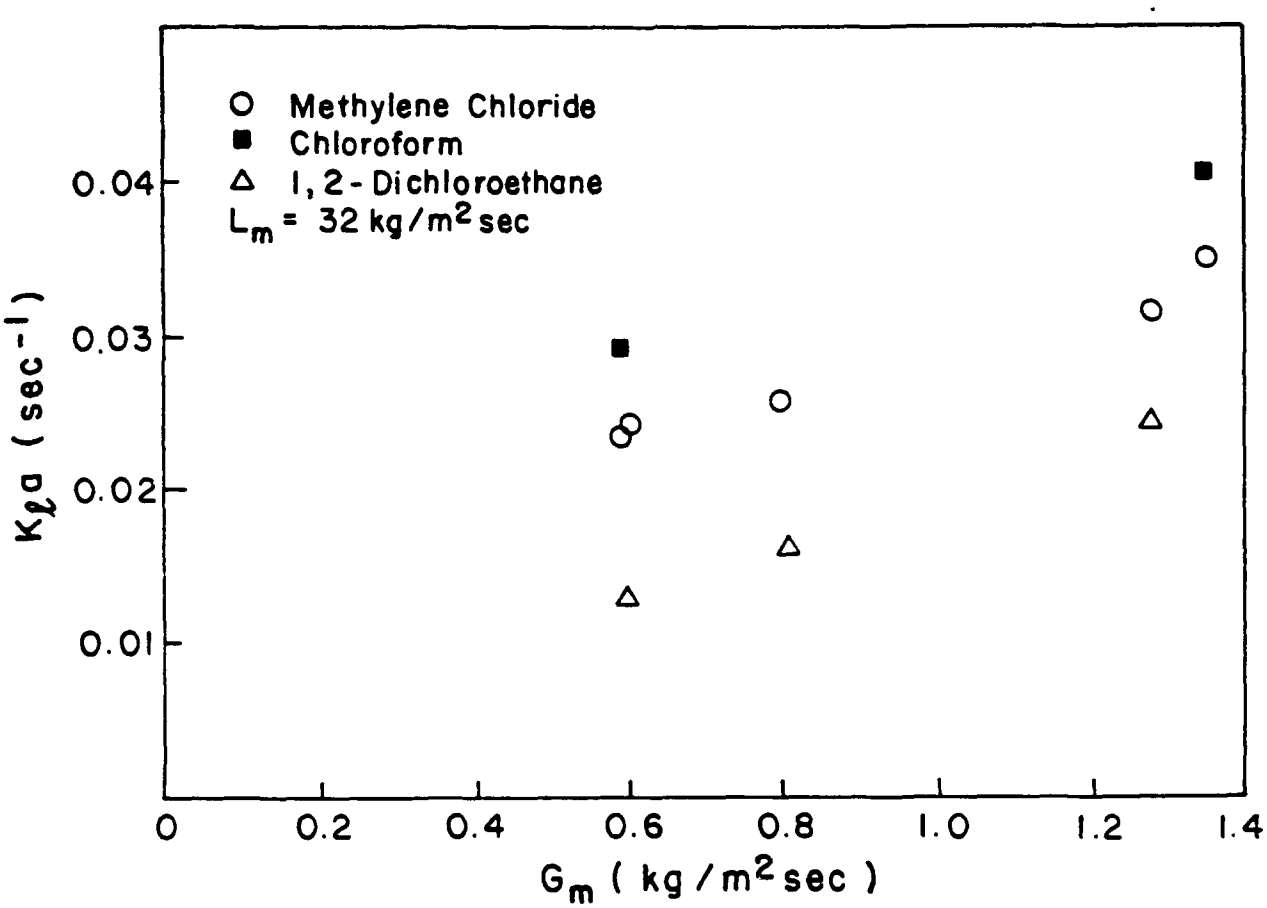

Figure 30. Mass Transfer Coefficients Versus Gas Loading Rates at L_m = 32 kg/m^2.s on the 12-Inch Pilot-Scale Column.

for the 6-inch column, the dependence on α should be marginal. However, the surprising result that we observed was a general decrease in $K_\ell a$ as compared to the equivalent operation in the 6-inch column. The values for the 12-inch column were in most cases 20-30 percent lower than those for the 6-inch column, even though the efficiencies were similar. Whether this is a result of decreasing gas-liquid crossflow contact efficiency with increasing column diameter is unknown at the present time.

E. EVALUATION OF MASS TRANSFER CORRELATIONS

As described earlier, four different mass transfer correlations were tested. They were:

1. Cornell's correlation, Equation (15) with Equation (18) for a_ℓ
2. Shulman's correlation, Equations (16) and (17) with Equation (18) for a_ℓ
3. Onda's correlation, Equations (19) and (20) with Equation (21) for a_w
4. Onda's correlation, Equations (19) and (20) with Equation (22) for a_w, which we call modified Onda.

Since in crossflow operation we have the additional variable α to contend with, the correlations were all modified slightly. It was assumed that the crossflow operation does not significantly alter the values of k_ℓ but that the change in α will affect the gas phase velocity and hence the gas phase mass transfer coefficient, k_g. The results described earlier showed the effect to be marginal except for 1,2-DCA which had a larger gas-phase resistance at low gas loadings. However, we made minor modifications in the gas-phase coefficients in both Onda's and Shulman's correlations with the hope of better predicting the k_g values for such compounds. With increasing α, the area for gas flow, A_g, increases and correspondingly G_m decreases and hence causes k_g to decrease. Therefore increasing α for a given set of operating conditions should decrease the overall $K_\ell a$. However, at high gas rates for most volatile organic compounds, the contribution of k_g to $K_\ell a$ is only marginal and hence incorporating α in the correlation should have little or no effect. This correction will be important only for low volatile compounds.

The $K_\ell a$ values obtained using the four different correlations were compared with the experimental values as parity plots. These are shown in Figures 31-40 for all the VOCs studied. The solid diagonal line in each case represents perfect agreement while the dashed lines represent ±30 percent and ±20 percent deviations between predicted and observed values.

Figures 31 and 32 show that the modified Onda correlation is capable of predicting $K_\ell a$ values for both methylene chloride and chloroform at α = 1.0, 2.0 and 3.3 to within ±20 percent, which is about the accuracy claimed by Onda for his $K_\ell a$ correlation. For methylene

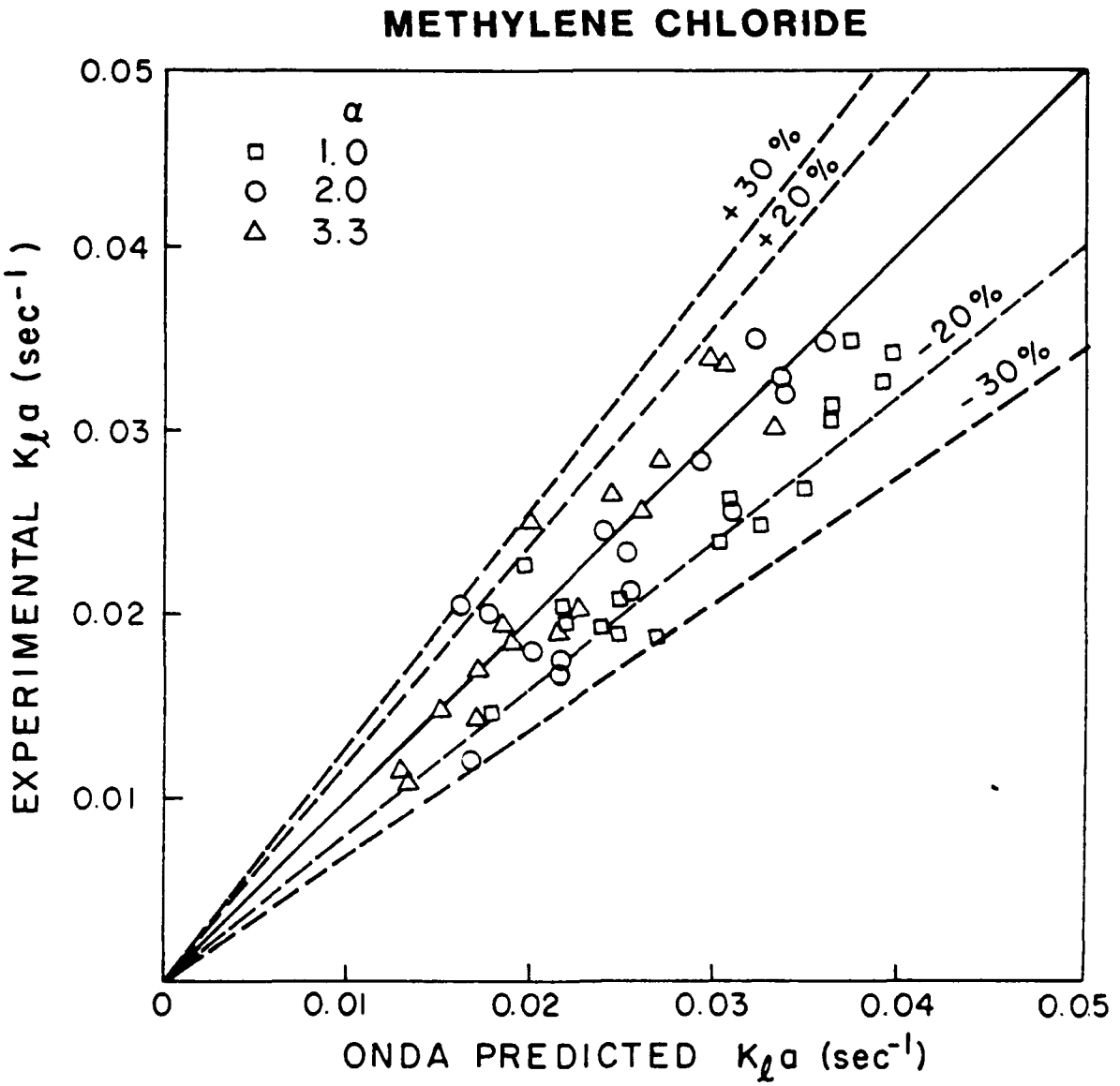

Figure 31. Modified Onda Predicted $K_l a$ versus Experimental $K_l a$; Methylene Chloride.

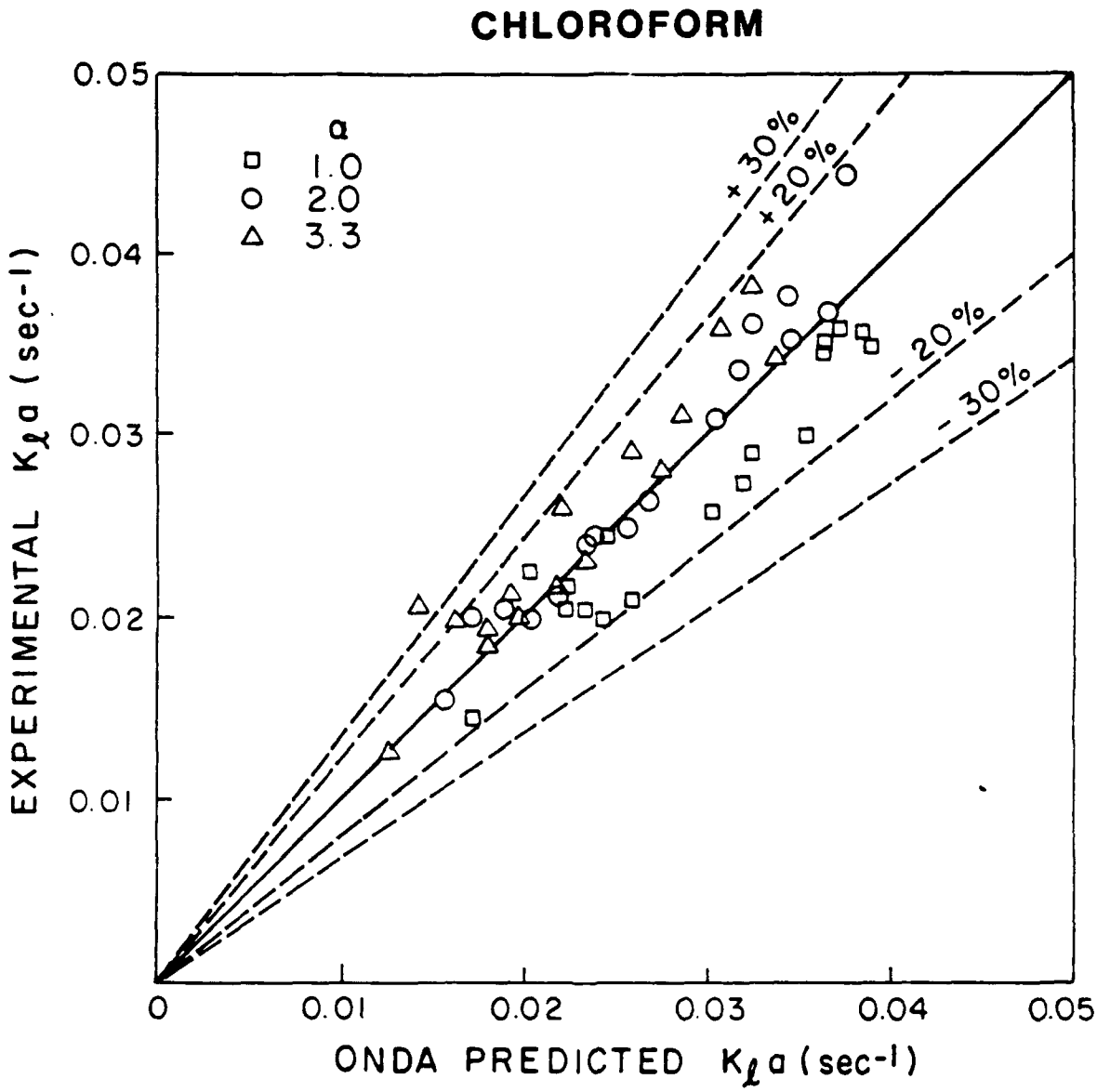

Figure 32. Modified Onda Predicted $K_l a$ versus Experimental $K_l a$; Chloroform.

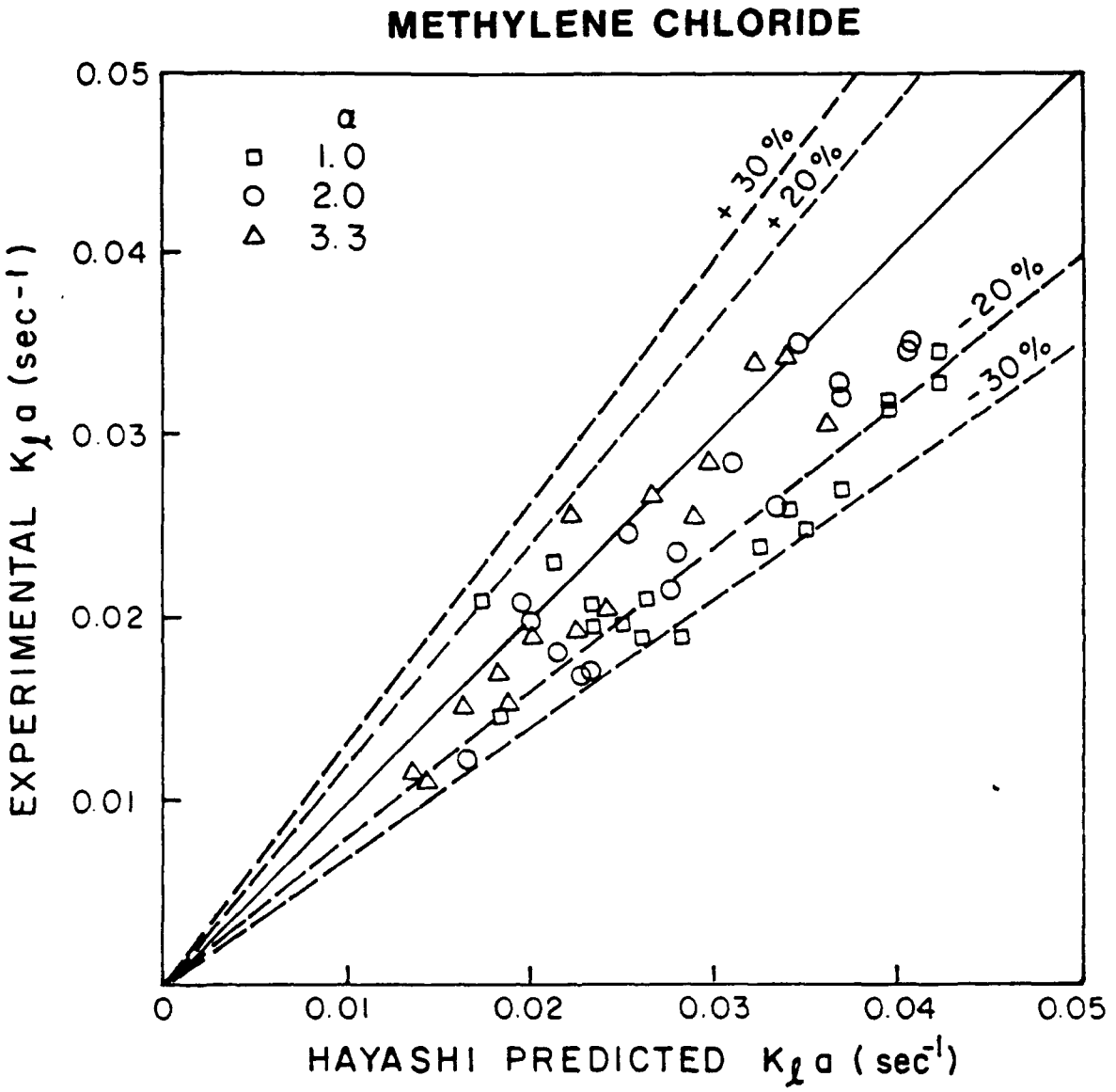

Figure 33. Experimental $K_l a$ versus Modified Onda/Hayashi $K_l a$; Methylene Chloride.

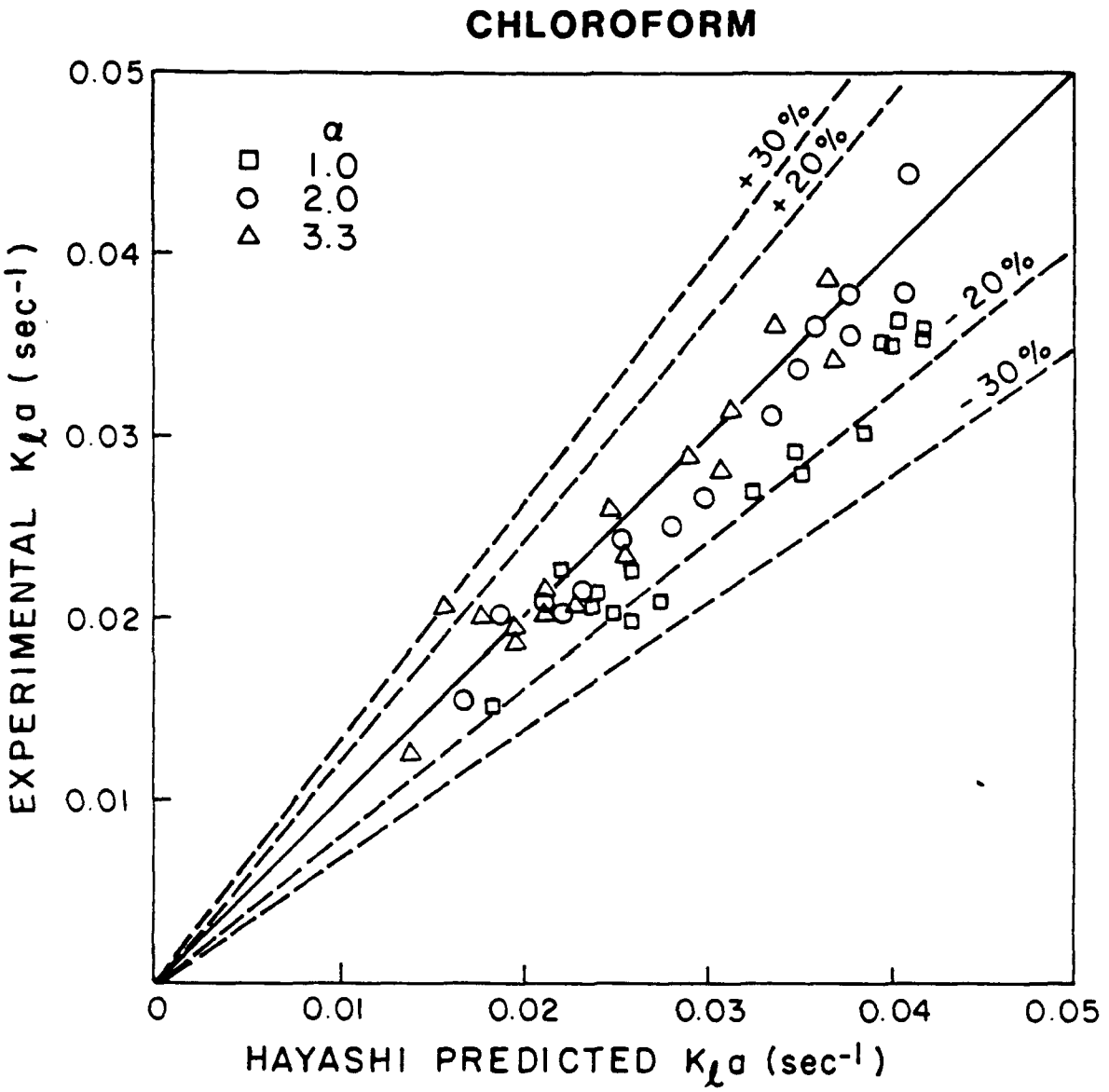

Figure 34. Experimental $K_l a$ versus Modified Onda/Hayashi $K_l a$; Chloroform.

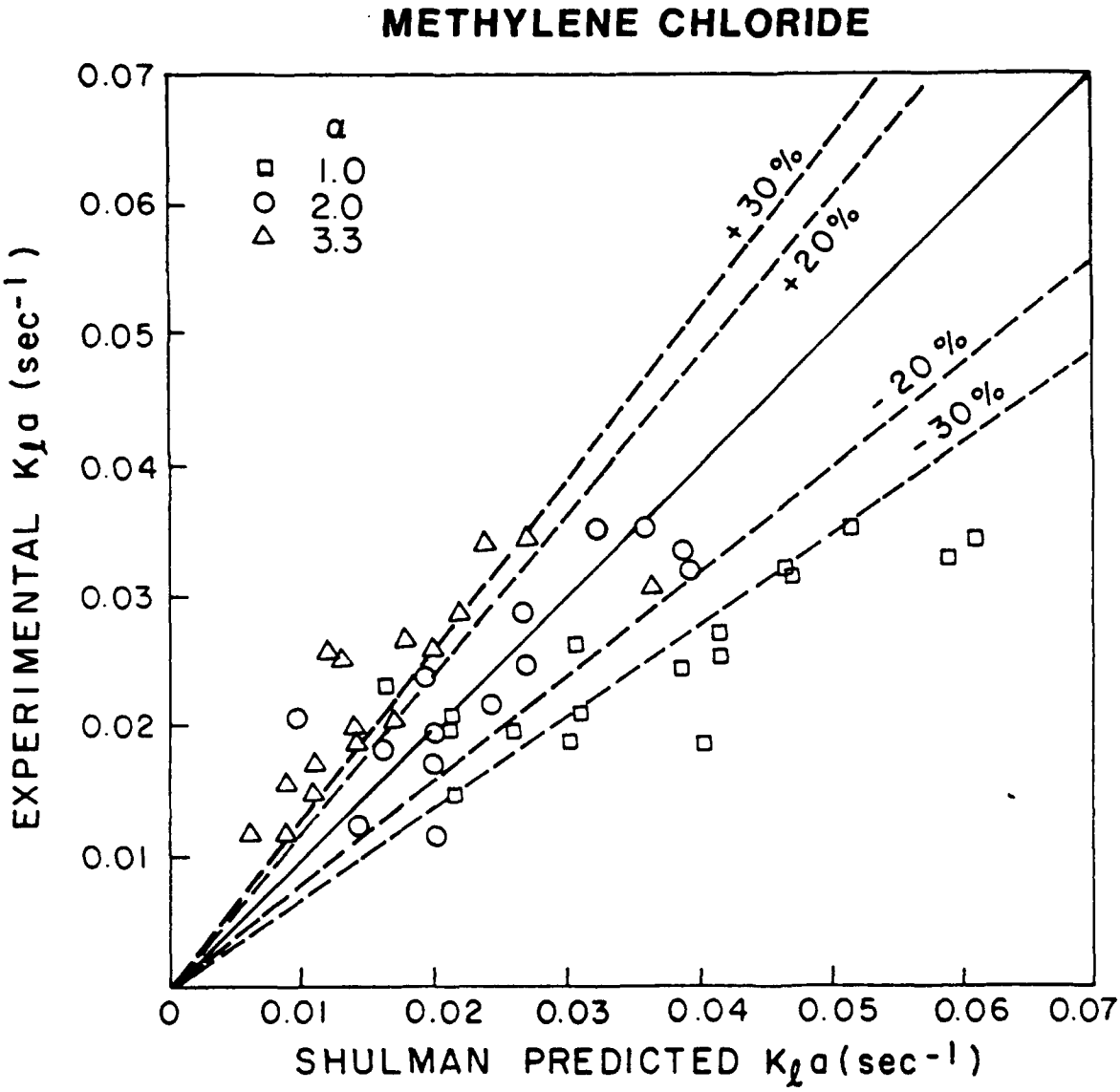

Figure 35. Experimental $K_l a$ versus Modified Shulman $K_l a$; Methylene Chloride.

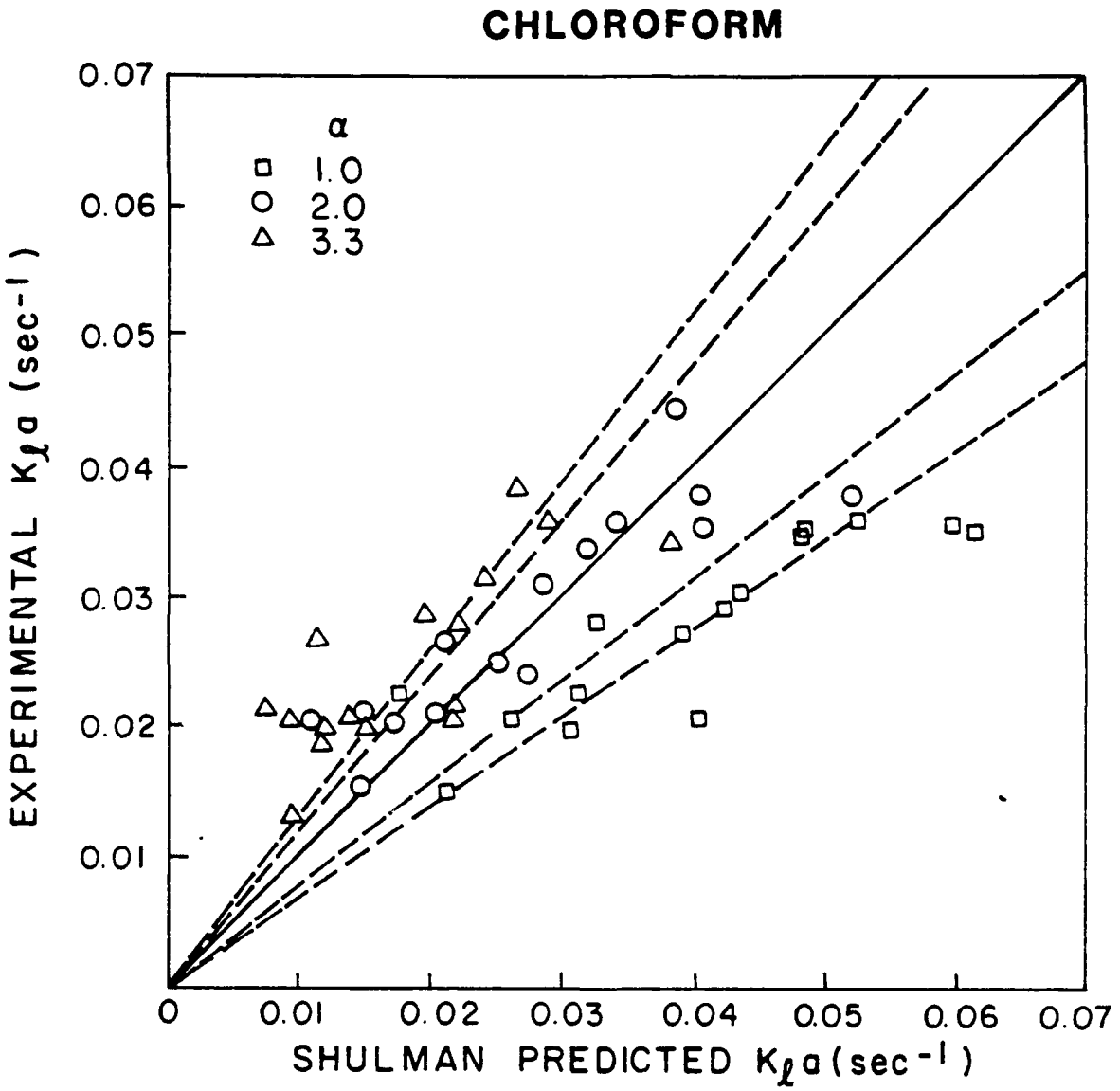

Figure 36. Experimental $K_l a$ versus Modified Shulman $K_l a$; Chloroform.

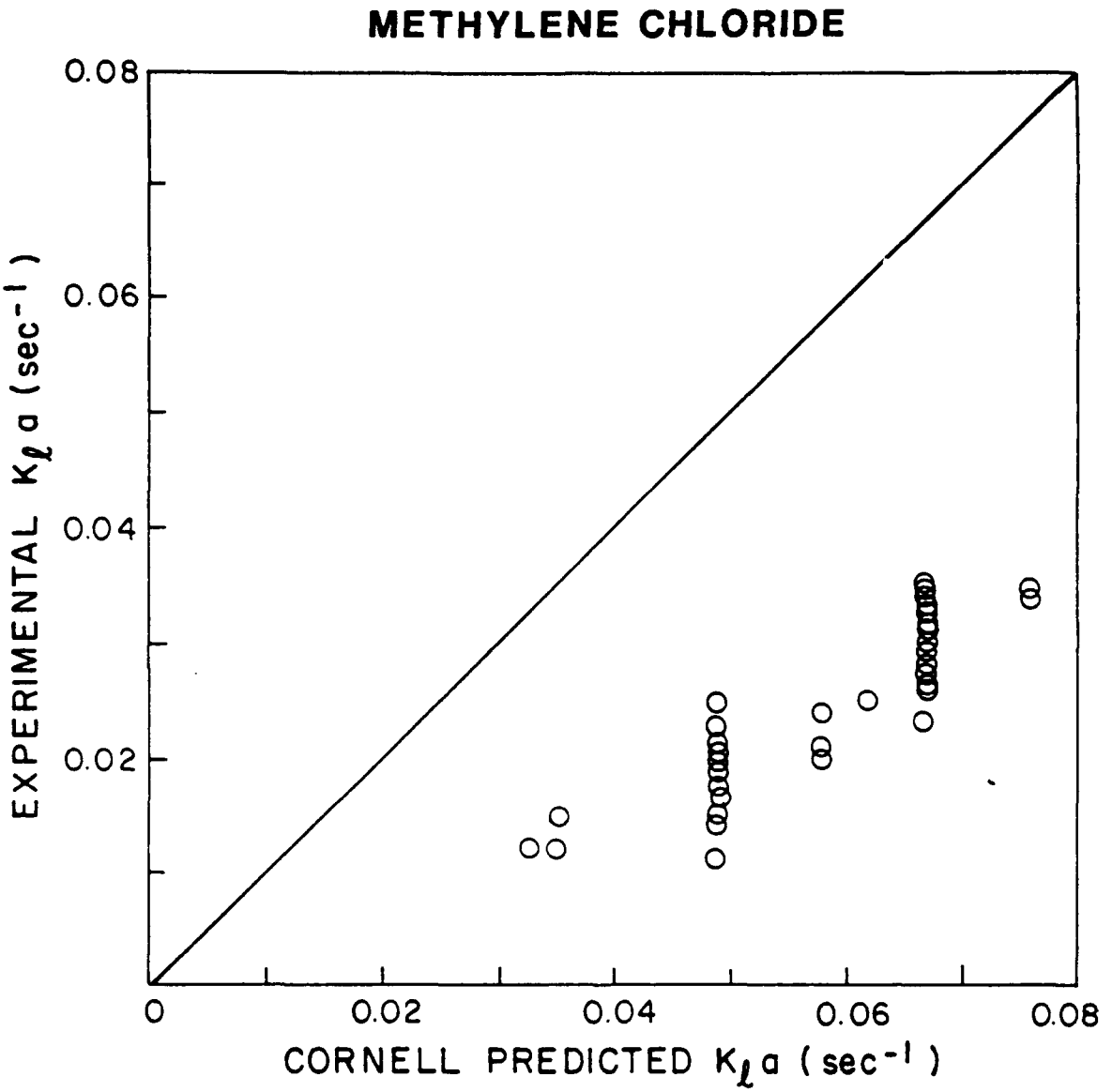

Figure 37. Experimental $K_l a$ versus Cornell Predicted $K_l a$; Methylene Chloride.

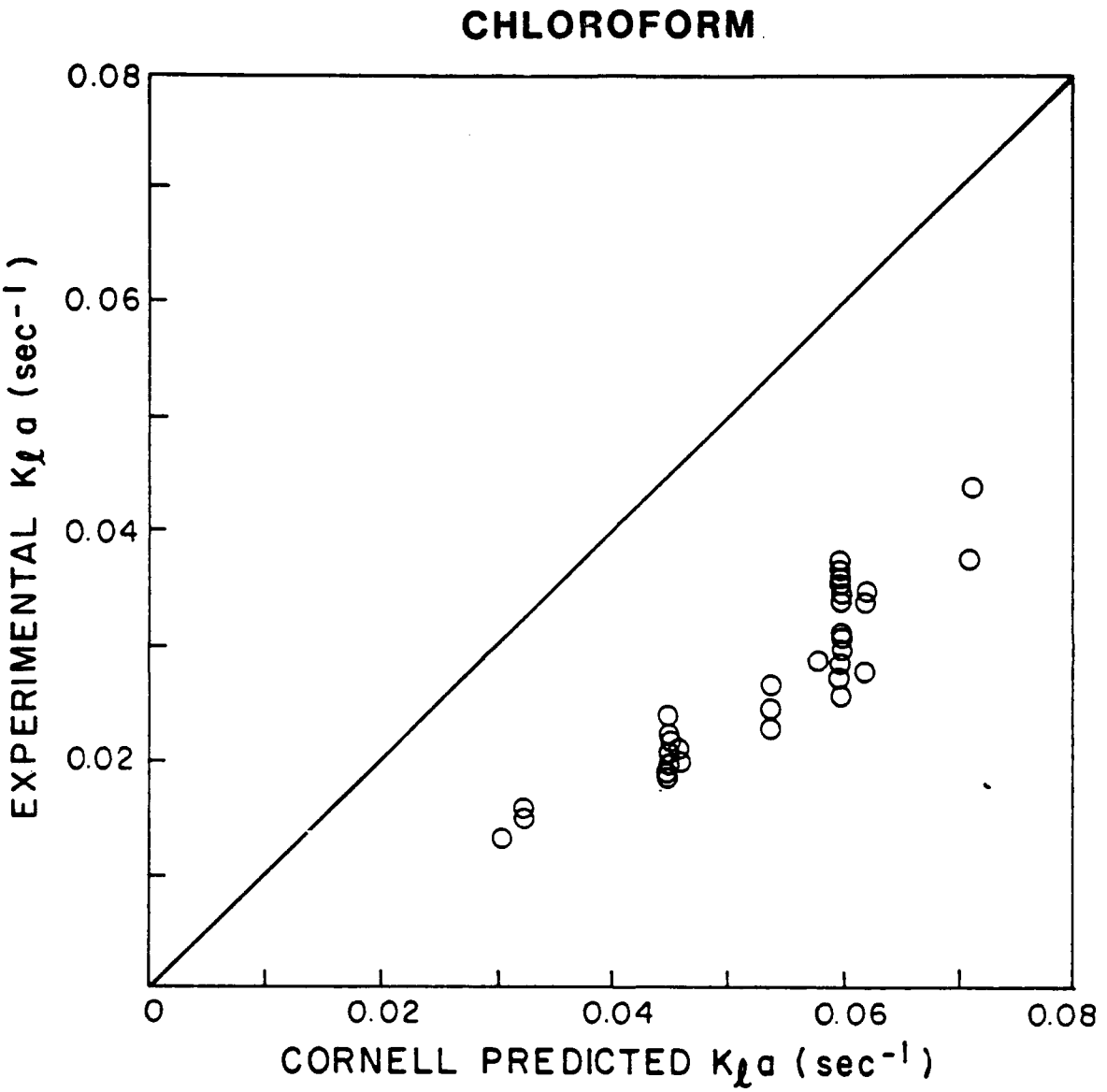

Figure 38. Experimental $K_l a$ versus Cornell Predicted $K_l a$; Chloroform.

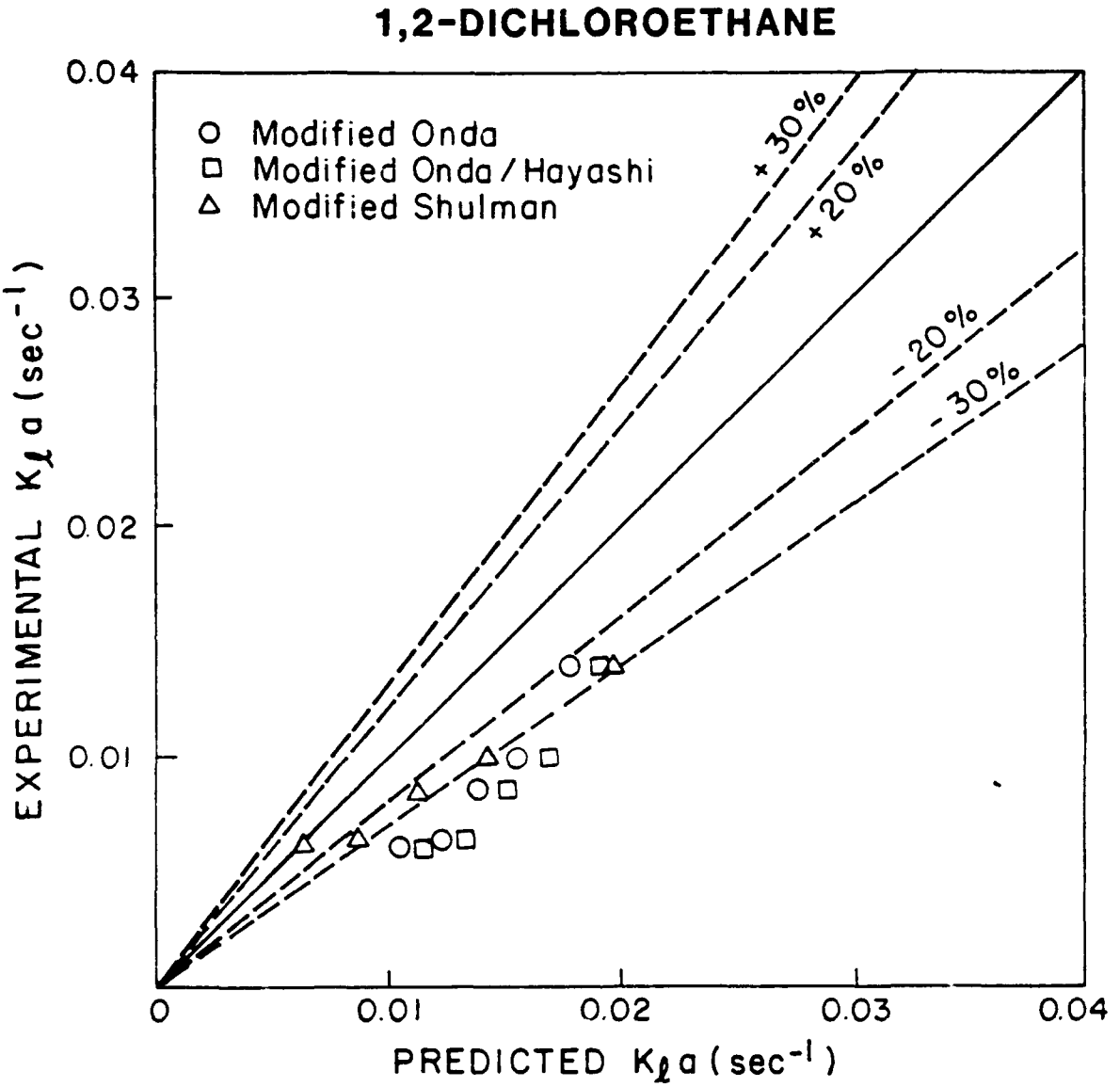

Figure 39. Experimental $K_l a$ versus Predicted $K_l a$; 1,2-Dichloroethane.

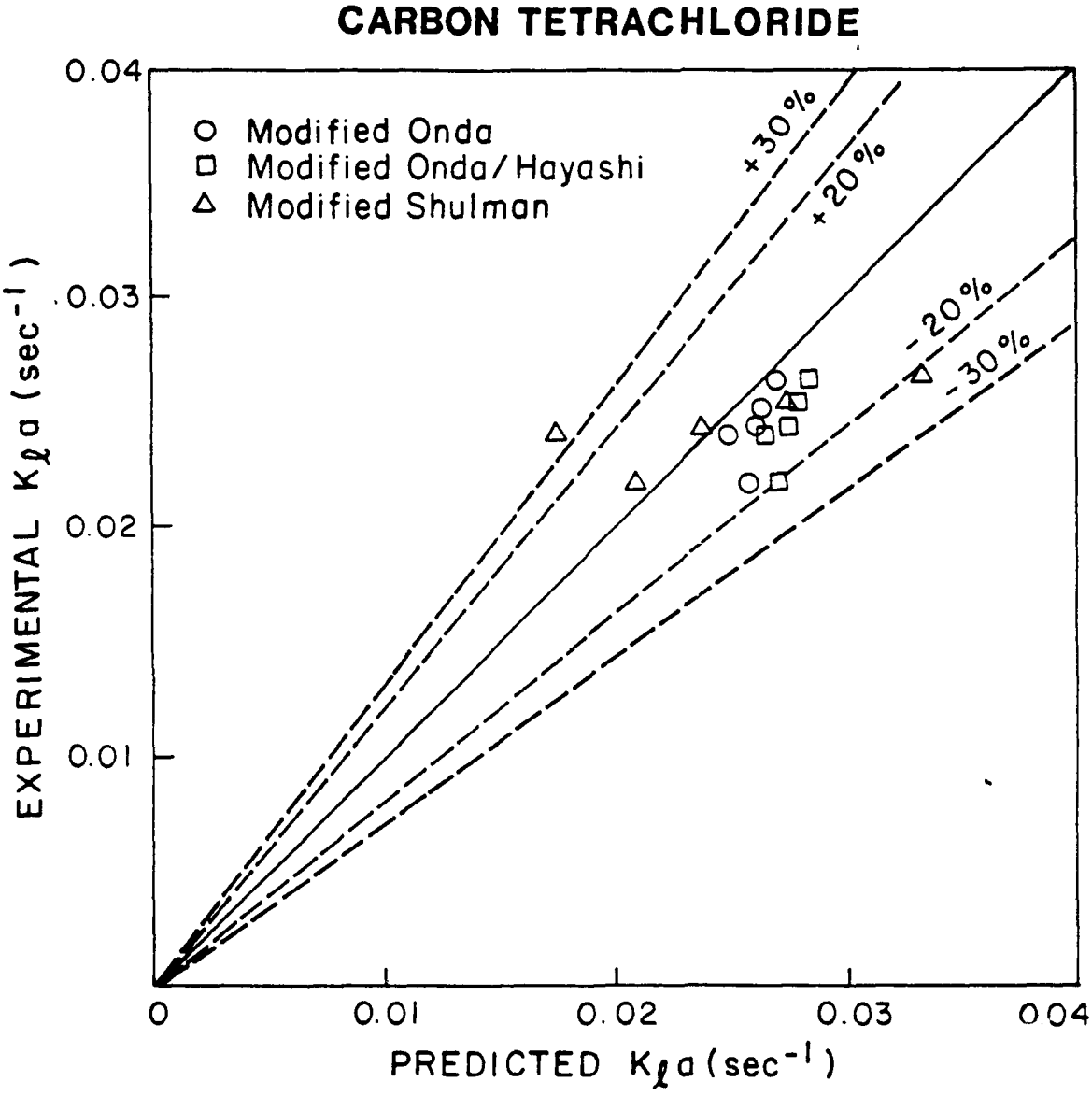

Figure 40. Experimental $K_l a$ versus Predicted $K_l a$; Carbon Tetrachloride.

chloride, a majority (65 percent) of experimental $K_\ell a$'s were 0-20 percent less than the corresponding values predicted by the modified Onda correlation. Approximately 65 percent of the experimental data for chloroform agreed within ±10 percent of the predicted Onda values. As shown in Figure 39, the predictions for carbon tetrachloride were excellent with a deviation of less than 10 percent in four out of the five conditions examined. However, for 1,2-dichloroethane the modified Onda correlation consistently overpredicted the $K_\ell a$ values by more than 30 percent (Figure 40). It was apparent that the modified Onda correlation did a credible job of predicting $K_\ell a$ for crossflow stripping for those compounds that were highly volatile, but seriously overestimated $K_\ell a$ for a moderately volatile compound such as 1,2-DCA. The level of agreement was inversely proportional to the calculated percent gas-phase resistance as shown in Figure 41. Similar observations have been made in conventional countercurrent columns by Gossett and co-workers (Reference 21). The original Onda's correlation was proposed for L_m values of 1-15 kg/m²·s and G_m values of 0.02-1.7 kg/m²·s. Our results were based on G_m values of 0.1-1.0 kg/m²·s while L_m values were 10.7-42.7 kg/m²·s. Thus it appears that extending the liquid loading rate did not affect the validity of Onda's correlations.

The use of Hayashi's proposed correlation for a_w in place of Onda's a_w correlation produced larger deviations from experimental values as can be seen from Figures 33 and 34. For methylene chloride, approximately 70 percent of the predictions were 10-30 percent greater than experimental values, while for chloroform they were 0-20 percent greater than experimental. The same trend was observed for carbon tetrachloride and dichloroethane (Figures 39 and 40). Onda's correlation for a_w is a function of liquid surface tension as well as Reynolds (Re), Froude (Fr) and Weber (We) numbers, while Hayashi's correlation for a_w is dependent on the packing diameter and Re, Fr and We numbers. Although surface tension appears in the Weber number in both cases, it seems that the explicit inclusion of liquid surface tension in Onda's a_w correlation is more appropriate than its exclusion in Hayashi's correlation. Similar results have been found in distillation and absorption experiments (Reference 31). Hayashi's correlation was developed using absorption data for only a single system and was based on limited data. Hence its applicability may be limited to systems similar to the one for which it was originally developed. In fact, it has been observed that for crossflow distillation experiments Hayashi's correlation improves the agreement with experiments (Reference 32).

The modified Shulman correlation proved less effective in predicting $K_\ell a$ values than the Onda model. For both methylene chloride and chloroform the deviations between predicted and experimental values were between ±45 percent (Figures 35 and 36). As shown in Figure 40, the modified Shulman's correlation consistently overpredicted $K_\ell a$ values for 1,2-dichloroethane by more than 30 percent while for carbon tetrachloride the level of disagreement ranged from +30 to -20 percent.

It was not surprising that the single resistance correlation of Cornell was completely ineffective in predicting $K_\ell a$'s for the compounds chosen for this study (Figures 37 and 38). Ignoring gas-phase resistance may have a dramatic effect on the predictions of $K_\ell a$ for VOCs

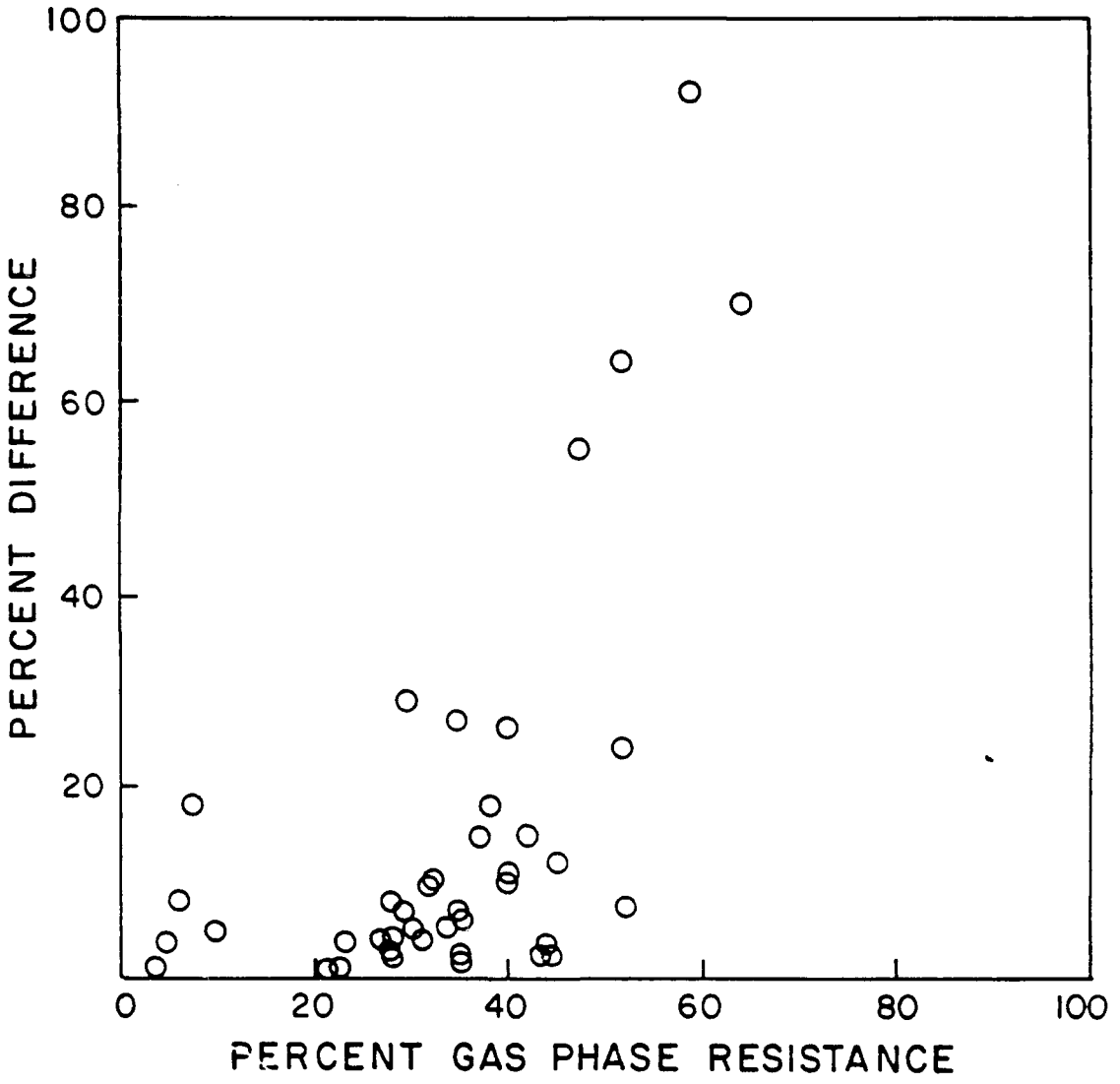

Figure 41. Percent Difference Between Onda Predicted and Measured $K_L a$ Values versus Onda Predicted Gas Phase Resistance; $\alpha = 2.0$

that are only partly volatile. Similar observations by Riojas et al. (Reference 33) support our finding.

In summary, the results of our attempts to predict mass transfer coefficients in crossflow for VOCs indicate that the frequently cited Onda's correlation did a credible job as far as liquid phase controlled chemicals were concerned. When gas-phase resistance becomes important, Onda's correlations may have to be further modified.

F. COLUMN PRESSURE DROP

One of the main advantages of a crossflow column over a conventional countercurrent column is the large decrease in pressure drop which may be achieved. As indicated earlier, in a conventional countercurrent column, the gas and liquid phases compete for the same flow cross-sectional area. In a crossflow unit these two flow areas are disconnected. This introduces the new variable α which is the ratio of the cross-sectional area for gas and liquid flow. Increasing α decreases the gas flow velocity through the packing and hence decreases the pressure drop. This flexibility does not exist in conventional countercurrent flow and hence the higher operating pressure drop limits the range of gas and liquid flow rates which may be employed.

Gas phase pressure drops were measured between taps located in the packed section 4.1 meters apart for the 6-inch crossflow and the 6-inch countercurrent flow tests. Data were collected at α values of 1.0, 2.0, 3.3, 6 and 8 for crossflow for various G_m and L_m values. Pressure drop data for each baffle arrangement in crossflow are given in Figures 42-46. Both gas and liquid loading rates in these figures are based upon the area for liquid flow through the packing, i.e., gas loading rates were not adjusted for α . In this manner, one can show the actual effects of α on gas phase pressure drop and can easily compare the values with conventional countercurrent pressure drops.

At all α values investigated, the pressure drops increased with increasing liquid and/or gas loading rates. In most cases, the relationship between log Δp, where Δp is the pressure drop per unit height of packing, and log G_m, was linear. In certain cases, for example α = 1.0 and L_m = 17.6 kg/m²·s. in Figure 42, there was an increase in pressure drop and deviation from linearity as the gas loading rate increased. This behavior, which is attributed to increased liquid holdup on baffles, is rather random and hence the effects are inconclusive.

For no liquid flow (unirrigated packing), the pressure drop data for all α values are shown in Figure 47. In addition, we also show the data for the 6-inch countercurrent column in the same figure. The pressure drop was approximately proportional to G_m^2 as expected from theory. Increasing α decreases the column pressure drop significantly. For example, at G_m = 1.62 kg/m²·s, the pressure drop for α = 1.0 was 2.4 times greater than the pressure drop for α = 2.0 and 4.4 times greater than for α = 3.3.

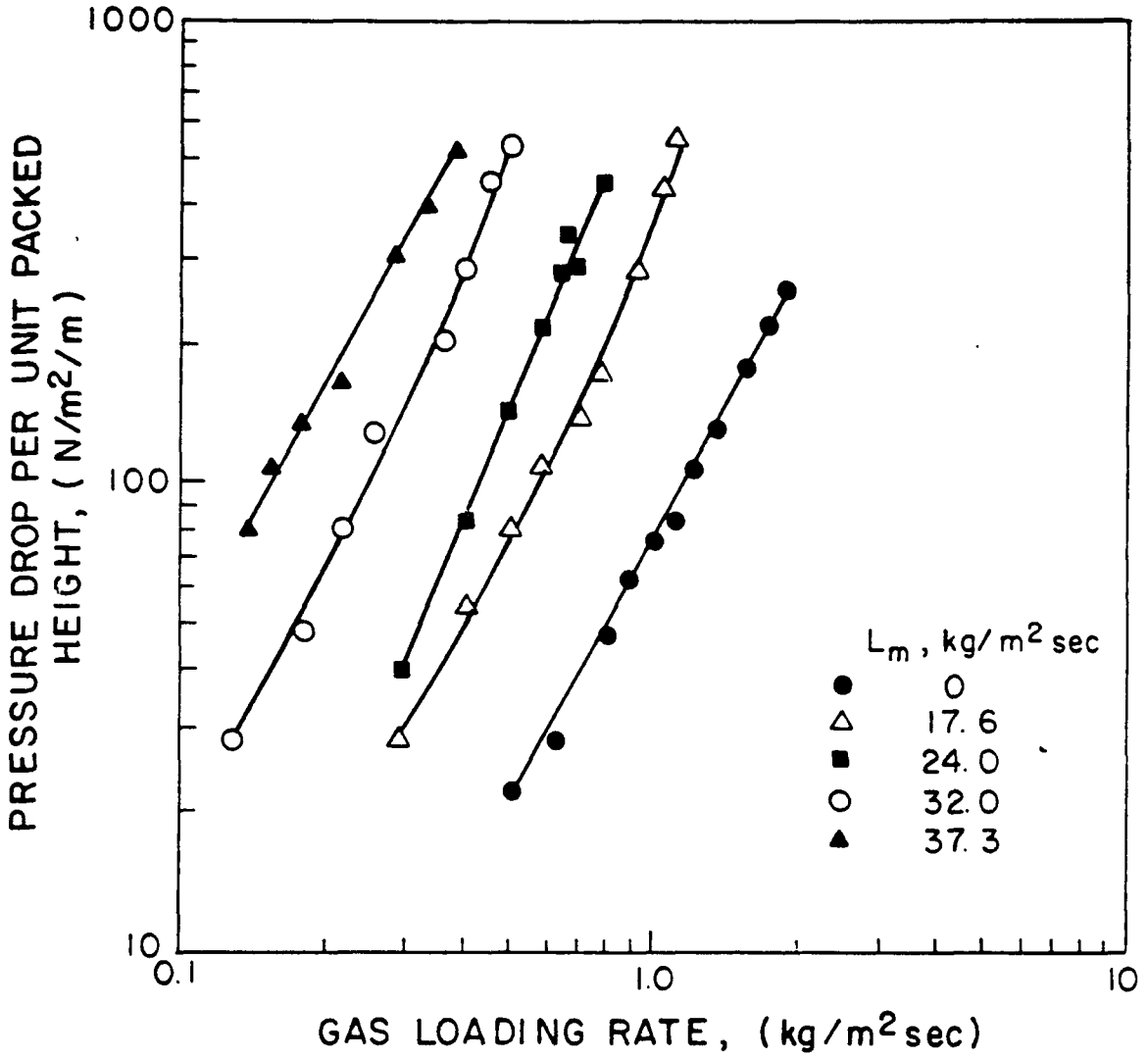

Figure 42. Column Pressure Drop versus Gas Loading; α = 1.0

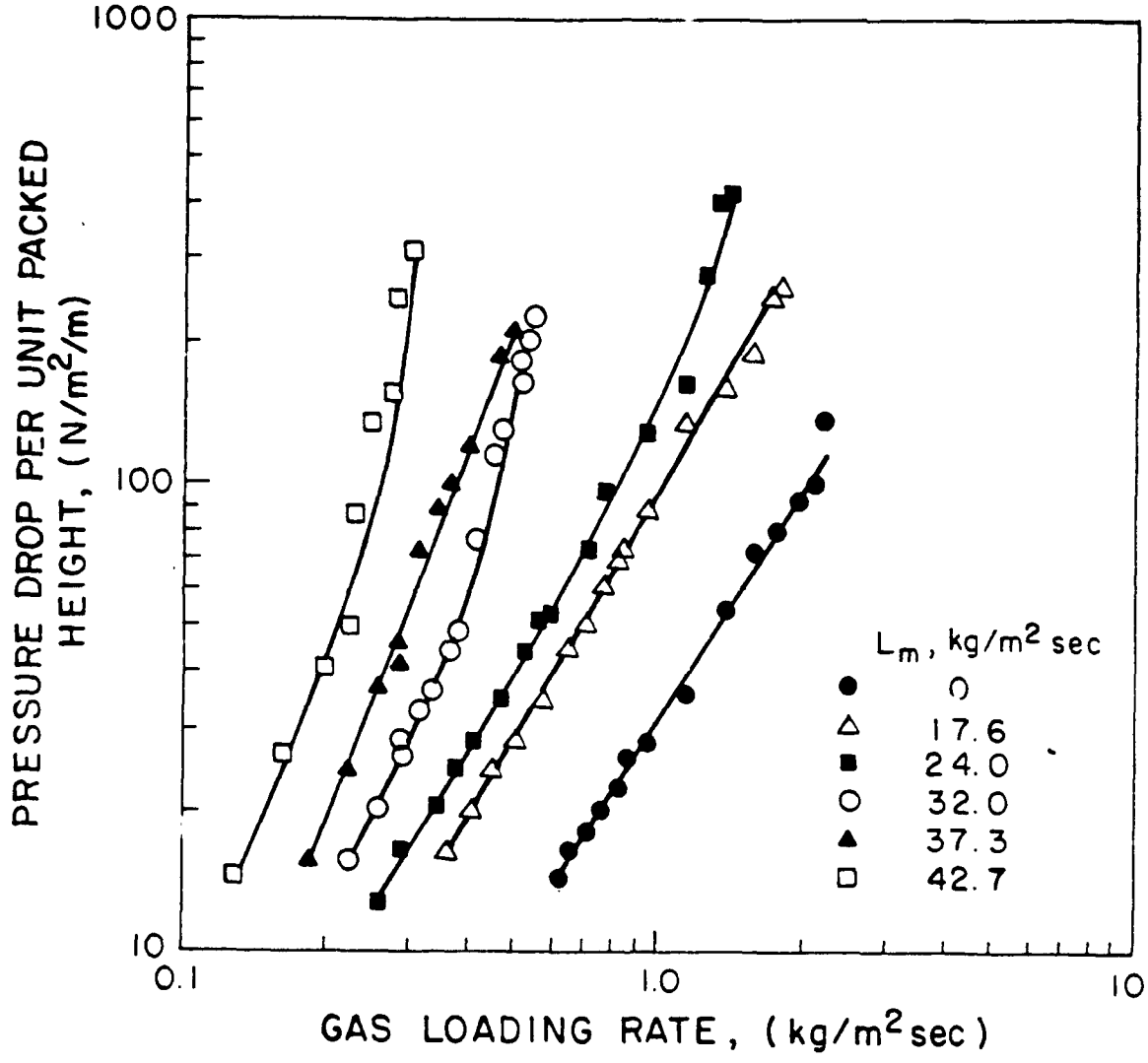

Figure 43. Column Pressure Drop versus Gas Loading. α = 2.0.

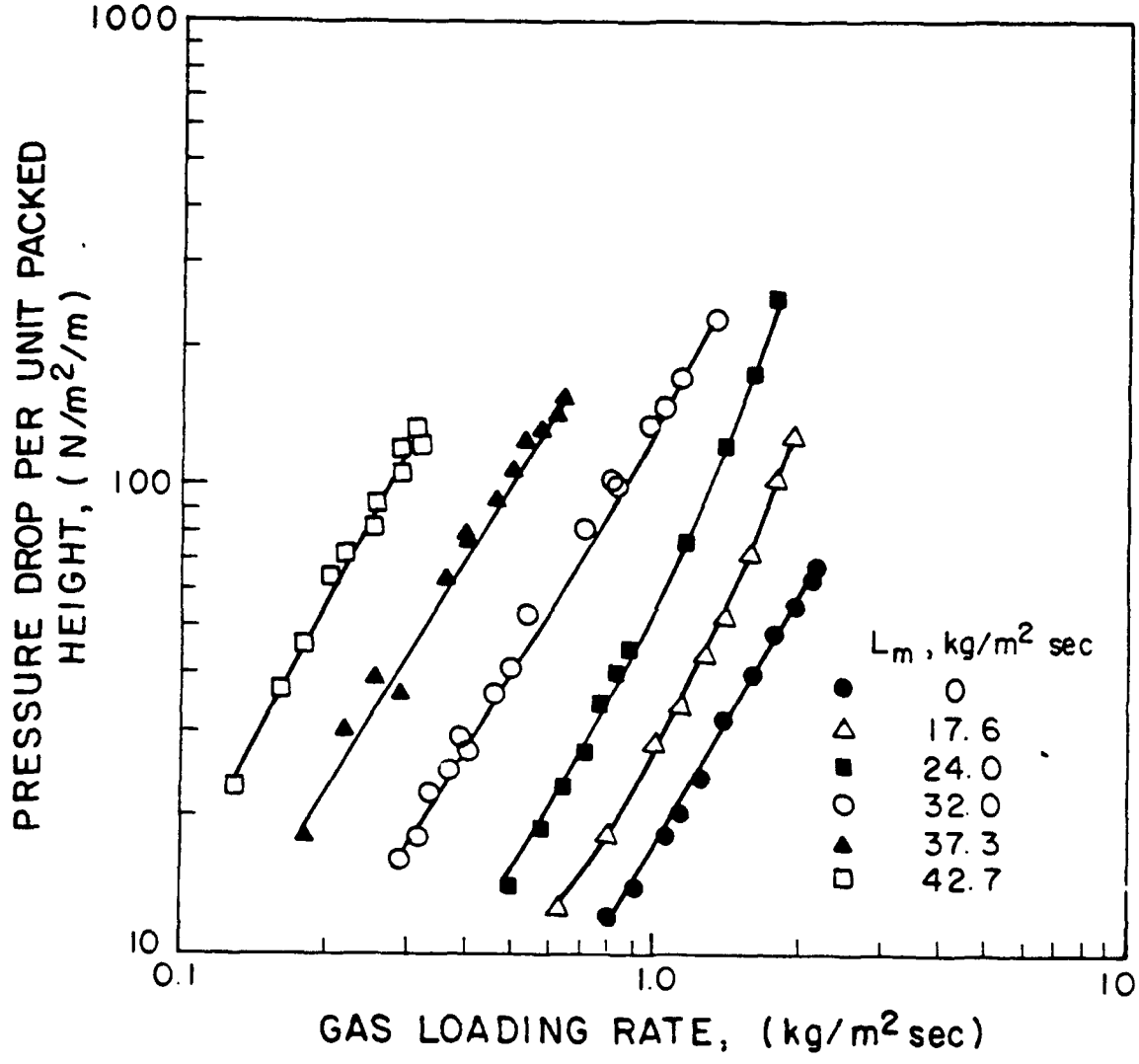

Figure 44. Column Pressure Drop versus Gas Loading; α = 3.3.

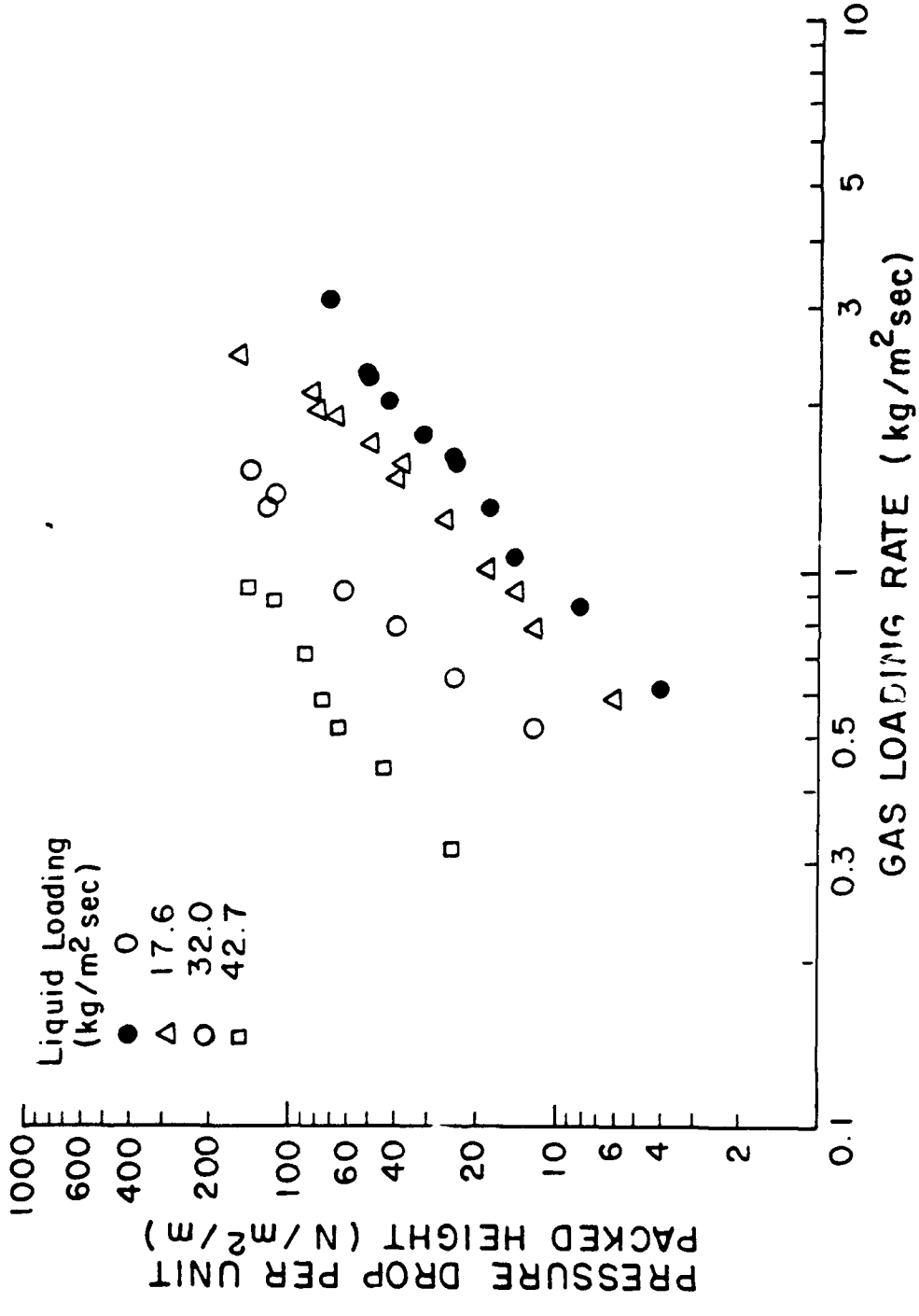

Figure 45. Column Pressure Drop versus Gas Loading; alpha = 6.

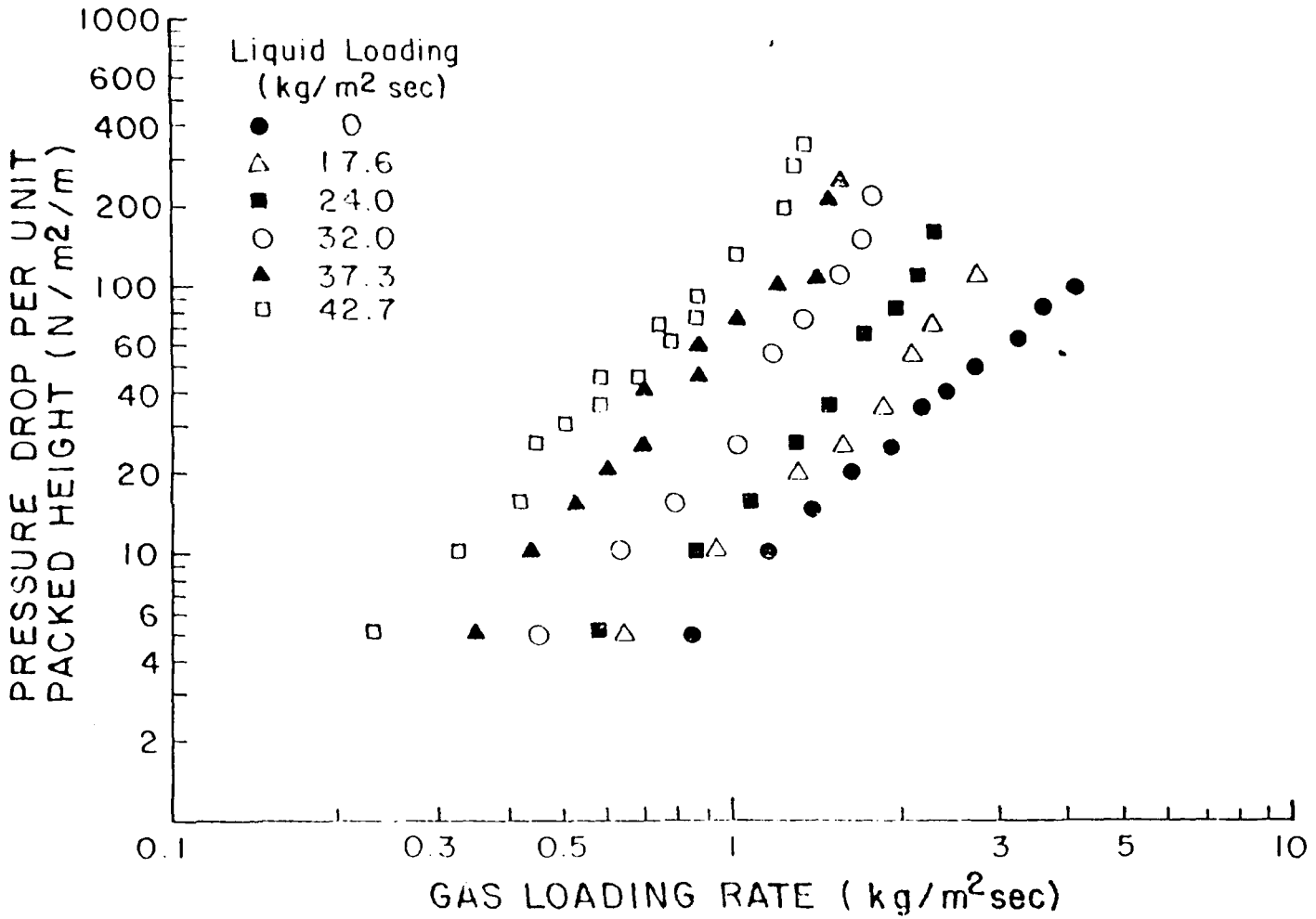

Figure 46. Column Pressure Drop versus Gas Loading; alpha = 8.

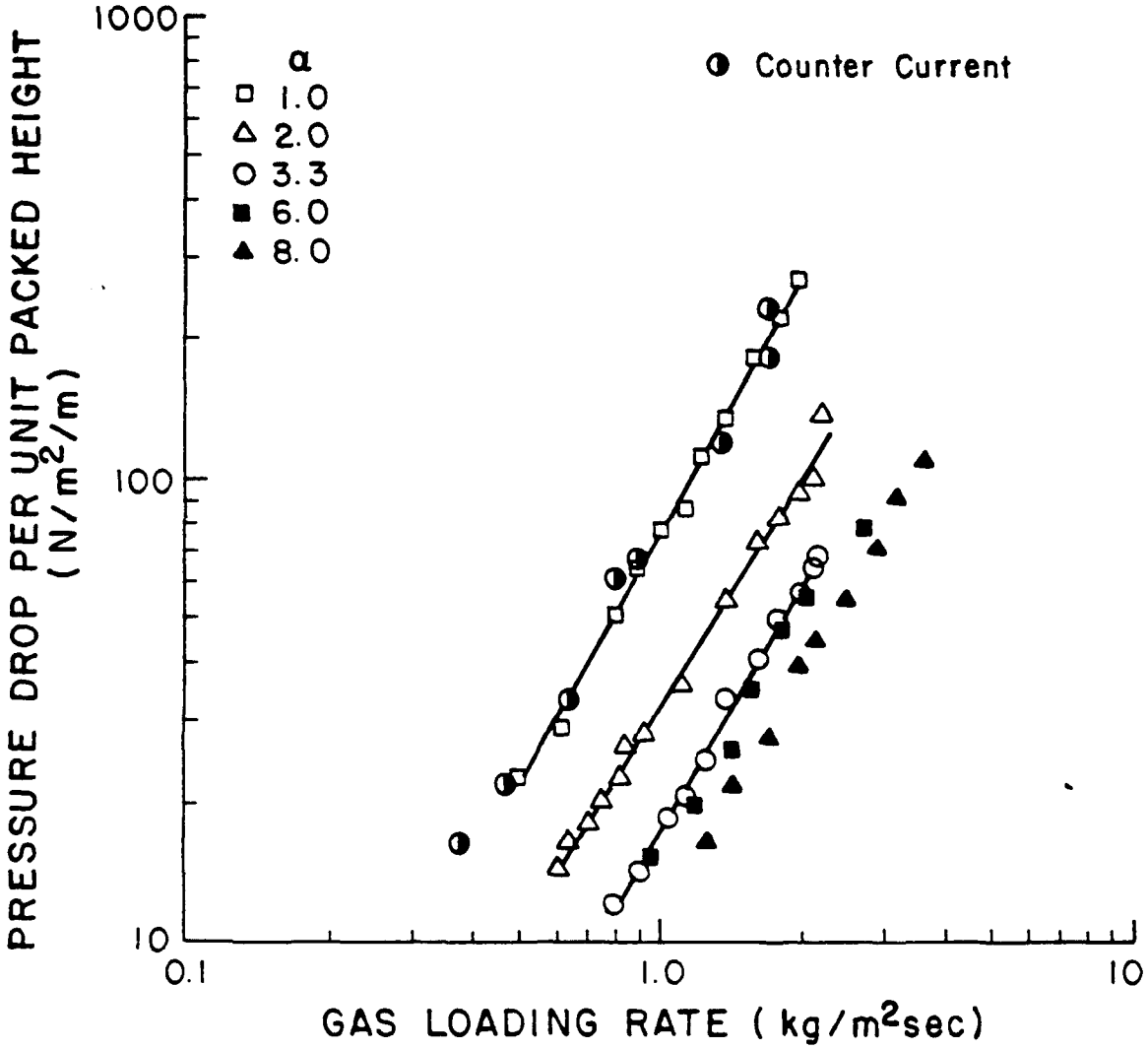

Figure 47. Column Pressure Drop versus Gas Loading; Dry Packing.

Compared to the countercurrent data (Figure 48), the pressure drop for α = 3.3 was approximately an order of magnitude less than that for the countercurrent column. This advantage becomes even greater at α = 6.0 and 8.0. For irrigated packing, as shown in Figures 42-46, the increasing baffle spacing also decreased the pressure drop in crossflow. Once again, it was observed that the pressure drops for the equivalent countercurrent column were as much as an order of magnitude larger than for crossflow. An α = 1 in crossflow is approximately equivalent to countercurrent flow since at α = 1, the gas and liquid flow areas are equal and the length of the gas path in the packing is nominally identical to the countercurrent path. This suggests that the pressure drop for α = 1 in crossflow should be close to that for the countercurrent flow, which was what we observed.

As mentioned earlier, the ability to manipulate α is a unique feature of crossflow. Reduced pressure drops at higher α values, when combined with practically the same stripping efficiency as that of a countercurrent device, suggests that the crossflow system may be an attractive alternative for the air stripping of those compounds which require large G/L values.

The pressure drop for the 12-inch crossflow column at different liquid loading rates is presented in Figure 49. The same trend as was observed for the 6-inch column was seen. A more detailed discussion of pressure drop including the correlation of measured values for design purposes will be given in the succeeding section.

In addition to producing reduced pressure drop, the cascade crossflow column can operate at a wider range of G/L ratios than conventional countercurrent columns. The countercurrent columns are limited in their operating range at the so-called "flooding" point, where operation becomes impossible, and mass transfer efficiency ceases. "Flooding" in a conventional countercurrent column is the situation when gas can no longer be forced upward and liquid hold-up increases dramatically in the column. Such behavior was not observed in the crossflow columns. Both the 6-inch and 12-inch columns operated stably at points that would have constituted flooding of equivalent countercurrent columns. Figure 50 is a Sherwood-Eckert plot (Reference 35) covering the range of gas and liquid flow rates used in the 6-inch crossflow column for both air stripping and pressure drop measurement. According to Ludwig (Reference 34), the onset of loading in a countercurrent column corresponds to the deviation in linearity in the $\ln \Delta P - \ln G_m$ plots, and occurs in the vicinity of a pressure drop of 250 $N/m^2/m$. Clearly the crossflow tower was operable at conditions above initial loading in conventional counterflow operations. This region in a countercurrent column is undesireable because of loss in efficient gas/liquid contacting. The crossflow column did not show any loss in mass transfer efficiency at these points. At conditions beyond the flooding point in a countercurrent column, the crossflow column still operated stably. However, large liquid buildup on the baffles was observed. It is possible that serious loss in mass transfer efficiency may not occur since the liquid is still turbulently mixed by the gas as it crosses the baffles.

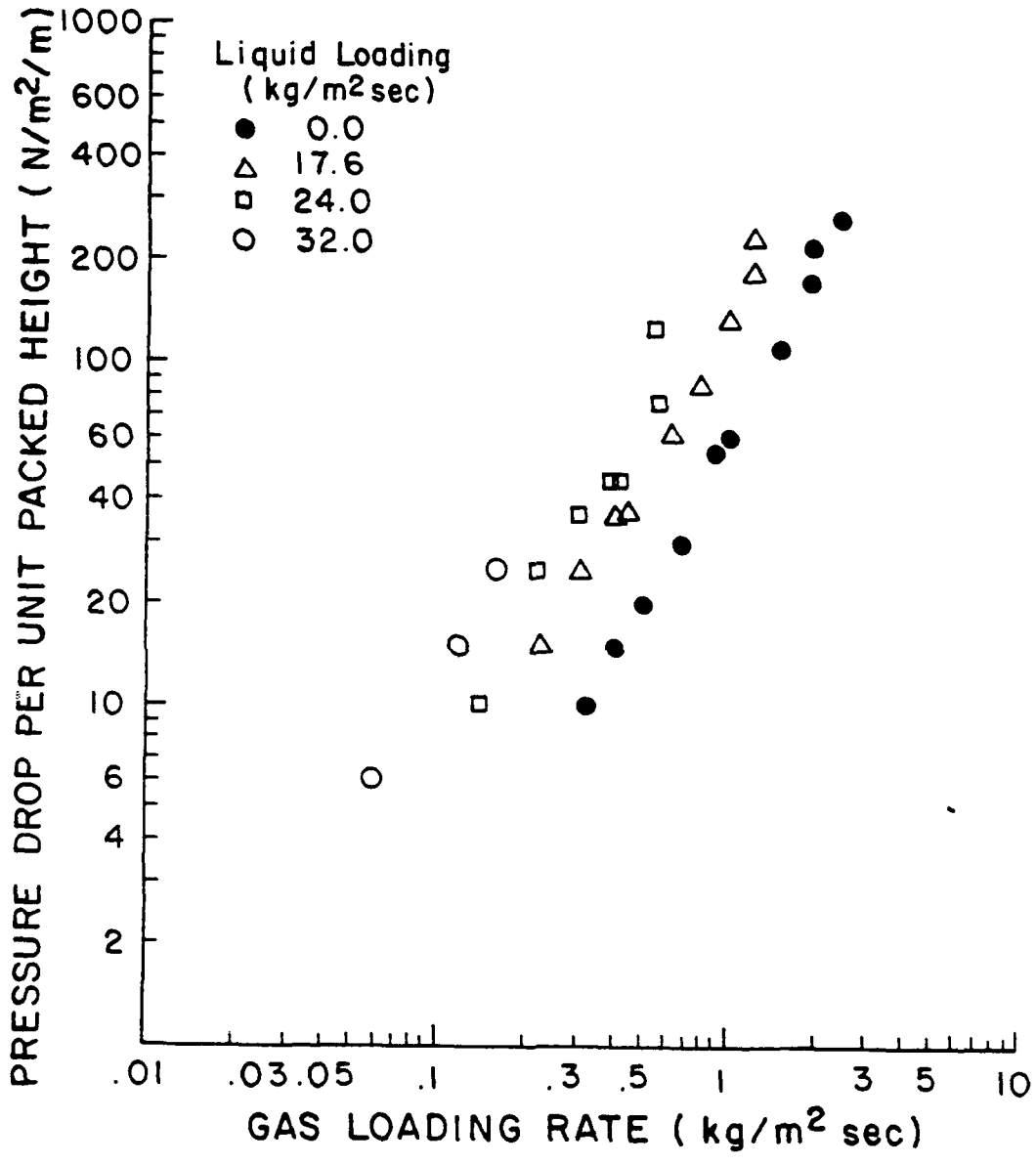

Figure 48. Countercurrent Column Pressure Drop versus Gas Loading.

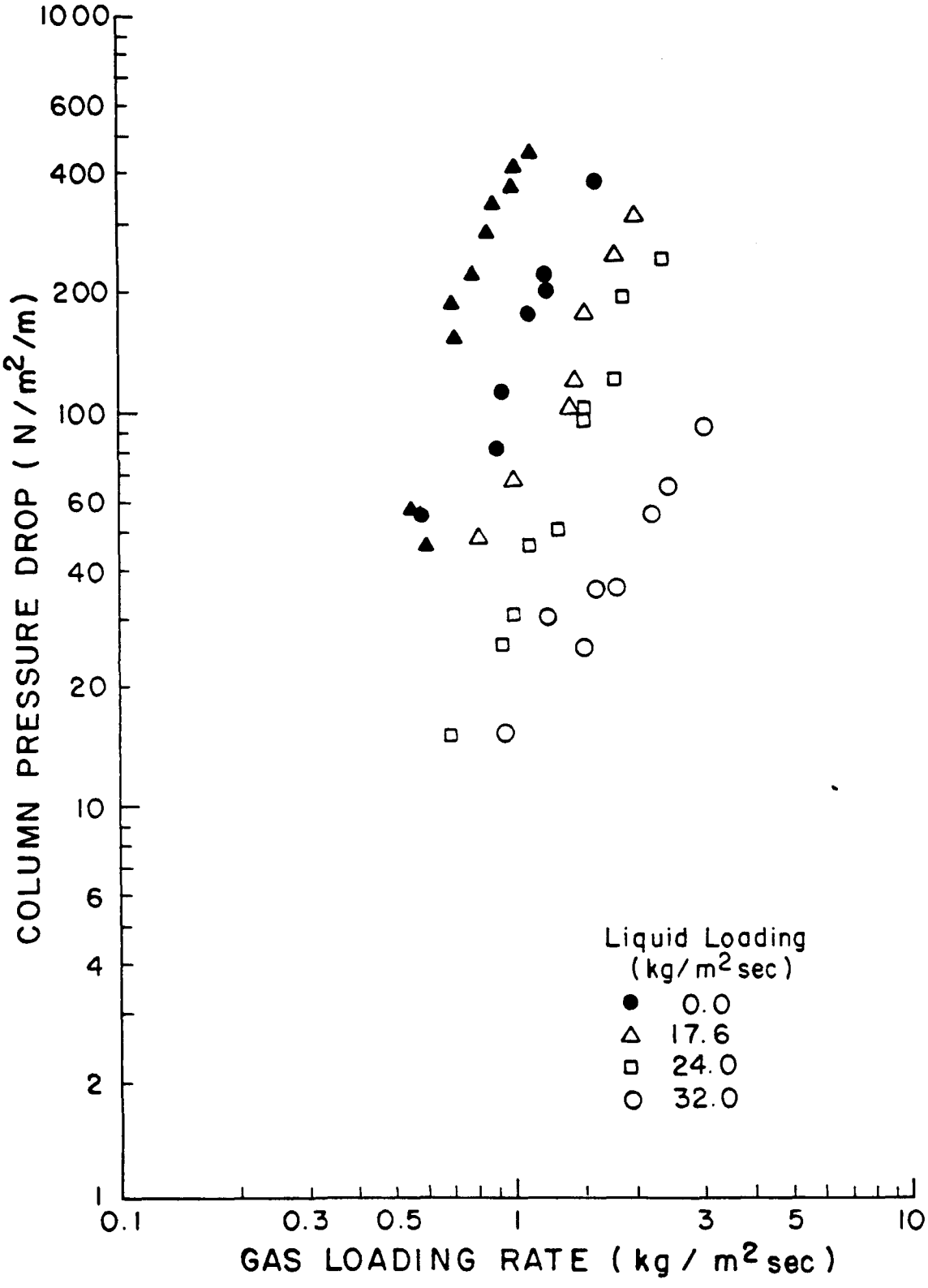

Figure 49. Column Pressure Drop for the 12-inch Pilot-Scale Column.

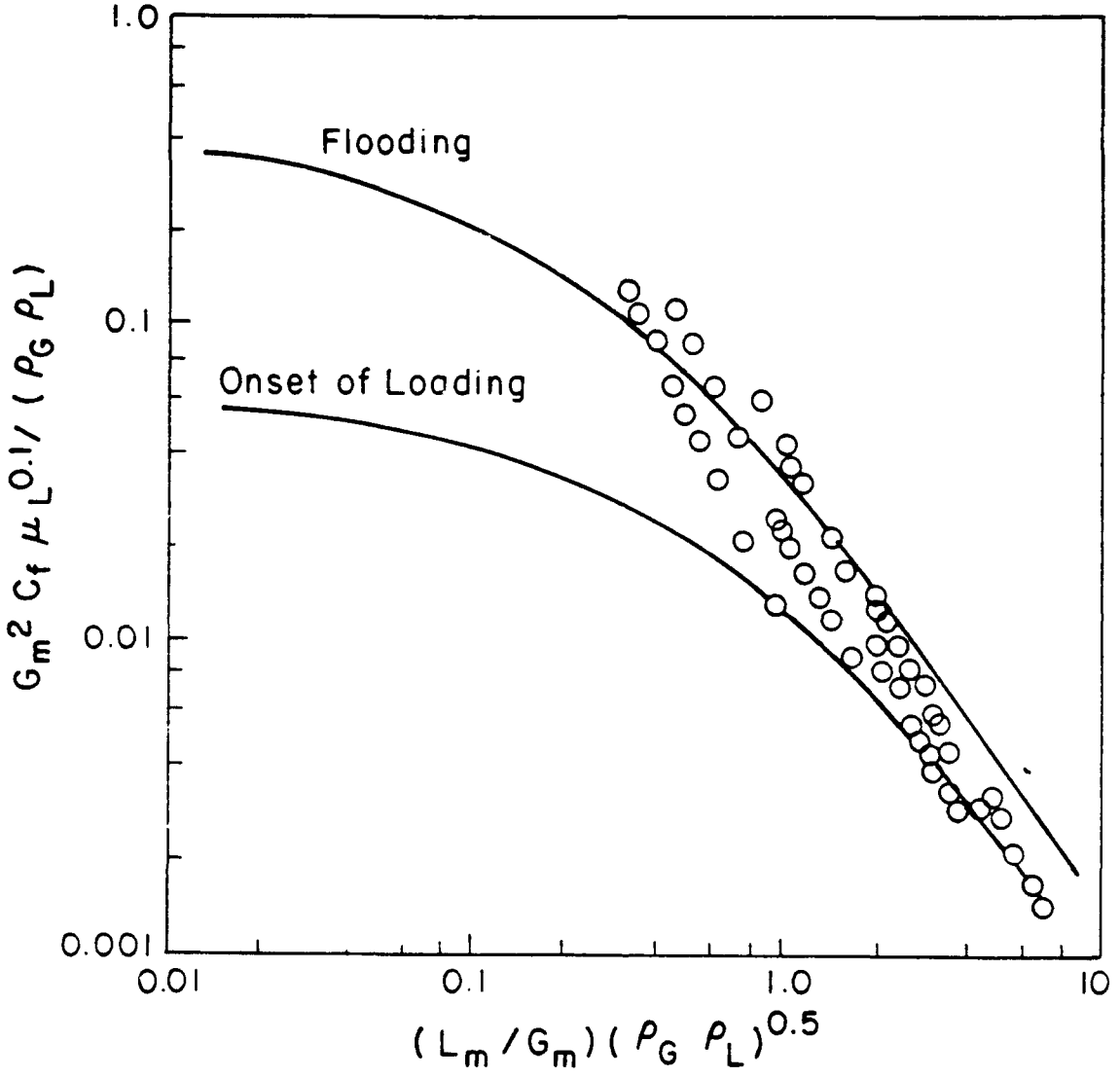

Figure 50. Sherwood-Eckert Plot.

SECTION V

PRELIMINARY ECONOMIC COMPARISON OF CROSSFLOW AND COUNTERCURRENT STRIPPING

A. OBJECTIVES

Experimental results from the 6-inch and 12-inch crossflow stripping columns proved the technical feasibility of crossflow air stripping for the removal of volatile organic contaminants from groundwater. Mass transfer coefficients were found to be comparable in both countercurrent and crossflow systems while gas-phase pressure drop, when compared at equal liquid loading rates (mass/time·area), was as much as one order of magnitude lower in the crossflow mode. These results suggest that crossflow stripping could provide an economically attractive option to countercurrent stripping in situations where the operational cost savings associated with reduced pressure drop would outweigh the possible increased capital costs associated with the installation of retainer screens and baffles within the crossflow tower.

Therefore, comparative economic evaluations were carried out to identify conditions where the crossflow mode of operation would prove economically attractive. The approximate nature of both the design and economic calculations at this time must be emphasized. Existing literature correlations should permit countercurrent flow systems to be designed with reasonable accuracy; however, the level of uncertainty increases considerably for crossflow operation. Similarly, uncertainties exist in several aspects of the cost estimation for both flow modes. The procedures used in both the design and economic evaluations are carefully described and areas of significant uncertainty are identified.

In line with current custom, all design and economic calculations have been expressed using typical American engineering units. For example, column pressure drop is expressed as inches of water per foot of packing rather than Newtons per square meter per meter of packing used in previous sections of this report. Similarly, air and water flow rates are expressed as cubic feet per minute (cfm) and gallons per minute (gpm), respectively, instead of cubic meters per second used previously.

B. DESIGN CASES

Design calculations have been carried out for six combinations involving two water treatment rates - 200 and 1500 gpm - and three volatile species - trichloroethylene, 1,2-dichloroethane, and methyl ethyl ketone. The two treatment rates illustrate the effect of scale on treatment costs. The three species exhibit large differences in volatility (Henry's constant) ranging from the quite volatile trichloroethylene to the low volatility methyl ethyl ketone.

Constant operating temperature of 283K and pressure of 1 atm were assumed in all cases, and 99 percent removal of the contaminating organic was required. Because the air stripping operation is linear

with liquid concentration, the final design for 99 percent removal is independent of the inlet contaminant concentration. That is, the same column size and air flow rate would be required to reduce the liquid concentration from 100 mg/L (100 ppm) to 1 mg/L (1 ppm) and from 5 mg/L to 0.05 mg/L (5 ppm to 0.05 ppm). At the operating temperature of 283K the Henry's constants for the three species were taken to be (Reference 37)

	H ($atm \cdot m^3/g \cdot mol$)
Trichloroethylene	0.00538
1,2 Dichloroethane	0.00117
Methy ethyl ketone	0.00028

In all cases, the packing was assumed to be 5/8 inch polypropylene Pall rings such as used in the experimental portions of the study. While larger packing sizes would normally be used in larger columns it was necessary to limit the economic comparison to the single packing since no crossflow stripping data are available for other packing sizes or types.

In countercurrent operation for each of the six cases, column diameter and gas flow rate were varied in the design calculations. For crossflow operation, column diameter, gas flow rate and the additional parameter of baffle spacing (characterized by α) were varied. A broad range of each of the design parameters was considered to ensure that the economic optimum conditions would be included. Altogether, more than 700 separate design cases were evaluated.

C. DESIGN METHOD

Once operational parameters such as liquid and gas flow rates, column diameter, stripping efficiency, and in crossflow operation, baffle spacing were fixed, it was necessary to estimate the overall mass transfer coefficient and the pressure drop per unit of packed height to complete the design calculation.

1. Mass Transfer Coefficient

For both countercurrent and crossflow operation the mass transfer coefficient was calculated using the Onda correlation, Equations (19), (20), and (21). Countercurrent calculations were based upon the Onda correlation without modification while, for crossflow calculations, the Onda correlation was modified only to the extent that gas loading was based upon the actual gas flow area, which was a function of the parameter α. The validity of this approach for volatile compounds in small-scale systems was established during the experimental portion of this study. For example, Figures 31 and 32 have shown that the mass transfer coefficients for methylene chloride and chloroform predicted by the Onda correlation agree with experimental results within approximately ±30 percent.

However, as the volatility of the contaminant decreases and the resistance due to gas phase mass transfer increases, it appears that the Onda correlation is less accurate. This is generally true and independent of the contacting mode. Limited data for 1,2-dichloroethane in crossflow operation shown in Figure 39 supports this conclusion. Consequently, it is necessary to consider the predicted mass transfer coefficients for both 1,2-dichloroethane and methyl ethyl ketone in both countercurrent and crossflow operation as less reliable than the coefficient for trichlorethylene. While it may be reasonable to assume that the magnitude of the error would be comparable in countercurrent and crossflow, there are no experimental data available at this point to confirm the assumption.

2. Packed Height

Once the estimated value of the overall mass transfer coefficient was available, the required packed height was calculated by rearranging Equation (11) so that Z_T became the unknown

$$Z_T = \frac{L}{A\ K_\ell a} \frac{\ell n\ [\frac{1}{1-E} - (\frac{E}{1-E})\ \frac{L}{G\ H_c}]}{1 - \frac{L}{G\ H_c}} \qquad (24)$$

This equation was used for both countercurrent and crossflow modes of operation.

3. Pressure Drop

In countercurrent operation, gas phase pressure drop per unit length of packing is available from the packing manufacturer as shown in Figure 51. In this figure, the pressure drop expressed as inches of H_2O per foot of packed height is plotted versus the gas loading rate, G_m (lb/hr ft^2), both on logarithmic scales. The liquid loading rate (also in lb/hr ft^2) is shown as the parameter in this figure. For dry packing at all gas rates and for irrigated packing at sufficiently low gas rates, the curves are linear with a slope of approximately 2. As gas rate increases curvature becomes evident and the slope of the lines increases. The onset of curvature is taken as the onset of loading. All lines terminate at a pressure drop of 2.0 to 2.5 in H_2O/ft which defines flooding in the countercurrent column.

For calculation purposes it was necessary to express the Figure 51 data in mathematical form. Leva (Reference 39) proposed the following equation to describe pressure drop in the operating region prior to loading as a function of gas and liquid rates

$$\Delta P' = \gamma 10^{(\varphi L_m)} \frac{G_m^2}{\rho_g} \qquad (25)$$

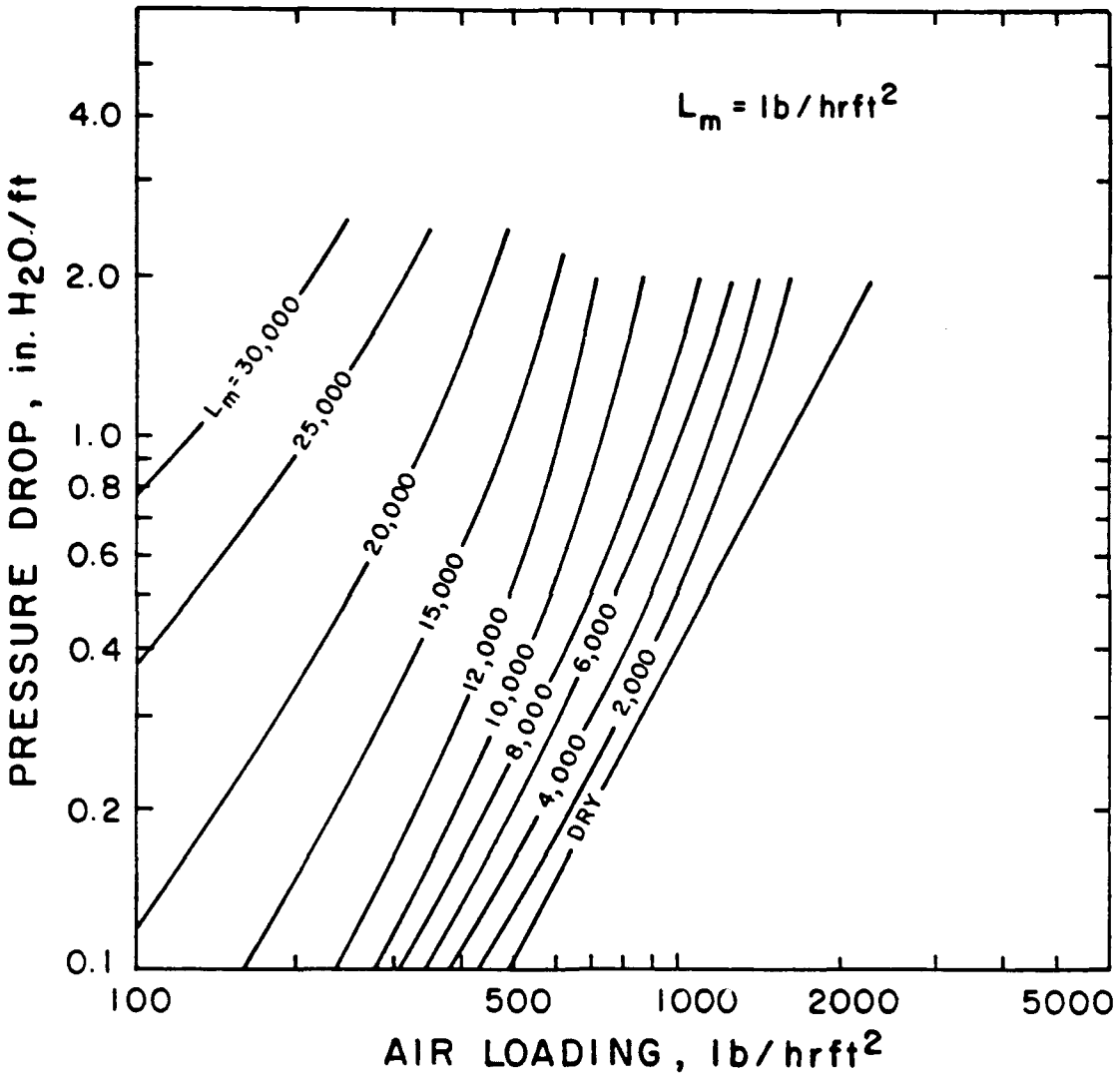

Figure 51. Manufacturer's Data for Pressure Drop in a Countercurrent Column using 5/8-Inch Pall Rings.

where $\Delta P'$ = pressure drop, inches H_2O/ft

L_m = liquid loading rate, lb/hr ft^2

G_m = gas loading rate, lb/hr ft^2

ρ_g = gas density, lb/ft^3

The constants in Equation (25) were evaluated using a least-squares fit to the linear portion of the data in Figure 51 and found to be

$$\gamma = 0.299 \tag{26}$$

$$\varphi = 0.267 \tag{27}$$

Figure 52 compares the pressure drop calculated from Equation (25) with Figure 51 data for liquid loading rates of 6000 and 15000 lb/hr ft^2. The agreement is generally within ±10 percent for $\Delta P'$ less than 1 inch H_2O/ft; however, the equation underpredicts pressure drop in the loading region and fails completely to predict flooding. In the countercurrent design calculations, Equation (25) was used, with the loading region taken to correpond to calculated $0.75 \leq \Delta P' \leq 2.0$ inches H_2O/ft. In the following sections where design case results are reported, no cases corresponding to calculated $\Delta P' > 2.0$ inches H_2O/ft (flooding) are included and cases in which the calculated $\Delta P'$ is in the loading region are clearly designated.

For crossflow operation, the experimental pressure drop data reported in Figures 42 through 46 was correlated into a mathematical expression which could, with reasonable justification, be extrapolated to larger column sizes and different liquid and gas flow rates associated with the design study. The mathematical description required that a new model be developed to describe gas and liquid contacting in the crossflow mode. The new model concept is shown schematically in Figure 53 and described in the following sections.

Figure 53a shows a top view of a column of diameter D. It is assumed that 65 percent of the total cross-sectional area is packed leaving 17.5 percent of the total area on each side of the packing for air flow. A_ℓ represents the cross-sectional area for liquid flow, d is the gas flow distance corresponding to gas and liquid contact in one crossflow pass, and w is the length of the cord corresponding to the packing retainer screen. Geometric analysis can be used to show that

$$A_\ell = 0.65 \left[\frac{\pi D^2}{4}\right] = 0.511D^2 \tag{28}$$

$$d = 0.537D \tag{29}$$

$$w = 0.842D \tag{30}$$

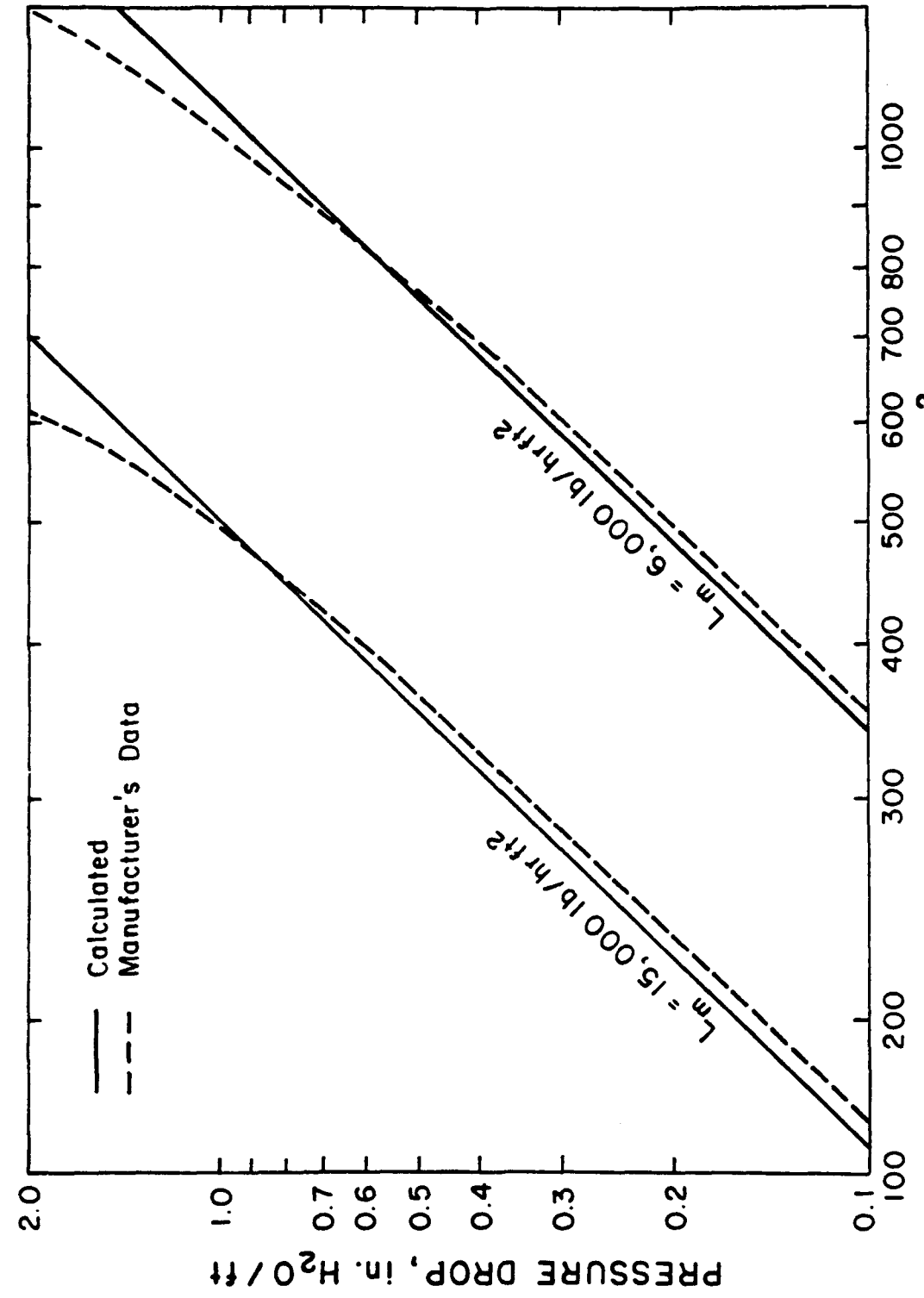

Figure 52. Comparison of Calculated Countercurrent Pressure Drop with Manufacturer's Data.

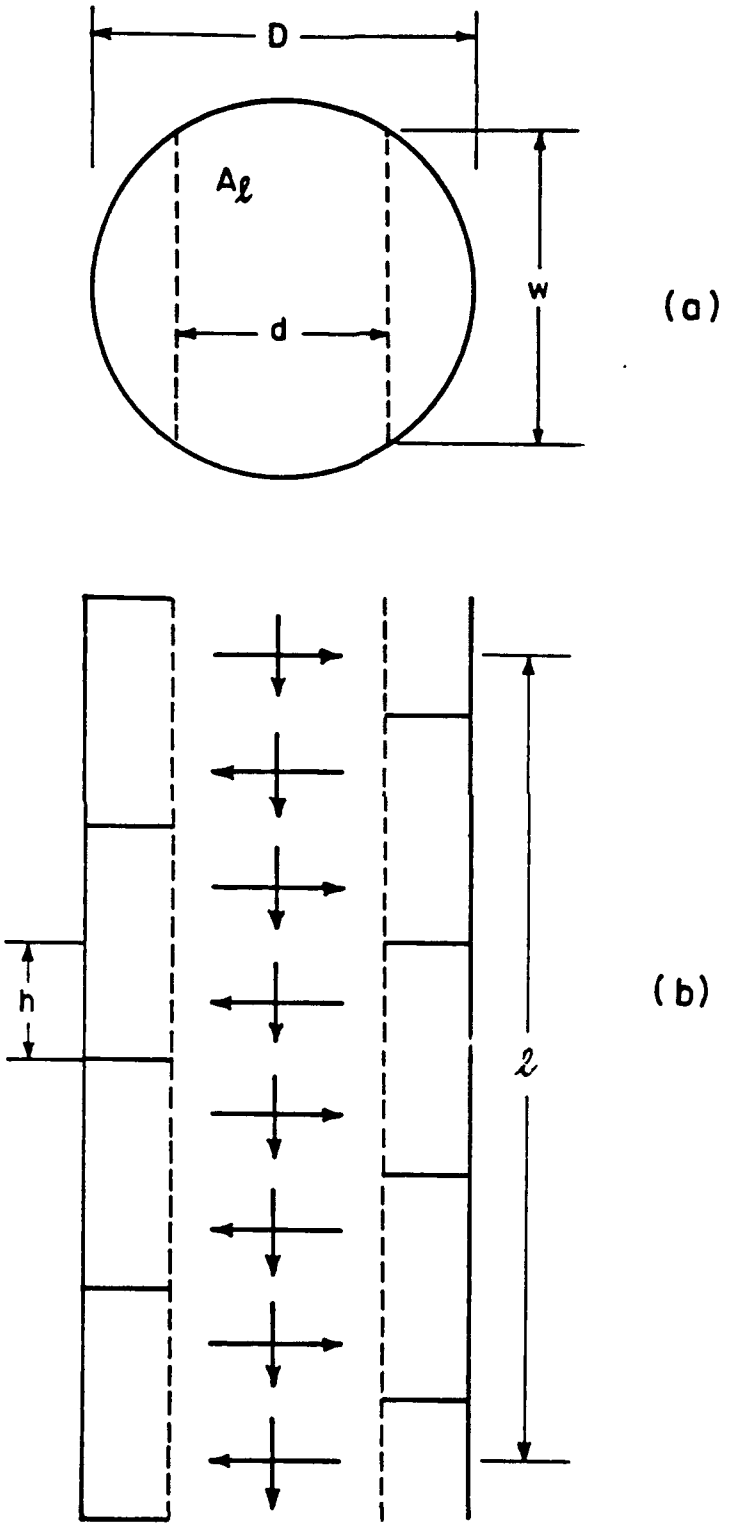

Figure 53. Schematic of Crossflow Pressure Drop Model

In Figure 53b, the dimension, ℓ, represents the vertical distance between the taps used in the pressure drop measurements, and h represents the vertical distance between baffles on opposite sides of the column. The distance h depends upon the parameter α in the following manner

$$h = \frac{\alpha A_{\ell}}{w} = \frac{\alpha [0.511 D^2)}{0.842 D} = 0.607\alpha D \qquad (31)$$

The number, N, of gas and liquid crossflow passes between the pressure taps is therefore

$$N = \frac{\ell}{h} = \frac{\ell}{0.607\alpha D} \qquad (32)$$

In each crossflow pass the vapor travels a distance, d, in contact with the liquid. The total distance, L, through which the vapor must flow against liquid resistance is

$$L = Nd = \frac{\ell}{0.607\alpha D} [0.537D] = \frac{0.885\ell}{\alpha} \qquad (33)$$

We assume that the entire pressure drop is associated with the vapor-liquid contact distance L, i.e., pressure drop associated with vapor flow through the open-plenum areas is neglected.

For $\alpha = 1$, the vapor-liquid contact distance is 88.5 percent of the vertical distance between pressure taps. Also for $\alpha = 1$ the areas for gas and liquid flow are equal, as is always the case in countercurrent flow. This accounts for the fact that the measured pressure drops for crossflow with $\alpha = 1$ are approximately equal to expected pressure drops for countercurrent flow at equal gas and liquid volumetric flows.

In order to convert the raw crossflow pressure drop data expressed as inches H_2O/ft packed height, $\Delta P'$, to inches H_2O/ft of gas-liquid contact distance, $\Delta P''$, it is necessary to multiply by the ratio of ℓ/L

$$\Delta P'' = \Delta P' \left(\frac{\ell}{L}\right) = 1.13\ \alpha\ \Delta P' \qquad (34)$$

The gas loading rate through the packed section is also a function of α. If G_m' is the loading rate based upon unit liquid flow area and G_m'' represents the same flow rate, but based upon gas flow area, then

$$G_m'' = \frac{G_m'}{\alpha} \tag{35}$$

According to Equation (25), pressure drop prior to loading is proportional to the square of the gas loading rate. Combination of Equations (25), (34) and (35) suggests that crossflow pressure drop should be inversely proportional to α^3, i.e., the crossflow pressure drop at $\alpha = 2$ should be 8 times less than the countercurrent pressure drop at the same gas and liquid flow rates. However, measured pressure drop reduction was less than that predicted by these simple arguments. At fixed gas and liquid flow rates the measured pressure drop in countercurrent flow was approximately four times greater than the measured pressure drop in crossflow at $\alpha = 2$. Therefore the experimental results turned out to be more nearly proportional to α^{-2} than α^{-3}.

Initial attempts to correlate crossflow pressure drop results using a direct modification of the Leva equation were unsuccessful because of the less than expected dependence of pressure drop on α. However, reasonable success was achieved by modifying the Leva equation to the following form

$$\Delta P'' = \gamma' \, \alpha^{1.25} \, 10^{\varphi' L_m} \, \frac{G_m''^2}{\rho_g} \tag{36}$$

By fitting all of the crossflow data from the 6-inch column, best values of γ' and φ' were found to be

$$\gamma' = 0.059 \tag{37}$$

$$\varphi' = 0.293 \tag{38}$$

The overall success of the crossflow pressure drop correlation is shown in Figure 54, a parity plot of calculated pressure drop versus measured pressure drop (both expressed as inches H_2O per foot of gas-liquid contact distance). A great deal of scatter exists in the data as indicated by numerous points which fall outside the ±50 percent limits. However, most of the outlying data correspond to low pressure drops and better agreement is achieved as pressure drop increases.

Collecting accurate experimental data at a low pressure drop is quite difficult because the error in the pressure drop reading approaches the actual pressure drop. In addition, correlation of column pressure drop data, even in the often-studied countercurrent system, is not totally satisfactory. The Leva correlation, Equation (25), proved adequate in this study but it is not universally accepted. Therefore, in spite of the wide data spread, Equation (36) is considered to provide the best correlation of crossflow pressure drop data presently available. This equation was used to predict pressure drop in the crossflow design cases to be reported.

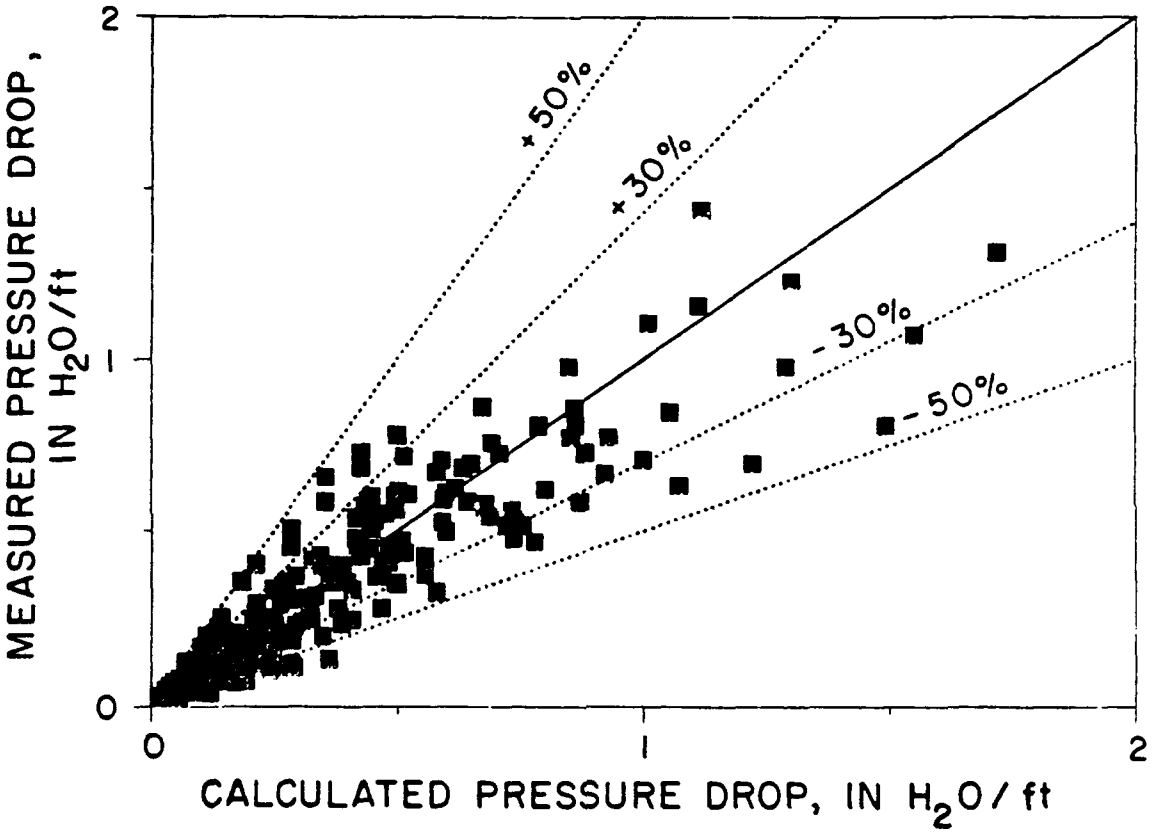

Figure 54. Parity Plot Comparing Calculated and Measured Column Pressure Drop for Crossflow.

4. Pump and Blower Power Requirements

The theoretical horsepower required to drive the pump and the air blower were calculated directly from equations taken from Perry (Reference 38). For the pump

$$P_{hp} = \frac{Z' \, Q_\ell}{3960} \qquad (39)$$

Z', the total hydraulic head, was taken to be the packed height as calculated from Equation (24) plus 10 feet to allow for adequate distance above and below the packing. Q_ℓ is the water flow rate in gallons per minute, and P_{hp} is the theoretical horsepower.

For the blower

$$B_{hp} = 0.000157 \, Q_g \, \Delta P_T \qquad (40)$$

Q_g is the air flow rate in cubic feet per minute and ΔP_T is the total gas-phase pressure drop in inches of water. For countercurrent operation, ΔP_T is the product of $\Delta P'$ from Equation (25) and Z_T from Equation (24). For crossflow operation, ΔP_T is the product of $\Delta P''$ from Equation (34) and the total distance corresponding to air-water contact given by Equation (33).

D. DESIGN RESULTS

As indicated previously, design studies were carried out for three organic contaminants at two water flow rates in both countercurrent and crossflow operation. Column diameter and gas flow rate were considered as design parameters in countercurrent flow while the additional parameter of baffle spacing was considered for crossflow operation. Selected results are presented and discussed in the following sections.

Figure 55 shows the required packed volume as a function of the air to water volumetric ratio for the countercurrent stripping of TCE with 99 percent removal efficiency. The water flow rate is 200 gpm and results for four column diameters are shown. As the actual G/L ratio approaches G_{min}/L, the exit air approaches equilibrium with the inlet water, the mass transfer rate goes to zero, and infinite packed volume is required. As the actual gas rate is increased above G_{min}, the required packed volume initially decreases rapidly and eventually approaches an asymptote for each column diameter. Normal column operation with respect to pressure drop is represented by the solid lines for each diameter. The onset of loading was taken to correspond to a pressure drop of 0.75 inches H_2O/ft of packing, and the loading region is represented by the dashed lines. For these calculations, flooding was assumed to occur at a pressure drop of 2.0 inches H_2O/ft and each of the lines terminates at this condition.

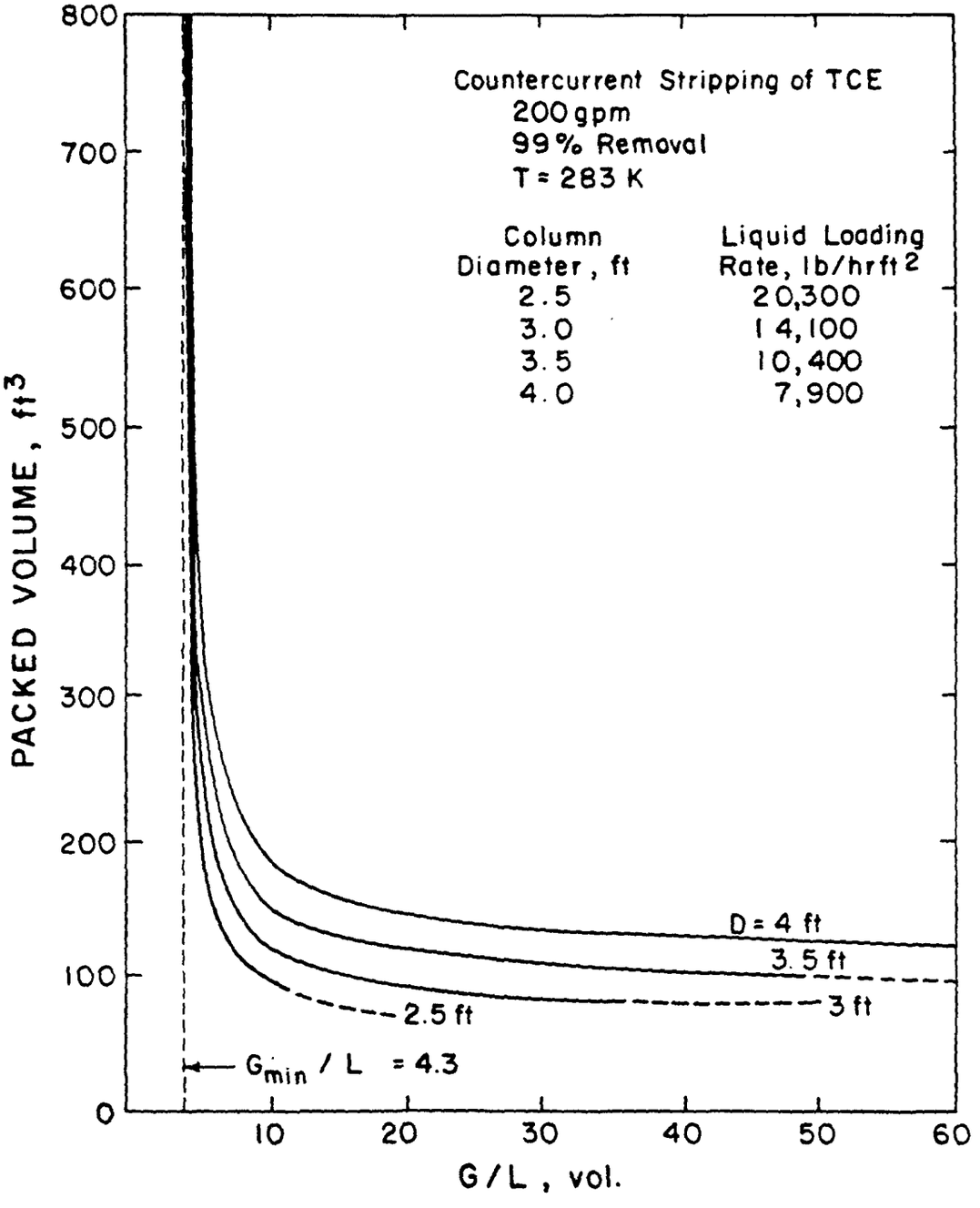

Figure 55. Design Calculations Showing Packed Volume as a Function of Column Diameter and Gas Flow Rate: 99 Percent Removal of TCE at 200 gpm using Countercurrent Flow.

The figure shows that while minimum packed volume may be achieved by using a small diameter column, the range of permissible gas flow rates is severely restricted. For example, G/L values greater than 60 may be used without entering the loading region in a 4-foot diameter column; however, in a 2.5-foot diameter column loading is predicted to begin at G/L ~ 12 and flooding to occur at G/L ~ 20.

Figure 56 shows the variation in packed height and theoretical pump and blower horsepower as a function of gas flow rate for a fixed column diameter of 3 feet. This is a companion to Figure 55 and also uses the parameters of 99 percent removal of TCE from 200 gpm of water in countercurrent operation. Packed height decreases rapidly as gas flow increases above the minimum value. However, for G/L greater than approximately 15, the packed height is relatively constant in the range of 11 to 14 feet. The theoretical pump horsepower curve tracks the packed height curve almost exactly, as shown by Equation (39). Since the liquid flow rate is constant, the horsepower is directly proportional to column height. Theoretical blower horsepower approaches infinity as the gas flow approaches the theoretical minimum because of the infinitely large packed height at this condition. Initial increases in gas flow above the minimum result in a rapid decrease in horsepower. In this region, the decrease in packed height, which reduces the total pressure drop, is more important than the increase in gas flow rate. The required horsepower reaches a minimum value at G/L ~ 5, after which the blower horsepower increases. In this region the increased flow rate outweighs the further small decreases in packed height. The pump and blower horsepower requirements become equal at G/L ~ 28 after which the required blower horsepower exceeds the pump horsepower.

Increasing the water feed rate from 200 to 1500 gpm necessitates a larger diameter column and increases the required pump and blower horsepowers. The stripping of lower volatility (lower Henry's constant) contaminants such as 1,2-DCA or MEK results in a larger G_{min}/L which in turn requires a larger column diameter and increased blower horsepower. In contrast, the packed height and pump horsepower are relatively independent of the volatility of the contaminant. Although the magnitudes of the parameters in Figures 55 and 56 change with flow rate and component volatility, the general shape of the curves remains the same.

The shapes of the curves for crossflow operation are also similar. However, crossflow operation introduces the additional design parameter of baffle spacing or α. Figure 57 compares the required packed volume for countercurrent and crossflow operation for 99 percent removal of TCE at 200 gpm in a 3-foot diameter column. The packed volume for crossflow operation is relatively independent of baffle spacing as indicated by the curves for $\alpha = 1$ and $\alpha = 4$. The packed volume is considerably less in crossflow; however, since only 65 percent of the total cross-sectional area is packed, the packed height is slighly greater. The absence of a strong dependence of packed volume on α for crossflow operation is due to the fact that liquid phase mass transfer resistance is the most important factor for TCE stripping. Variation in α alters the gas loading rate but does not change the liquid loading rate, and

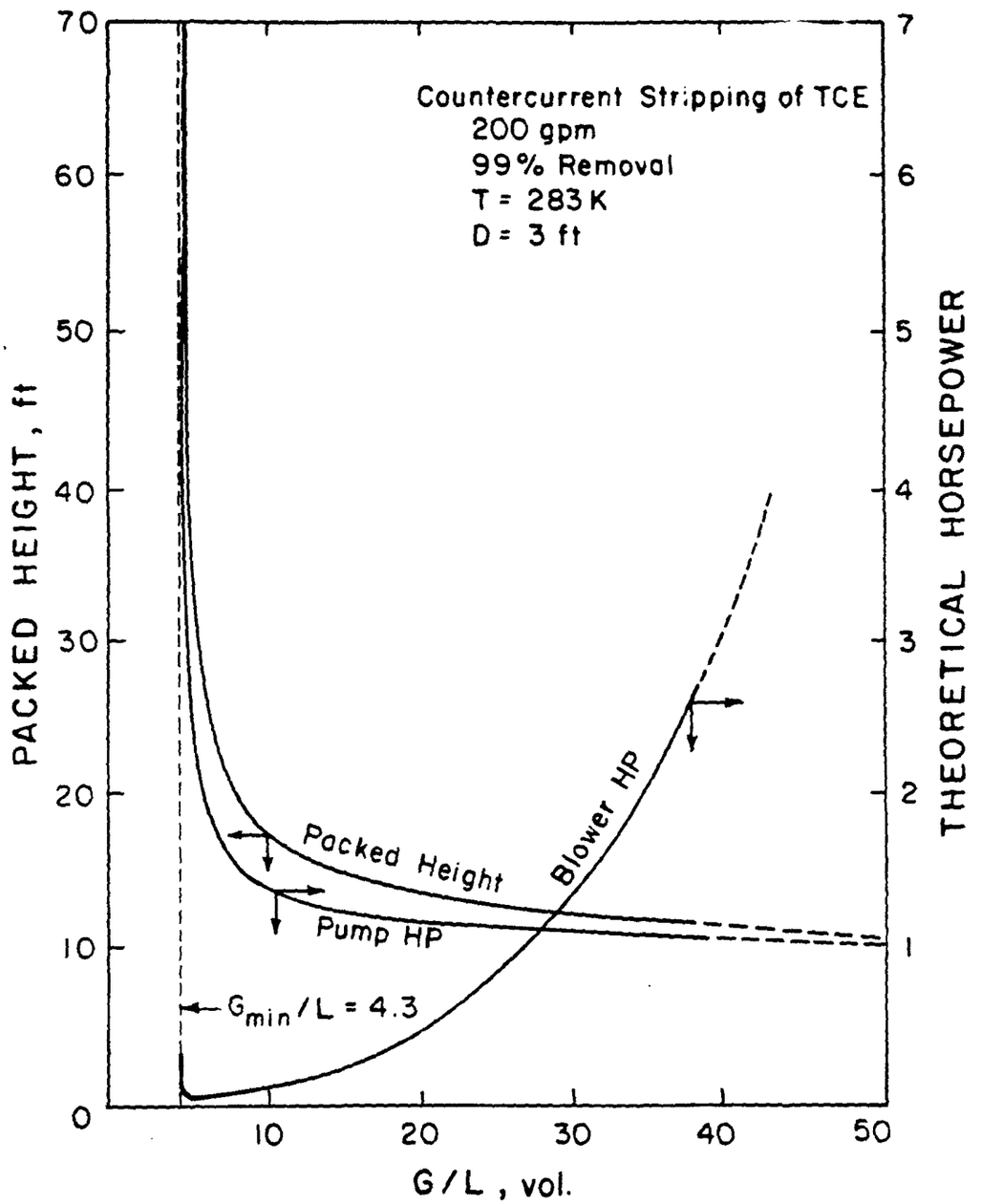

Figure 56. Design Calculations Showing Packed Height and Theoretical Pump and Blower Horsepowers as a Function of Gas Flow Rate: 99 Percent Removal of TCE at 200 gpm using a 3-Foot Diameter Countercurrent Column.

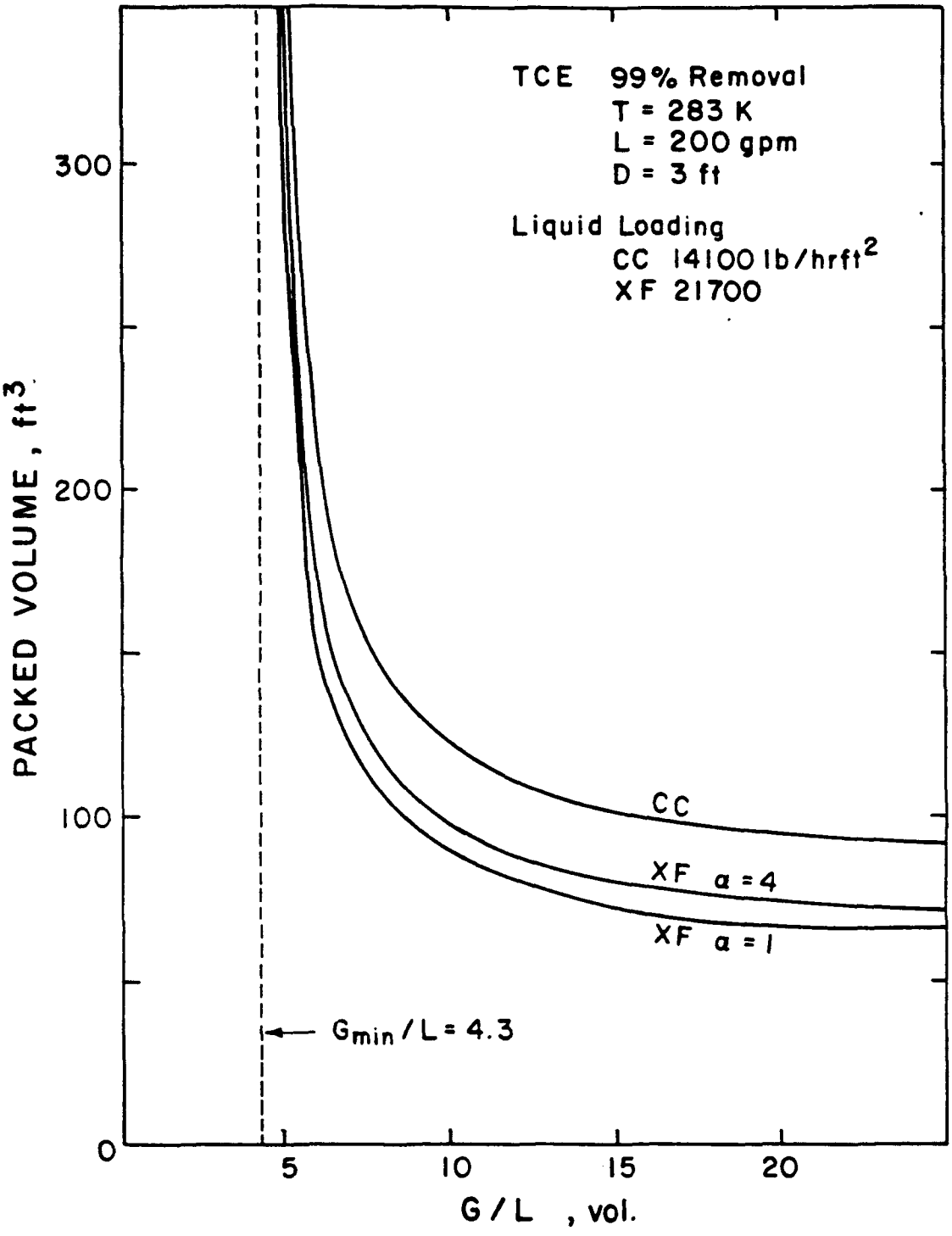

Figure 57. Design Calculations Comparing Packed Volume in Crossflow and Countercurrent Operation as a Function of Gas Flow Rate and Baffle Spacing: 99 Percent Removal of TCE at 200 gpm in a 3-Foot Diameter Column.

the overall mass transfer coefficient is primarily a function of liquid loading.

Blower and pump theoretical horsepower comparisons for the same system are shown in Figure 58. The estimated pump horsepower for countercurrent operation is somewhat less than for crossflow since pump horsepower is determined by column height rather than column volume. Variation in α in crossflow operation has little effect on packed height and, therefore, on pump horsepower. Large blower horsepower requirements for all operating modes at low gas rates are due to the very large packed heights required at these conditions. As gas rate is increased the added power needed to process larger quantities of gas is more than offset by the decreased packed height and the required blower horsepower decreases. The effect of the increased gas flow rate quickly becomes more significant than the decreased packed height and a minimum in the blower horsepower curve is reached, in this case at a G/L ratio of approximately 6. Further increases in gas flow rate then result in increased blower horsepower.

In crossflow operation, blower horsepower is a strong function of α, and, for this example case, the blower horsepower required for countercurrent operation lies between the horsepower required for crossflow operation with $\alpha = 2$ and $\alpha = 3$. Since only 65 percent of the cross-section is packed in crossflow, a water flow rate of 200 gpm in a 3-foot diameter column produces a liquid loading rate of 21,700 lb/hr ft^2 compared to 14,100 lb/hr ft^2 in countercurrent flow. The higher liquid loading rate increases the term $10^{\phi L_m}$ in Equation (36). A reduction in gas loading to that corresponding to $\alpha = 3$ is required to offset the increased liquid loading and produce an overall pressure drop reduction.

For components having lower volatility the relative importance of the blower horsepower to pump horsepower increases as the total quantity of air to be processed increases. This is illustrated in Figures 59 and 60, which are analogous to Figures 57 and 58, except that the contaminant is 1,2-DCA having a Henry's constant of 0.00117 $atm \cdot m^3/gmol$, approximately 78 percent less than TCE. 200 gpm of water flow with 99 percent stripping efficiency is applicable in both cases. However, the column diameter for 1,2-DCA stripping is 5 feet, compared to 3 feet for TCE. The larger column diameter is required to accomodate the larger air flow.

The shapes and relative positions of the curves relating packed volumes and G/L in Figures 57 and 59 are similar. Greater packed volume is required for countercurrent operation and the crossflow packed volume is relatively independent of baffle spacing. The minimum G/L for 1,2-DCA is 19.6 compared to 4.3 for TCE, with the increase due to the reduction in Henry's constant. Liquid loading rates are reduced in both countercurrent and crossflow columns because of the larger diameter, and the difference in loading rates is again due to the fact that only 65 percent of the area is packed during crossflow.

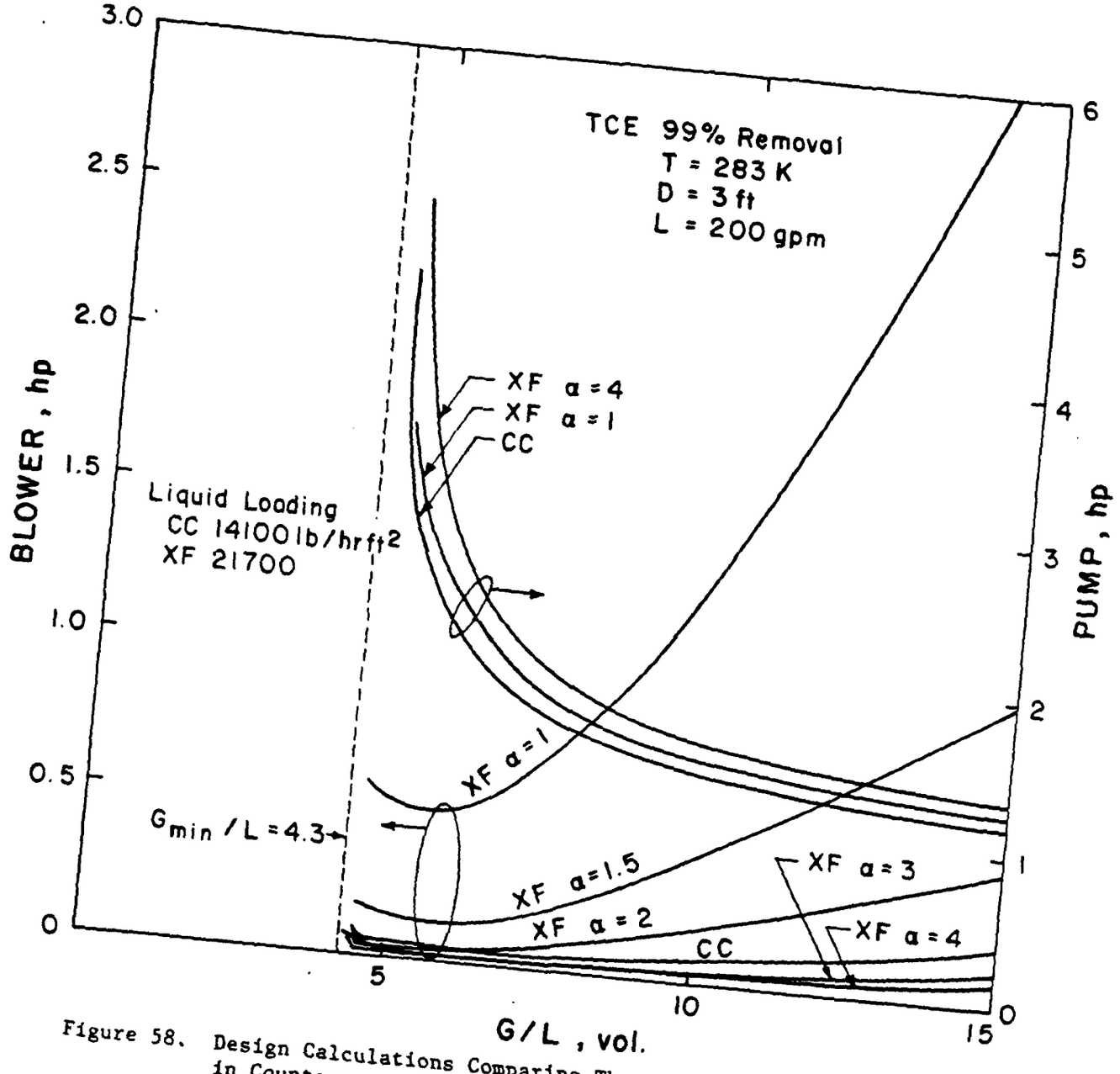

Figure 58. Design Calculations Comparing Theoretical Power Requirements in Countercurrent and Crossflow Operation as a Function of Gas Flow Rate and Baffle Spacing: 99 Percent Removal of TCE at 200 gpm in a 3-Foot Diameter Column.

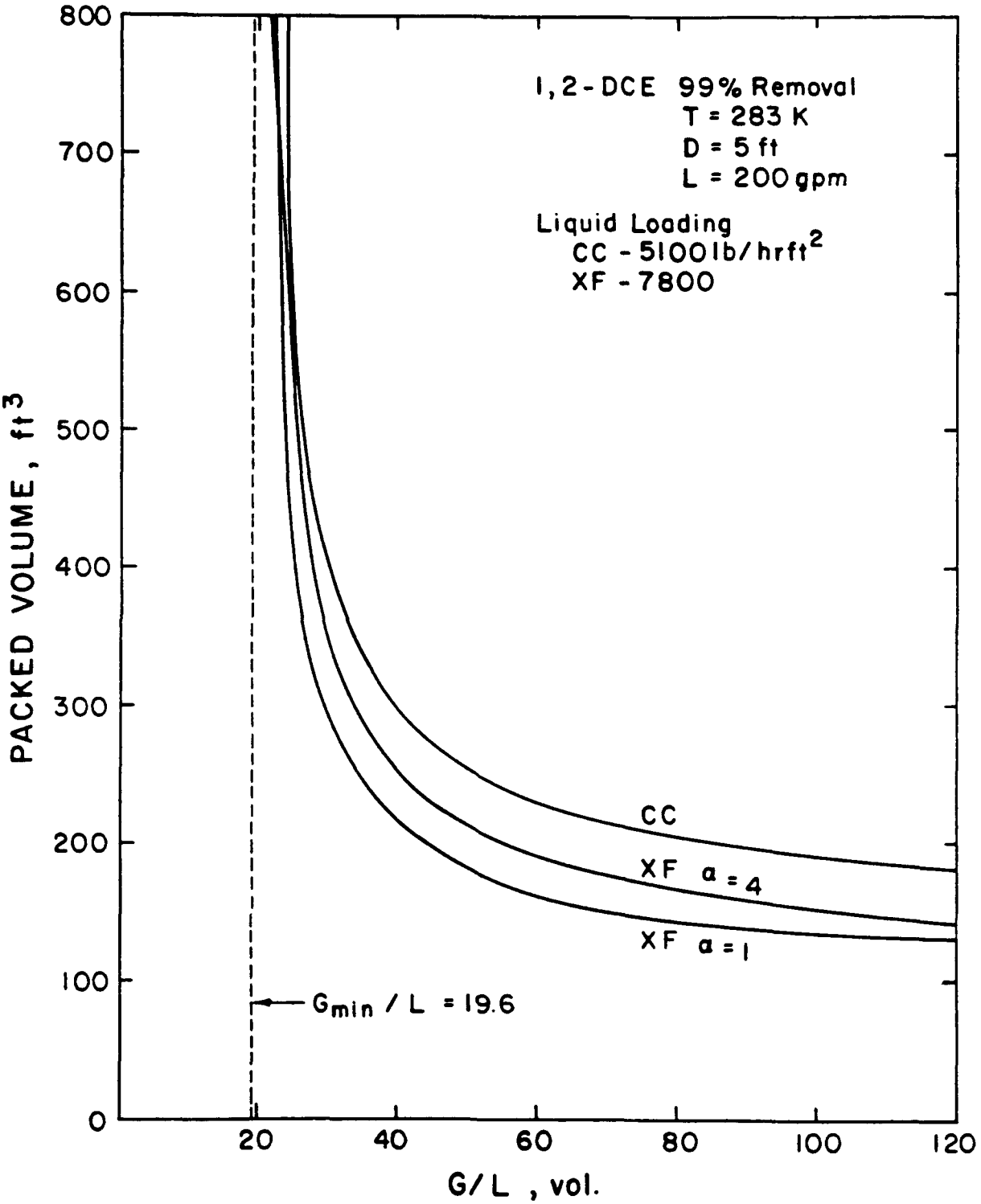

Figure 59. Design Calculations Comparing Packed Volume in Countercurrent and Crossflow Operation as a Function of Gas Flow Rate and Baffle Spacing: 99 Percent Removal of 1,2-DCA at 200 gpm in a 5-Foot Diameter Column.

In Figure 60, the general shapes of the pump and blower horsepower curves are similar to those in Figure 58. The blower horsepower required for countercurrent operation lies between the values for $\alpha = 1$ and $\alpha = 2$ for crossflow operation. However, the blower power requirements for 1,2-DCA are significantly higher than for TCE, due to the increased volume of air required, while pump power requirements are approximately the same.

Complete design calculations similar to those illustrated were carried out for each of the three compounds using both crossflow and countercurrent flow modes. Column diameter and G/L ratio served as primary design parameters while the additional parameter of baffle spacing was considered in crossflow. Results of the design calculations then served as input to the comparative economic analysis to be described in the following section.

E. ECONOMIC EVALUATION METHOD

The purpose of the preliminary economic evaluation was to compare the costs of countercurrent and crossflow stripping and to identify situations in which crossflow stripping could provide significant cost savings. In order to meet this objective, only items involving significant cost difference were considered. For example, on the basis of current knowledge, it was presumed that maintenance costs for the two flow modes would be equivalent; consequently, maintenance costs were omitted from the comparison.

Purchased equipment costs for individual equipment items were estimated using published cost charts. Individual costs were updated to 1989 costs using cost indices, and then summed to give the total purchased equipment cost. Total capital investment was then estimated by multiplying the total purchased equipment cost by an appropriate factor. Annual capital costs were estimated based upon a specified interest rate and expected equipment lifetime. Total annual costs were taken to be the sum of the annual capital costs and the cost of electricity for pump and blower operation.

Due to the uncertainties involved in cost estimations at this stage of process development, multiple estimates based upon different assumptions were included. For example, two different cost factors were used to estimate total capital investment from puchased equipment cost. Similarly, because of the uncertainties involved in crossflow stripping, two methods were used to estimate the purchased equipment cost of packing and associated column internals. These and other differences are fully described below.

1. Purchased Equipment Cost

Six separate equipment items were considered:

a. tower
b. packing plus tower internals
c. pump
d. blower
e. pump motor
f. blower motor

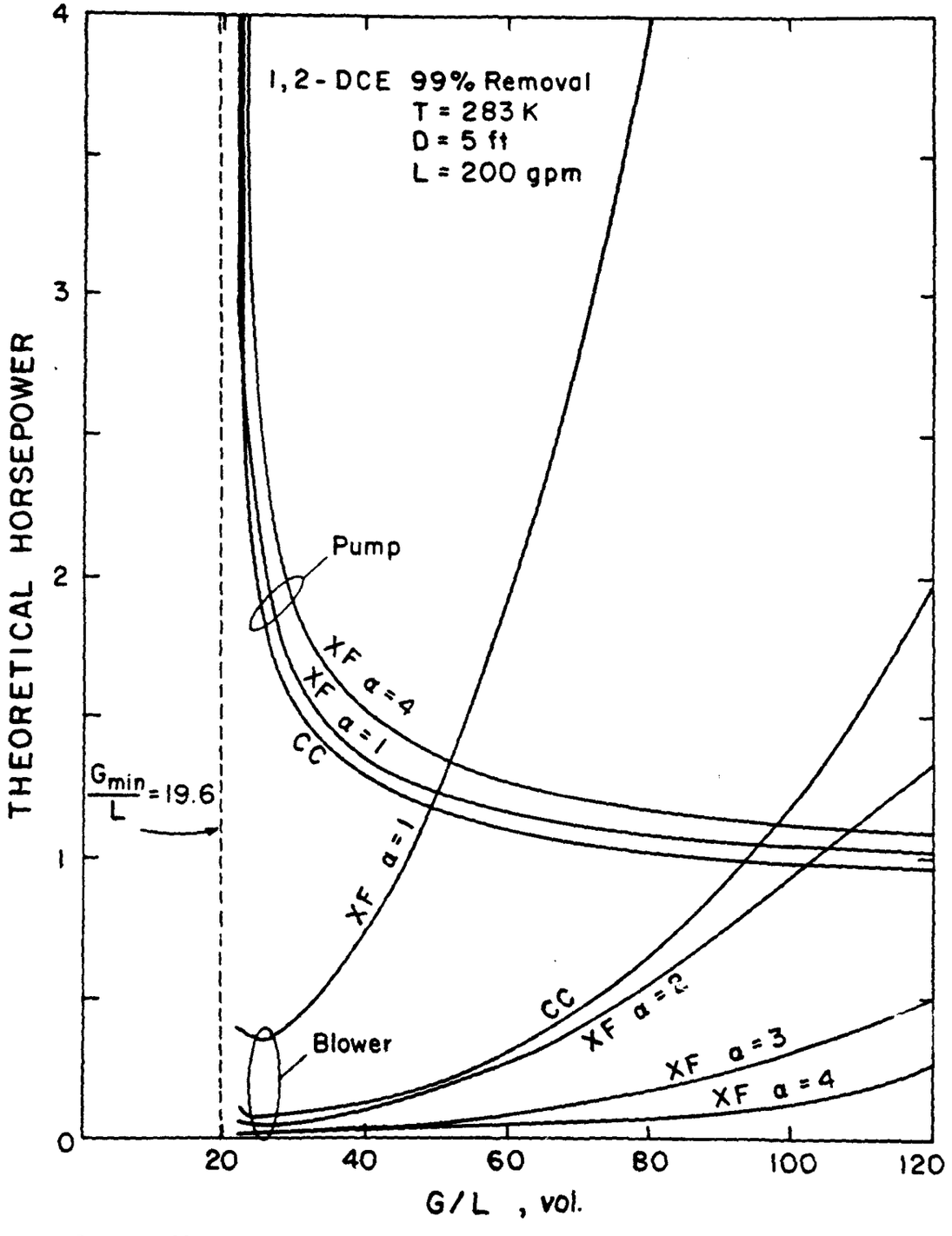

Figure 60. Design Calculations Comparing Theoretical Power Requirements in Countercurrent and Crossflow Operation as a Function of Gas Flow Rate and Baffle Spacing: 99 Percent Removal of 1,2-DCA at 200 gpm in a 5-Foot Diameter Column.

The purchased cost of the tower as a function of diameter and height was estimated from a cost chart from Page 307 of Ulrich (Reference 40). The cost data are for carbon steel construction and the applicable CE Plant Cost Index was 315. A correction factor representing fiberglass-reinforced plastic (FRP) construction as shown in Figure 61 was applied to the raw cost data. The correction factor curve was based upon actual estimates of specific column costs for both FRP and carbon steel construction for 3-foot and 5-foot diameter columns. A cost saving associated with FRP is indicated for diameters less than 6 feet. For larger columns ($\geq$ 6-foot diameter) carbon steel construction was assumed and the estimated costs from Ulrich were used directly. The CE Plant Cost Index in mid-1989 was 355, and all tower cost estimates were multipled by 355/315 = 1.13 to represent current costs. There was no difference in the tower cost estimation procedure for the countercurrent and crossflow modes of operation. Both were determined from the height and diameter results of the design study.

The purchased cost of packing plus tower internals was also estimated using a cost chart from Ulrich (Reference 40). For countercurrent flow, cost estimates were made directly from the chart and updated to present cost by the factor of 1.13. In crossflow, the amount of packing required for a specified diameter and packed height is only 65 percent of the total volume. However, the column internals are more complex than in countercurrent flow. Since the added cost associated with the more complex internals is not known, two separate estimates were made (Methods II and III). In Method II, the cost estimate from Ulrich's chart was first reduced by 35 percent to account for the lower amount of packing needed, and then multiplied by a factor of 2 to represent the more complex internal structure. The net result was a packing plus internals cost 1.3 times the cost of packing plus internals costs for a comparably sized countercurrent system. In Method III, the internal complexity factor was reduced to 1.5, producing an overall factor of 0.975. This factor indicates that cost saving associated with reduced packing volume is almost exactly offset by the cost increase associated with the more complex internals.

The costs of the blower, pump, and motors to drive both were estimated from cost charts in Peters and Timmerhaus (Reference 41). The base Marshall and Stevens (M&S) cost index for each of these charts was 561. The current M&S cost index is 903 so that a cost multiplier of 1.61 was applied to each item. The estimation procedure for each of these items was the same for countercurrent and crossflow operation. A general purpose centrifugal pump was assumed and the cost was fixed solely by the water flow rate and the liquid head.

The type of blower specified depended upon the predicted pressure drop across the column. For pressure drops less than 3 1/2 inches of water, the cost was based upon the purchase of a relatively inexpensive centrifugal fan. For larger pressure drops, the cost estimate was based upon the purchase of a more expensive turbo blower. Since at a fixed air flow rate, the turbo blower is approximately 10 times more expensive than the centrifugal fan, there is a significant economic incentive to keep the pressure drop below 3 1/2 inches of water. This factor works in favor of crossflow operation. The cost of both the pump and blower

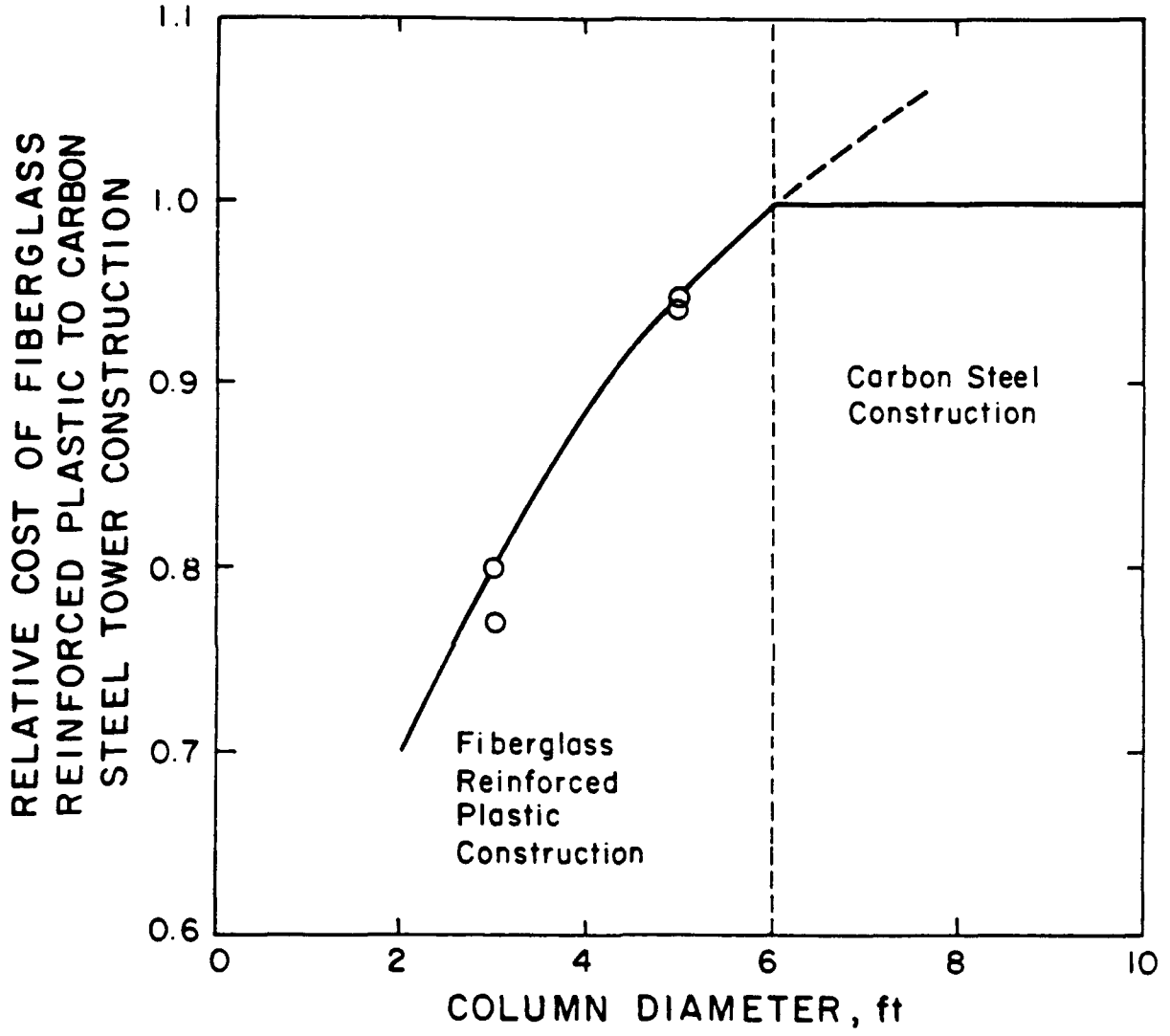

Figure 61. Material of Construction Factor for Fiberglass Reinforced Plastic Towers.

motors was based upon the use of alternating current and explosion proof housing. A pump efficiency of 75 percent and blower efficiency of 50 percent were assumed for converting theoretical horsepower to delivered horsepower.

In summary, for each design case subjected to economic analysis, three separate puchased equipment cost estimates were made. One cost estimate was for countercurrent flow and the other two were for crossflow. The two crossflow estimates differed in the way that the "packing plus tower internals" component was handled. In the first case, the puchased cost from the cost chart was multiplied by 1.3 reflecting a higher cost of column internals. In the second case, the multiplying factor was 0.975 reflecting a more moderate column internals cost. Individual puchased equipment cost estimates for an example design case are summarized in Table 3. The example case represents 99 percent removal of TCE from 200 gpm of water using a column diameter of 3 feet and an air flow rate of twice the minimim. In crossflow operation the baffle spacing corresponds to $\alpha = 3$. A slightly taller tower is required in crossflow operation which accounts for the higher tower cost. Packing plus internals cost for crossflow is also higher both because of the greater packed height and the more complex internals. All of the remaining costs are relatively small and the only equipment item which results in a cost saving for crossflow is provided by the blower.

2. Total Capital Investment

Total capital investment, which includes such items as piping, instrumentation, and equipment installation, was estimated as a factor of the purchased equipment cost. Because of the large uncertainty in the factor and the desire to examine the sensitivity of the economics to a wide variety of conditions, two cases were developed. In case A, which is referred to as a capital intensive case, the total capital investment was taken to be 4.0 times the purchased equipment cost. In case B, operating costs are stressed, and the total capital investiment was calculated as 2.4 times the purchased equipment costs. Other differences between Cases A and B will be developed in the following discussion.

The two capital investment cost cases result in a total of six cost estimates associated with each design case. Item 2 in Table 4 summarizes the six total capital investment estimates generated from the three purchased equipment cost estimates from Table 3 and reproduced as Item 1 in Table 4. Other entries in Table 4 are explained in the following sections. It should be recognized that the chosen example case does not represent an economic optimum for either countercurrent or crossflow operation. The example is chosen only to illustrate the procedure.

TABLE 3. 1989 PURCHASED EQUIPMENT COST ESTIMATES FOR COUNTERCURRENT AND CROSSFLOW OPERATION

99 percent Removal of TCE
Water Flow - 200 gpm
Column Diameter - 3 ft.
Air Flow Rate - 2 x G_{min}
Crossflow - $\alpha = 3$

Item	Countercurrent	Crossflow	
	Method I ($)	Method II ($)	Method III ($)
Tower	14,100	15,000	15,000
Packing Plus Internals	5,100	7,300	5,500
Pump	1,500	1,500	1,500
Blower	1,100	970	970
Pump Motor	430	450	450
Blower Motor	240	240	240
Total	22,500	25,500	23,700

TABLE 4. EXAMPLE METHOD FOR ESTIMATING TOTAL COST

99 percent Removal of TCE
Water Flow - 200 gpm
Column Diameter - 3 ft
Air Flow Rate - 2 x G_{min}
Crossflow - $\alpha = 3$

	Countercurrent	Crossflow	
	Method I	Method II	Method III
1. Purchased Equipment Cost (PEC), $	22,500	25,500	23,700
2. Total Capital Investment (TCI)			
Case A (4 x PEC), $	90,000	102,000	94,800
Case B (2.4 x PEC), $	54,000	61,200	56,800
3. Annual Capital Cost			
Case A (0.131 x TCI), $/yr	11,800	13,400	12,400
Case B (0.117 x TCI), $/yr	6,300	7,200	6,600
4. Operating Cost			
Pump			
Case A, $/yr	680	650	650
Case B, $/yr	710	800	800
Blower			
Case A, $/yr	20	20	20
Case B, $/yr	30	20	20
5. Total Cost			
Case A			
$/yr	12,400	14,100	13,100
$/$10^3$ gal	0.143	0.162	0.152
Case B			
$/yr	7,060	8,000	7,480
$/$10^3$ gal	0.067	0.075	0.071

3. Annual Capital Cost

Annual capital costs were calculated using the formula

$$ACC = TCI \left[\frac{i(1 + i)^n}{(i + 1)^n - 1}\right] \quad (41)$$

where i is the interest rate and n is the lifetime of the equipment. For both Cases A and B, i was taken to be 0.1. In keeping with the capital cost emphasis for Case A, a 15-year equipment lifetime was used, while in Case B the equipment was assumed to have a 20-year lifetime. As a result

$$\text{Case A} \quad ACC = 0.131 \times TCI \quad (42)$$

$$\text{Case B} \quad ACC = 0.117 \times TCI \quad (43)$$

Annual capital costs calculated from these equations are summarized as Item 3 of Table 4 for the example case.

4. Operating Cost

As previously mentioned the only operating costs considered in this comparative economic study were the costs of power to drive the pump motor and blower motor. In all calculations the cost of electricity was taken to be \$0.055/kwh. The pump and blower efficiencies were assumed to be 75 percent and 50 percent, respectively. The other parameter required to calculate operating cost is the time on stream, i.e., the days per year during which the stripping column is operated. In Case A, the system was assumed to operate 300 days per year while full-time operation, i.e., 365 days per year was assumed for Case B. These time on stream assumptions are consistent with the previously stated capital cost emphasis for Case A and operating cost emphasis for Case B.

Operating costs for the example case are summarized as Item 4 of Table 4. Blower operating costs are small compared to pump operating costs because of the low air flow associated with the example case. Also there is no significant operating cost savings associated with crossflow stripping because the blower operating costs are small in both modes of operation. Both of these factors change, however, as the air flow rate is increased.

5. Total Cost

The total comparative cost was taken to be the sum of the annual capital cost and the operating costs for the pump and blower. All other costs factors were assumed to be equal for the two modes of operation. Total cost estimates for the example case are summarized in Item 5 of Table 4. The total cost is expressed in two sets of units, \$/yr and $\$/10^3$ gal.

Traditional countercurrent stripping would be more economical in this example case. As will be shown in the following sections, this is generally true for highly volatile components such as TCE and for relatively low water treatment rates such as 200 gpm. The economic attractiveness of crossflow stripping increases with increasing treatment rate and decreasing component volatility.

F. ECONOMIC EVALUATION RESULTS

Economic evaluations were carried out at selected column diameters and air flow rates for each of the six design cases representing water flow rates of 200 and 1500 gpm and three contaminants - TCE, 1,2-DCA, and MEK. Crossflow calculations were limited to a baffle spacing corresponding to $\alpha = 3$ since, as previously shown, smaller values of α do not result in the desired pressure drop saving. Trends in the various cost components as a function of column diameter and air flow rate for the example design case involving a water treatment rate of 200 gpm with 99 percent TCE removal are discussed in the following.

Figure 62 shows the effect of air flow rate, expressed as a multiplier of the minimum air rate, on 1989 purchased equipment costs for a 3-foot diameter countercurrent column. The tower is the most costly equipment item at all air rates. Both the tower and packing plus tower internals costs decrease with increasing air rate, while the blower cost increases with air rate. The sharp increase in blower cost at an air flow rate approximately three times the minimum is caused by the need to shift from a centrifugal fan to a turbo blower necessitated by increased gas-phase pressure drop. Costs of the pump, pump motor, and blower motor are small throughout. The abrupt increase in blower cost causes a similar increase in total purchased equipment cost. The overall minimum purchased equipment cost of about $19,900 occurs at an air rate approximately 2.6 times the minimum. Note that the minimum purchased equipment cost is approximately 12 percent less than associated with the example case in Tables 3 and 4. The previous example case utilized an air flow rate of 3 times the minimum value compared to the optimum air rate of 2.6 times the minimum rate.

Comparable 1989 purchased equipment cost estimates as a function of column diameter at a fixed air flow rate corresponding to $(G/L) = 2.6 \times (G/L)_{min}$ are shown in Figure 63. Tower and packing costs increase significantly with increasing diameter, while pump, pump motor, and blower motor costs are approximately constant. There is a significant decrease in blower costs between 2.5 and 3.0 feet diameter caused by the shift from a turbo blower to a centrifugal fan. At diameters above 3.0 feet the blower costs are approximately constant. The total purchased equipment cost is a minimum ($19,400) at 2.5 feet diameter. There is a slight increase to $19,900 at 3.0 feet diameter followed by a more rapid increase thereafter.

Total annual cost, expressed in $/yr, for a countercurrent column having a diameter of 3.0 feet as a function of air flow rate is shown in Figure 64. Annual capital costs and operating costs in this figure are based upon parameters corresponding to economic Case A. The minimum total cost of $11,000/yr occurs at an air rate corresponding to (G/L) =

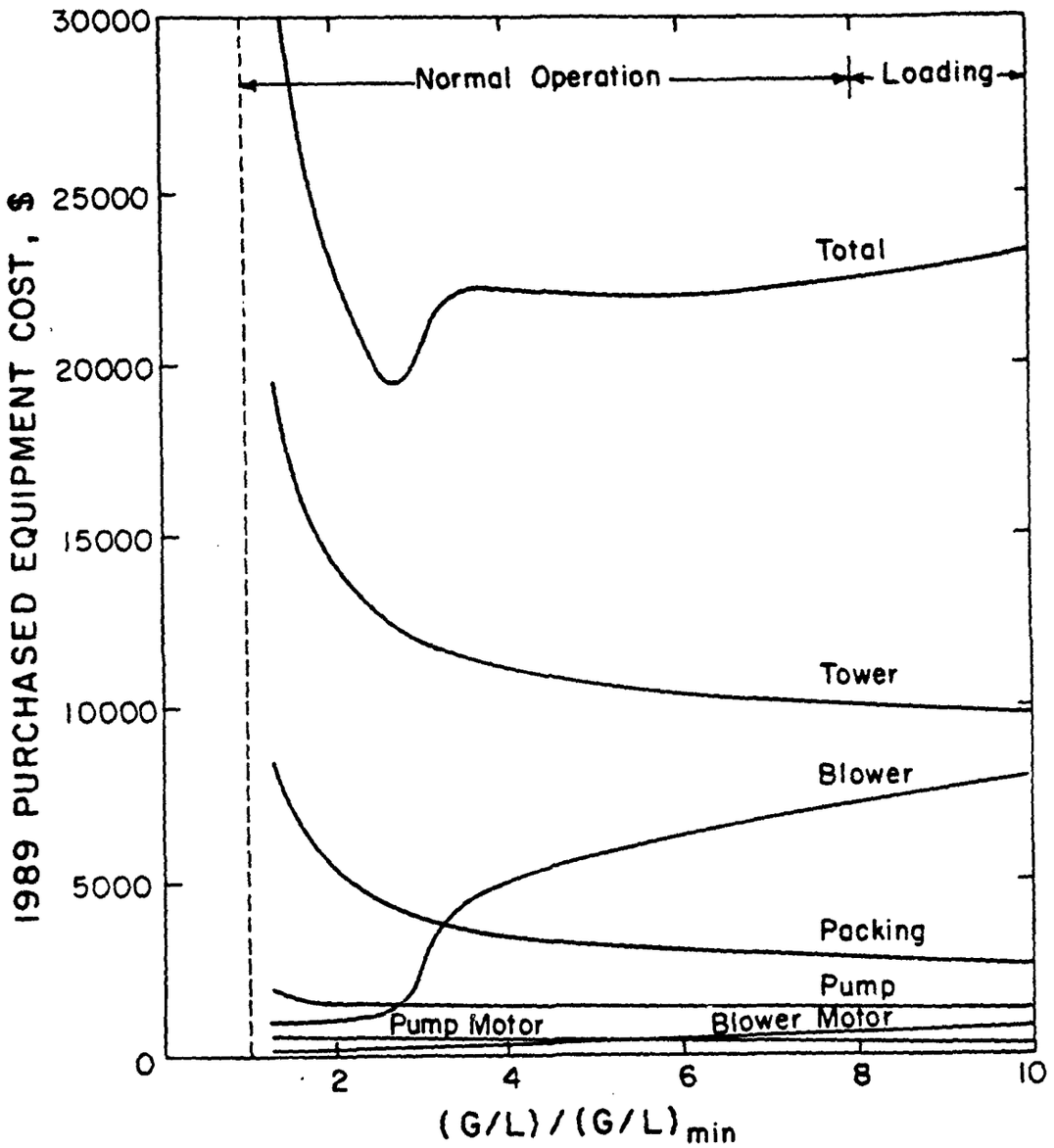

Figure 62. Purchased Equipment Costs as a Function of Gas Flow Rate: 99 Percent Removal of TCE at 200 gpm in a 3-Foot Diameter Countercurrent Column.

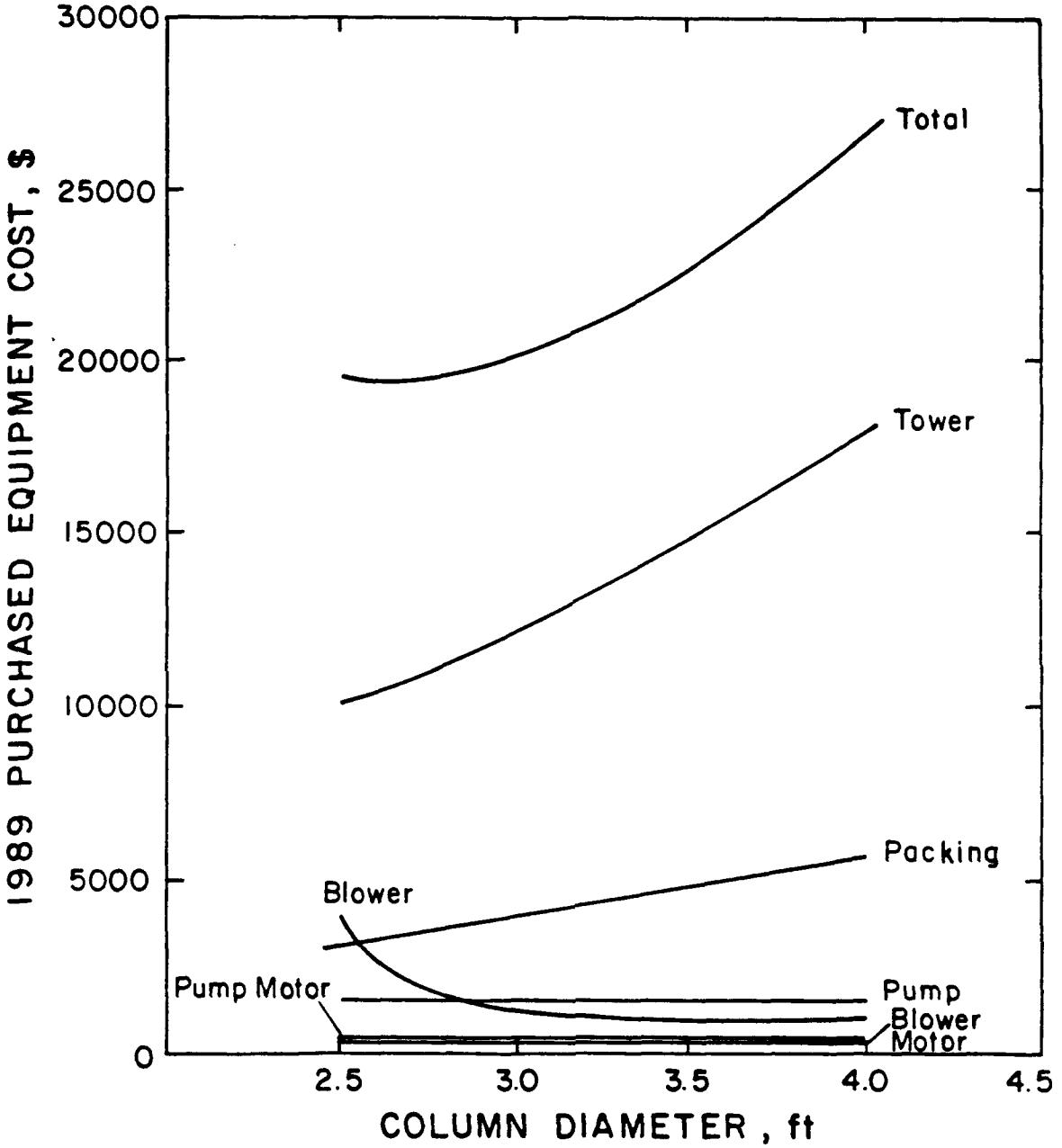

Figure 63. Purchased Equipment Costs as a Function of Column Diameter: 99 Percent Removal of TCE at 200 gpm in Countercurrent Operation using an Air Flow Rate of 2.6 Times the Minimum Flow Rate.

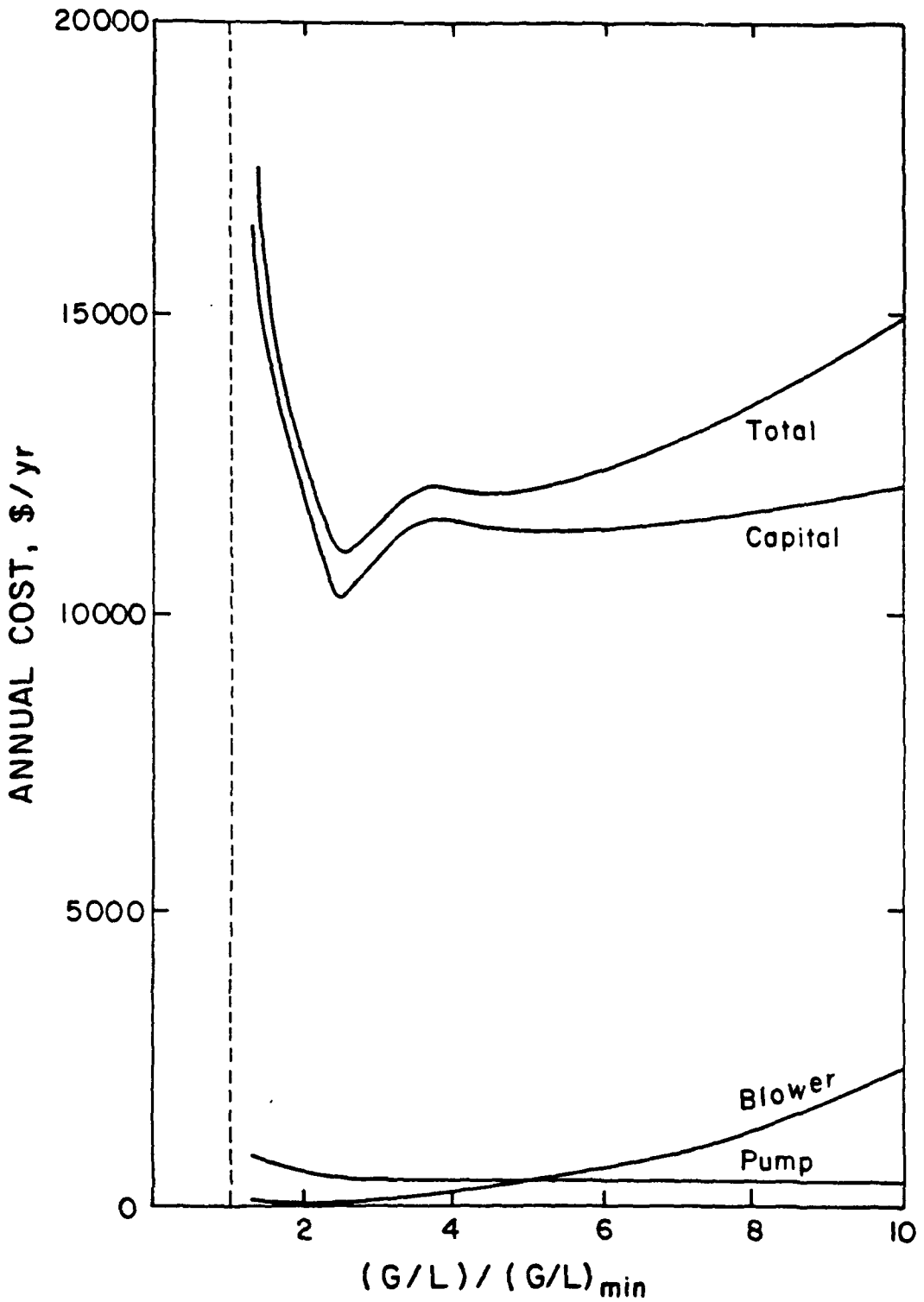

Figure 64. Annual Cost as a Function of Gas Flow Rate: 99 Percent Removal of TCE at 200 gpm in a 3-Foot Diameter Countercurrent Column.

2.6 x $(G/L)_{min}$. At these conditions the operating costs account for only about 5 percent of the total annual cost. It is only at the very high air rates, well above the economic optimum, that operating costs become significant. The \$11,000/yr total annual cost is equivalent to a treatment cost of $\$0.127/10^3$ gal.

Similar calculations for countercurrent stripping with the same column diameter and 99 percent removal of TCE from 200 gpm of water, but based upon the economic parameters of Case B, produce a minimum total cost estimate of \$6,300/yr, which corresponds to a treatment cost of $\$0.060/10^3$ gal. This minimum also occurs at a gas rate corresponding to $(G/L) = 2.6 \times (G/L)_{min}$. The lower annual cost for Case B is due primarily to the smaller factor used to relate total capital investment to purchased equipment cost. The lower treatment cost ($\$/10^3$ gal) is due to the lower capital investment and the fact that 100 percent on-stream operation corresponds to a 20 percent annual increase in the amount of water treated.

Figure 65 establishes the column diameter and gas flow rate corresponding to the overall minimum cost (Case A) for 99 percent removal of TCE from 200 gpm of water in countercurrent flow. Four column diameters were considered and the overall minimum cost corresponds to a 3.5-foot diameter column operated at an air rate corresponding to $G/L = 6.4 \times (G/L)_{min}$. The total estimated cost at these conditions is \$10,500/yr or $\$0.122/10^3$ gal. 94.3 percent of the total cost at these conditions is associated with annual captial costs; the pump operation amounts to 4.0 percent of the total and the blower operation is 1.7 percent of the total.

In addition to noting the minimum overall cost, it is instructive to examine the general shape of the curves. At low gas rates, the total cost decreases rapidly for each diameter. The curve for the 2.5-foot diameter column terminates at $(G/L)/(G/L)_{min} \sim 3.6$ which corresponds to the predicted flooding rate. As the diameter increases the minimum in the cost curve shifts to higher gas rates due to the fact that pressure drop limits, and therefore the blower equipment cost and operating cost, are associated with increasingly high gas rates in larger diameter columns. The sharp breaks in the 3-foot and the 3.5-foot diameter curves at $(G/L)/(G/L)_{min}$ of 2.6 and 6.5, respectively, are the result of the need to shift from a centrifugal fan to a turbo blower at these air rates. The magnitude of the economic impact of the shift is much greater at the 3.5-foot diameter because of the larger air rate involved.

Similar analyses were carried out for each contaminant at each flow rate using both countercurrent and crossflow contacting modes. Calculations were made using economic parameters corresponding to Cases A and B. In crossflow operation both cost Methods II and III were used to estimate the purchased cost of the packing plus internals. Results are summarized in the following section.

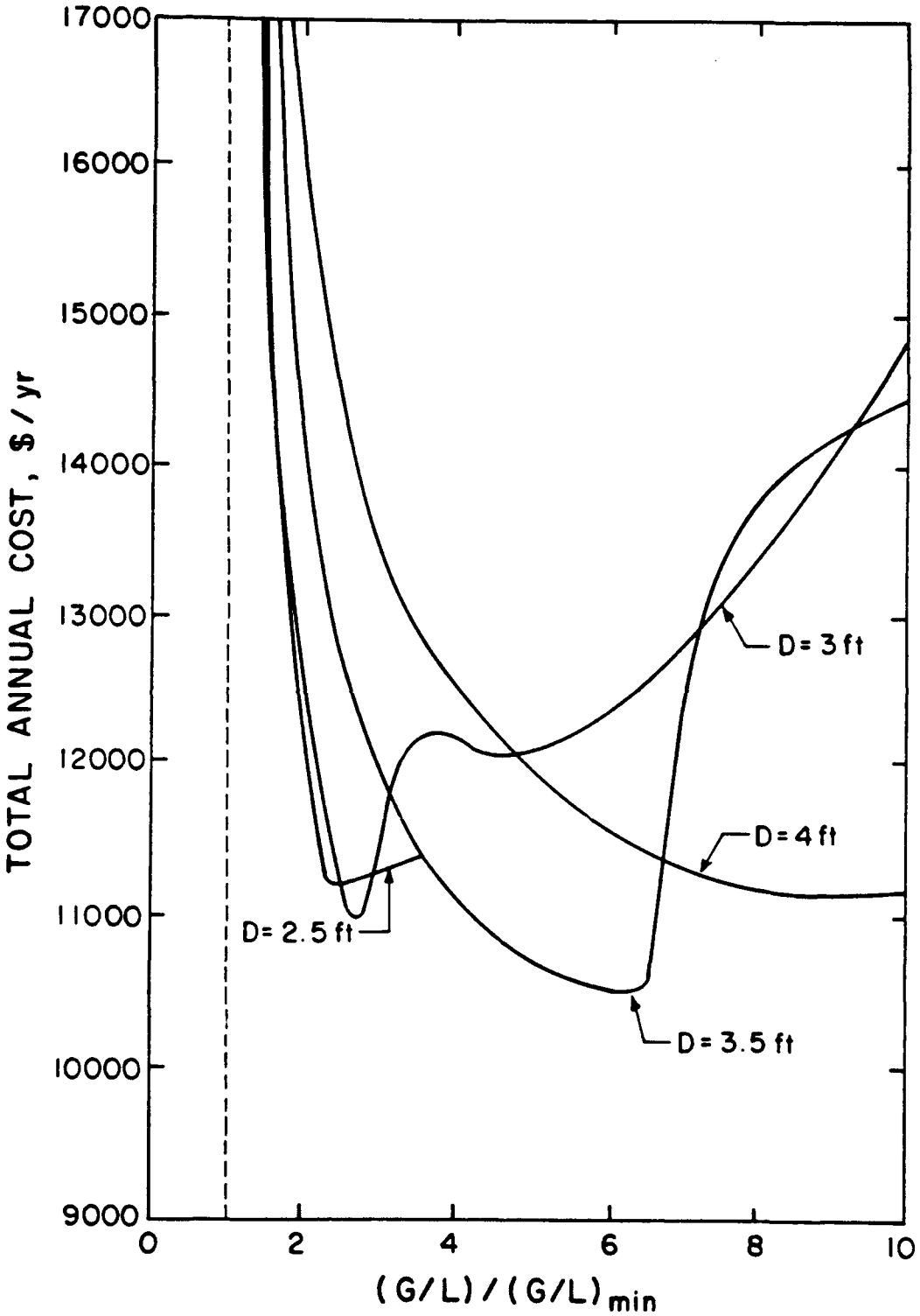

Figure 65. Annual Cost as a Function of Column Diameter and Gas Flow Rate: 99 Percent Removal of TCE at 200 gpm in Countercurrent Operation.

G. MINIMUM COST SUMMARY

The set of design and operating conditions resulting in minimum cost, plus the cost estimates at these conditions for the three contaminants at two flow rates are summarized in Tables 5 through 10. The procedures described in the previous example were used for all cases.

Table 5 summarizes results for 99 percent removal of TCE at a flow rate of 200 gpm. The first column of results applies to countercurrent flow using economic Case A which served as the example. Bottom-line cost estimates indicate that countercurrent stripping would be more economical with crossflow stripping projected to cost from 1 percent to 8 percent more, depending upon the factor used to estimate the cost of packing plus column internals. Because the projected economic advantages are relatively small, only minor cost reductions would be required to make crossflow stripping economically attractive. It should also be recognized that the estimated cost differences are, in all probability, smaller than the error in the cost estimates themselves.

The primary variation in the most economic design condition appears in the column diameter and gas flow rate columns of Table 5. The higher pressure drop in countercurrent operation dictates that a 3.5-foot diameter column should be used. The optimum value of $(G/L)/(G/L)_{min}$ = 6.5 corresponds to the largest estimated gas flow rate which can be achieved using a centrifugal fan. The lower pressure drop in crossflow permits the smaller column diameter of 3 feet, and the optimum gas flow rate again corresponds the maximum flow rate which can be achieved using a centrifugal fan. Although crossflow permits a smaller diameter column, the required packed height in crossflow is sufficiently greater to result in higher estimated capital costs. The operating costs are small in all cases and operating cost savings associated with crossflow are insufficient to offset the capital cost penalty.

Comparison of Tables 5 and 6 shows the effect of water flow rate on treatment cost for 99 percent TCE removal. Increasing the flow rate from 200 gpm to 1500 gpm results in an estimated cost reduction per thousand gallons treated of approximately 55 percent. The relative economics of crossflow versus countercurrent flow is also slightly improved because larger flow rates tend to reduce the importance of capital costs. Once again, the difference in the estimated costs is smaller than the error in the cost estimates. From the design standpoint it is interesting to note that the optimum column diameter is 8 feet in all cases and that, with equal diameter, the optimum gas flow rates are larger in the crossflow cases.

Tables 7 and 8 describe the optimum economic conditions for 99 percent removal of 1,2-DCA at 200 and 1500 gpm, respectively. The estimated cost for 1,2-DCA removal is approximately 50 percent greater than the comparable cost for TCE removal, primarily because of the lower Henry's constant for 1,2-DCA which necessitates a significant increase in air flow rate. The optimum column diameter for 1,2-DCA stripping at 200 gpm is increased to 5 feet, compared to 3 or 3.5 feet for TCE. Again, the larger diameter is required to accomodate the larger gas flow.

TABLE 5. DESIGN AND OPERATING CONDITIONS RESULTING IN MINIMUM COST: 99 PERCENT TCE REMOVAL at 200 GPM

ECONOMIC BASIS	Case A			Case B		
CONTACTING MODE*	CC	XF3	XF3	CC	XF3	XF3
PURCHASED EQPT. COST METHOD**	I	II	III	I	II	III
DESIGN						
Diameter, ft	3.5	3.0	3.0	3.5	3.0	3.0
Packed Height, ft	11.3	16.3	16.3	11.3	16.3	16.3
L_m, lb/hrft^2	10,400	21,700	21,700	10,400	21,700	21,700
$(G/L)/(G/L)_{min}$	6.5	3.8	3.8	6.5	3.8	3.8
(G/L)	27.8	16.3	16.3	27.8	16.3	16.3
G, cfm	741	433	433	741	433	433
ΔP_{TOT}, in H_2O	2.6	2.7	2.7	2.6	2.7	2.7
Pump, theo. hp	1.1	1.3	1.3	1.1	1.3	1.3
Blower, theo. hp	0.3	0.2	0.2	0.3	0.2	0.2
ECONOMICS						
Purchased Equip. Cost, $	18,960	20,450	19,210	18,960	20,450	19,210
Total Cap. Investment, $	75,800	81,800	76,800	45,500	49,100	46,100
Annual Capital Cost, $/yr	9,930	10,700	10,070	5,320	5,740	5,390
Pump Operating, $/yr	420	520	520	510	640	640
Blower Operating, $/yr	180	60	60	220	80	80
Total Annual Cost, $/yr	10,530	11,300	10,650	6,050	6,460	6,110
$/10^3 gal	.122	.131	.123	.058	.061	.058
COST DISTRIBUTION, PERCENT						
Capital	94.3	94.8	94.5	87.9	88.9	88.3
Pump Operating	4.0	4.6	4.9	8.5	9.9	10.4
Blower Operating	1.7	0.6	0.6	3.6	1.2	1.3
		+7.4%	+0.8%		+5.2%	+0.1%

*CC - countercurrent
XF3 - crossflow with baffle spacing correspond to $\alpha = 3$
** see p. 101 for explanation.

TABLE 6. DESIGN AND OPERATING CONDITIONS RESULTING IN MINIMUM COST: 99 PERCENT TCE REMOVAL at 1,500 GPM

ECONOMIC BASIS	Case A			Case B		
CONTACTING MODE*	CC	XF3	XF3	CC	XF3	XF3
PURCHASED EQPT. COST METHOD**	I	II	III	I	II	III
DESIGN						
Diameter, ft	8	8	8	8	8	8
Packed Height, ft	15.1	14.9	14.9	15.1	15.6	15.6
Lm, $lb/hrft^2$	14,900	22,900	22,900	14,900	22,900	22,900
$(G/L)/(G/L)_{min}$	3.1	5.5	5.5	3.1	4.6	4.6
(G/L)	13.2	23.5	23.5	13.2	19.6	19.6
G, cfm	2,660	4,710	4,710	2,660	3,940	3,940
ΔP_{TOT}, in H_2O	3.5	3.8	3.8	3.5	2.7	2.7
Pump, theo. hp	9.5	9.4	9.4	9.5	9.6	9.6
Blower, theo. hp	1.5	2.8	2.8	1.5	1.7	1.7
ECONOMICS						
Purchased Equip. Cost, $	55,600	57,600	53,300	55,600	59,100	54,700
Total Cap. Investment, $	222,500	236,300	213,300	133,500	141,800	131,200
Annual Capital Cost, $/yr	29,100	31,000	27,900	15,600	16,600	15,400
Pump Operating, $/yr	3,700	3,700	3,700	4,550	4,600	4,620
Blower Operating, $/yr	860	1,640	1,640	1,040	2,000	1,220
Total Annual Cost, $/yr	33,700	35,500	33,300	21,200	22,400	21,200
$/10^3$ gal	.052	.055	.051	.027	.028	.027
COST DISTRIBUTION, PERCENT						
Capital	86.4	85.0	84.0	73.7	73.9	72.4
Pump Operating	11.1	10.4	11.1	21.4	20.6	21.8
Blower Operating	2.5	4.6	4.9	4.9	5.5	5.8
		+5.8%	-1.9%		+3.6%	0.0%

*CC - countercurrent
XF3 - crossflow with baffle spacing correspond to $\alpha = 3$
** see p. 101 for explanation.

TABLE 7. DESIGN AND OPERATING CONDITIONS RESULTING IN MINIMUM COST: 99 PERCENT 1,2-DCE at 200 GPM

ECONOMIC BASIS	Case A			Case B		
CONTACTING MODE*	CC	XF3	XF3	CC	XF3	XF3
PURCHASED EQPT. COST METHOD**	I	II	III	I	II	III
DESIGN						
Diameter, ft	5	5	5	5	5	5
Packed Height, ft	10.5	11.4	11.4	11.8	11.4	11.4
Lm, lb/hrft^2	5,100	7,800	7,800	5,100	7,800	7,800
$(G/L)/(G/L)_{min}$	4.0	5.5	5.5	3.0	5.5	5.5
(G/L)	79	108	108	59	108	108
G, cfm	2,100	2,890	2,890	1,580	2,890	2,890
ΔP_{TOT}, in H_2O	1.9	0.8	0.8	1.2	0.8	0.8
Pump, theo. hp	1.0	1.1	1.1	1.1	1.1	1.1
Blower, theo. hp	0.62	0.4	0.4	0.3	0.4	0.4
ECONOMICS						
Purchased Equipment, $	30,500	30,900	29,050	30,900	30,900	29,050
Total Cap. Investment, $	122,100	123,400	116,200	74,200	74,200	69,700
Annual Capital Cost, $/yr	16,000	16,200	15,200	8,700	8,700	8,160
Pump Operating, $/yr	410	570	570	520	700	700
Blower Operating, $/yr	360	290	290	210	350	350
Total Annual Cost, $/yr	16,800	17,000	16,100	9,500	9,700	9,200
$/10^3 gal	.194	.197	.186	.090	.092	0.88
COST DISTRIBUTION, PERCENT						
Capital	95.4	95.0	94.7	92.2	89.2	88.6
Pump Operating	2.4	3.3	3.5	5.5	7.2	7.5
Blower Operating	2.2	1.7	1.8	2.3	3.6	3.8
		+1.5%	-4.1%		+2.2%	-2.2%

*CC - countercurrent
XF3 - crossflow with baffle spacing correspond to $\alpha = 3$
** see p. 101 for explanation.

TABLE 8. DESIGN AND OPERATING CONDITIONS RESULTING IN MINIMUM COST: 99 PERCENT 1,2-DCE at 1,500 GPM

ECONOMIC BASIS	Case A			Case B		
CONTACTING MODE*	CC	XF3	XF3	CC	XF3	XF3
PURCHASED EQPT. COST METHOD**	I	II	III	I	II	III
DESIGN						
Diameter, ft.	12	10	10	12	10	10
Packed Height, ft	12.3	18.3	18.3	13.7	18.3	18.3
Lm, $lb/hrft^2$	6,600	14,600	14,600	6,600	14,600	14,600
$(G/L)/(G/L)_{min}$	3.1	3.1	3.1	2.5	3.1	3.1
(G/L)	61	61	61	49	61	61
G, cfm	12,200	12,200	12,200	9,800	12,200	12,200
ΔP_{TOT}, in H_2O	2.9	2.4	2.4	2.1	2.4	2.4
Pump, theo. hp	8.4	9.9	9.9	8.9	9.9	9.9
Blower, theo. hp	5.5	4.6	4.6	3.2	4.6	4.6
ECONOMICS						
Purchased Equip. Cost, $	[illegible],400	92,900	84,100	96,700	92,900	84,100
Total Cap. Investment, $	[illegible],700	371,700	336,400	232,000	223,000	197,200
Annual Capital Cost, $/yr	49,500	48,700	44,100	27,100	26,100	23,100
Pump Operating, $/yr	3,300	3,900	3,900	4,300	4,700	4,700
Blower Operating, $/yr	3,300	2,700	2,700	2,300	3,300	3,300
Total Annual, $/yr	56,100	55,300	50,700	33,700	34,100	31,700
$/10^3$ gal	.087	.085	.078	.043	.043	.040
COST DISTRIBUTION, PERCENT						
Capital	88.3	88.0	86.9	80.4	76.4	74.6
Pump Operating	5.9	7.0	7.7	12.7	13.9	15.0
Blower Operating	5.8	4.9	5.4	6.9	9.7	10.5
		-2.3%	-10.3%		0.0%	-7.0%

*CC - countercurrent
XF3 - crossflow with baffle spacing correspond to $\alpha = 3$
** see p. 101 for explanation.

TABLE 9. DESIGN AND OPERATING CONDITIONS RESULTING IN MINIMUM COST: 99 PERCENT MEK at 200 GPM

ECONOMIC BASIS	Case A			Case B		
CONTACTING MODE*	CC	XF3	XF3	CC	XF3	XF3
PURCHASED EQPT. COST METHOD**	I	II	III	I	II	III
DESIGN						
Diameter, ft.	8	6	6	8	6	6
Packed Height, ft	10.9	13.8	15.2	14.4	15.2	15.2
Lm, $lb/hrft^2$	2,000	5,400	5,400	2,000	5,400	5,400
$(G/L)/(G/L)_{min}$	3	3.8	3.1	2	3.1	3.1
(G/L)	246	312	254	165	254	254
G, cfm	6,600	8,400	6,800	4,400	6,800	6,800
ΔP_{TOT}, in H_2O	1.7	2.5	1.8	1.0	1.8	1.8
Pump, theo. hp	1.1	1.2	1.3	1.2	1.3	1.3
Blower, theo. hp	1.8	3.2	1.9	0.7	1.9	1.9
ECONOMICS						
Purchased Equip. Cost, $	47,200	42,000	41,000	49,100	43,800	41,000
Total Cap. Investment, $	188,800	168,100	163,900	117,900	105,100	98,400
Annual Capital Cost, $/yr	24,700	22,000	21,500	13,800	12,300	11,500
Pump Operating, $/yr	410	470	500	590	610	610
Blower Operating, $/yr	1,050	1,910	1,150	490	1,400	1,400
Total Annual Cost, $/yr	26,200	24,400	23,100	14,900	14,300	13,500
$/10^3$ gal	.303	.282	.268	.142	.136	.129
COST DISTRIBUTION, PERCENT						
Capital	94.4	90.2	92.9	92.7	86.0	85.1
Pump Operating	1.6	1.9	2.2	4.0	4.3	4.5
Blower Operating	4.0	7.9	5.0	3.3	9.8	10.3
		-6.9%	-11.5%		-4.2%	-9.2%

*CC - countercurrent
XF3 - crossflow with baffle spacing correspond to $\alpha = 3$
** see p. 101 for explanation.

TABLE 10. DESIGN AND OPERATING CONDITIONS RESULTING IN MINIMUM COST: 99 PERCENT MEK at 1,500 GPM

ECONOMIC BASIS	Case A			Case B		
CONTACTING MODE*	CC	XF3	XF3	CC	XF3	XF3
PURCHASED EQPT. COST METHOD**	I	II	III	I	II	III
DESIGN						
Diameter, ft	14	13	13	16	13	13
Packed Height, ft	21.8	14.6	14.6	20.7	14.6	14.6
Lm, $lb/hrft^2$	4,900	8,700	8,700	3,800	8,700	8,700
$(G/L)/(G/L)_{min}$	1.6	2.0	2.0	1.6	2.0	2.0
(G/L)	131	164	164	131	164	164
G, cfm	26,300	32,900	32,900	26,300	32,900	32,900
ΔP_{TOT}, in H_2O	9.5	2.8	2.8	4.3	2.8	2.8
Pump, theo. hp	12.0	12.4	12.4	11.6	12.4	12.4
Blower, theo. hp	39.4	14.6	14.6	18.1	14.6	14.6
ECONOMICS						
Purchased Equip. Cost, $	203,100	171,500	151,500	234,800	171,500	151,500
Total Cap. Investment, $	812,400	686,000	606,000	563,500	411,600	363,600
Annual Capital Cost, $/yr	106,400	89,900	79,400	65,900	48,200	42,500
Pump Operating, $/yr	4,700	4,900	4,900	5,600	5,900	5,900
Blower Operating, $/yr	23,300	8,600	8,600	13,000	10,500	10,500
Total Annual cost, $/yr	134,400	103,400	92,900	84,500	64,600	59,000
$/10^3$ gal	.207	.160	.143	.107	.082	.075
COST DISTRIBUTION, PERCENT						
Capital	79.2	86.9	85.4	78.0	74.5	72.1
Pump Operating	3.5	4.7	5.3	6.6	9.2	10.0
Blower Operating	17.3	8.4	9.3	15.4	16.3	17.8
		-22.7%	-30.9%		-23.4%	-29.9%

*CC - countercurrent
XF3 - crossflow with baffle spacing correspond to $\alpha = 3$
** see p. 101 for explanation.

The economics of crossflow stripping relative to countercurrent stripping are improved for 1,2-DCA. At a flow rate of 200 gpm, the crossflow stripper is estimated to be slightly more expensive (~2 percent) when Method II is used to estimate purchased equipment cost. However, when the less expensive Method III is used to estimate crossflow purchased equipment costs, crossflow actually results in an estimated cost saving of about 3 percent. At 1500 gpm, the relative economic estimates range from break-even to a 10 percent cost advantage for crossflow.

For extremely low volatility compounds such as MEK, crossflow appears to be economically attractive for all conditions studied. Table 9 shows an estimated cost saving of 4 to 12 percent for crossflow at a flow rate of 200 gpm. At 1500 gpm, Table 10 shows that crossflow stripping of MEK is estimated be 25 percent to 30 percent less costly than countercurrent stripping.

SECTION VI

GENERAL CONCLUSIONS AND RECOMMENDATIONS

An innovative method of gas-liquid contact called cascade crossflow was evaluated for air stripping volatile organic compounds (VOCs) from aqueous solutions. Tests were conducted on a laboratory-scale 6-inch internal diameter, 8-foot tall crossflow column as well as a pilot-scale 12-inch internal diameter, 11-foot tall crossflow column. The compounds investigated were chloroform, methylene chloride, carbon tetrachloride and 1,2-dichloroethane. 5/8-inch polypropylene pall rings were used as packing material. Different combinations of gas and liquid flow rates were tested. From the experiments, we obtained both the stripping efficiencies and overall mass transfer coefficients in crossflow air stripping. We also performed tests on a 6-inch internal diameter, 8-foot tall countercurrent column to compare the performance with the crossflow operation under equivalent conditions. Extensive pressure drop measurements were also made in both modes of operation.

The stripping efficiencies and mass transfer coefficients for liquid phase controlled chemicals in crossflow operation were similar to those in countercurrent operation at equivalent air and water loading rates. However, pressure drops in crossflow operation were as much as an order of magnitude smaller than in countercurrent flow. The permissible ranges of gas and liquid flow rates were also larger in crossflow with several experiments conducted under conditions that would result in flooding in countercurrent columns.

Four different mass transfer correlations were tested to predict the mass transfer coefficients in crossflow air stripping. It was observed that the frequently cited Onda correlation for liquid phase controlled chemicals could be easily modified for crossflow operation and that it predicted experimental values within ±30 percent.

The overall conclusion was that laboratory-scale crossflow cascade systems are efficient mass transfer devices and can be used to strip VOCs from groundwater with efficiencies similar to those of conventional countercurrent flow devices. However the crossflow systems have the added advantages of reduced pressure drop and greater range of stable operation. Mass transfer correlations obtained from conventional countercurrent operation can be modified to predict crossflow mass transfer coefficients as well.

Conceptual design calculations were also performed for both countercurrent and crossflow modes of operation in order to estimate process equipment specifications for 99 percent removal of three contaminants of varying volatility. The contaminants considered were trichlorethylene (TCE) having a relatively high Henry's constant, 1,2-dichlorethane (1,2-DCA) having a moderate Henry's constant, and methyl ethyl ketone (MEK) having a low Henry's constant. Two water flow rates - 200 gpm and 1500 gpm - were considered in order to determine the effect of scale on the comparative economics.

An important factor in the economic comparison turns out to be a balance between reduced blower operating cost due to the lower pressure drop and increased capital costs associated with the more complex internal structure of the crossflow tower. For the highly volatile TCE, in which only moderate air flow rates are required to achieve 99 percent stripping efficiency, blower operating costs are relatively insignificant in both crossflow and countercurrent operation. Hence the higher capital cost for the more complex column internals results in a higher estimated cost for crossflow operation. For example, at a water rate of 200 gpm, crossflow operation is estimated to be from 0 to 7 percent more expensive than traditional countercurrent operation.

However, as the contaminant volatility decreases, greater volumetric flow rates of air are required to achieve 99 percent stripping efficiency, and the blower operating cost savings become significant. For example, for 99 percent removal of MEK from 200 gpm of water, crossflow operation is estimated to be from 4 to 12 percent less expensive than countercurrent operation.

The economic advantages of crossflow operation also improve as the quantity of water to be treated increases. Operating costs are directly proportional to flow rate while capital costs increase less rapidly. The effect of flow rate is also magnified as the Henry's constant of the contaminant decreases. For example, for 99 percent removal of TCE at 1500 gpm, the estimated cost of crossflow stripping ranges from 2 percent less to 6 percent greater than countercurrent (compared to 0 to 7 percent greater at 200 gpm). For 99 percent removal of MEK from 1500 gpm of water, however, crossflow operation is estimated to result in a cost savings of 20 to 30 percent.

REFERENCES

1. Bouwer, E., J. Mercer, M. Kavanaugh and F. Digiano, "Coping with Ground Contamination," J. Water Poll. Cont. Fed., 60, 1415 (1988).

2. Clark, R.M., C.A. Frank and B.W. Lykins, "Removing Organics from Groundwater," Environ. Sci. Technol., 22, 1126 (1988).

3. Billelo, L.J., and J.E. Singley, "Removing Trihalomethanes by Packed Column and Diffused Aeration," J. Amer. Wat. Wks. Assoc., 78, 62 (1986).

4. Baker, D.R., and H.A. Shryock, "Heat Transfer in Cross-flow Cooling Towers," J. Heat Transfer (AIME), 339 (1961).

5. Thibodeaux, L.J., "Continuous Crosscurrent Mass Transfer in Towers," Chem. Eng., 76, 165 (1969).

6. Roseler, J.F., R. Smith and R.G. Eilers, "Mathematical Simulation of Ammonia Stripping Towers for Wastewater Treatment," U.S. Dept. of Interior, FWPCA, Cinncinnati, OH (1970).

7. Althoff, W.F., R.W. Cleary and P.H. Roux, "Aquifer Decontamination of Volatile Organics - A Case History," Groundwater, 19, 495 (1981).

8. McCarty, P.L., "Removal of Organic Substances from Water by Air Stripping," in Control of Organic Substances in Water and Waste Water, B.B. Berger (ed.), EPA 600/8-83-001, April (1983).

9. Pittaway, K.R., and L.J. Thibodeaux, "Measurement of Oxygen Desorption Rate in a Single Stage Crossflow Packed Tower," Ind. Eng. Chem. Proc. Des. Dev., 19, 40 (1980).

10. Hayashi, Y., and E. Hirai, "Calculation Method of Overall Volumetric Mass Transfer Coefficients in Crossflow Gas Absorption Columns," Kagaku Kogaku, 35, 214 (1971).

11. Hayashi, Y., and E. Hirai, "Wetted Area in Crossflow Type Gas-Liquid Contacting Apparatus - Eliminator Type Packings," Kagaku Kogaku, 36, 1249 (1972).

12. Thibodeaux, L.J., D.R. Daner, A. Kimura, J.D. Millican and R.J. Parikh, "Mass Transfer Units in Single and Multiple Stage Packed Beds, Crossflow Devices," Ind. Eng. Chem. Proc. Des. Dev., 16, 325 (1977).

13. Thibodeaux, L.J., "Fluid Dynamic Observations on a Packed, Crossflow Cascade at High Loadings," Ind. Eng. Chem. Proc. Des. Dev., 19, 33 (1980).

14. Thibodeaux, L.J., and D.M. Moncada, "Performance Comparison of a Crossflow Cascade and a Conventional Countercurrent Operation in Packed Towers," Paper presented at the Symposium on Recent Advances in Separation Technology, AIChE National Meeting, Chicago, IL (1980).

15. Hayashi, S., E. Hirai and M. Okubo, "Volumetric Film Coefficients in Crossflow Cooling Towers," Kagaku Kogaku, 36, 204 (1972).

16. Velaga, A., L.J. Thibodeaux, K.T. Valsaraj, J.S. Cho, R.B. Eldridge and D.M. Moncada, "Packed Crisscross Flow Cascade Tower Efficiencies for Methanol-Water Separations - Experimental versus Calculated Values Based on Countercurrent Flow Correlations," Ind. Eng. Chem. Res., 27, 1481 (1988).

17. Bayan, T., "Mass Transfer in a Multiple Stage Crosscurrent Packed Column," Ph.D. Dissertation, Oregon State University, Corvallis, OR (1981).

18. Buchelli, A., "The Design, Set up and Operation of a Countercurrent Gas Crossflow Cascade Packed Distillation Tower," M.S. Thesis, University of Arkansas, Fayetteville, AR (1980).

19. Eldridge, R.B., "Distillation in a Packed Crossflow Column," M.S. Thesis, University of Arkansas, Fayetteville, AR (1981).

20. Velaga, A., "Estimation of Interfacial Area in a Packed Crossflow Cascade with Distillation of Ethanol-Water, Methanol-Water and Hexane-Heptane," Ph.D. Dissertation, University of Arkansas, Fayetteville, AR (1985).

21. Gossett, J.M., C.E. Cameron, B.P. Eckstrom, G. Goodman and A.H. Lincoff, "Mass Transfer Coefficients and Henry's Law Constants for Packed-Tower Air Stripping of Volatile Organics: Measurements and Correlation," U.S. Air Force Office of Scientific Research, Report No. ESL-TR-85-18, 278 pages, June (1985).

22. Munz, C., "Air-Water Phase Equilibrium and Mass Transfer of Volatile Organic Solutes," Ph.D. Dissertation, Dept. of Civil Engineering, Stanford University, Stanford, CA (1985).

23. Welty, J.R., C.E. Wicks and R.F. Wilson, Fundamentals of Momentum, Heat and Mass Transfer, Second Edition, John Wiley and Sons, Inc., New York, NY (1984).

24. Sherwood, T., and F.A. Holloway, "Performance of Packed Towers - Liquid Film Data for Several Packings," Trans. Am. Inst. Chem. Engr., 36, 39 (1940).

25. Bolles, W.L., and J.R. Fair, "Improved Mass Transfer Model Enhances Packed-Column Design," Chem. Eng., 89, 109 (1982).

26. Bolles, W.L., and J.R. Fair, "Mass Transfer Models for Packed Columns," Inst. Chem. Eng. Symp. Ser., 56, 3/35 (1979).

27. Shulman, H.L., C.F. Ullrich and N. Wells, "Performance of Packed Columns I. Total, Static and Operating Holdups," AIChE J., 1, 247 (1955).

28. Shulman, H.L., C.F. Ullrich, A.Z. Proulx and J.O. Zimmerman, "Performance of Packed Columns II. Wetted and Effective Interfacial Areas, Gas and Liquid Phase Mass Transfer Rates," AIChE J., 1, 253 (1955).

29. Bravo, J.L., and J.R. Fair, "Generalized Correlation for Mass Transfer in Packed Distillation Columns," Ind. Eng. Chem. Proc. Des. Dev., 21, 162 (1982).

30. Onda, K., H. Tadeuchi and Y. Okumoto, "Mass Transfer Coefficients Between Gas and Liquid Phases in Packed Columns," J. Chem. Eng. Japan, 1, 56 (1968).

31. Zuiderweg, F.J., and A. Harmens, "The Influence of Surface Phenomena on the Performance of Distillation Columns," Chem. Eng. Sci., 9, 89 (1958).

32. Velaga, A., K.T. Valsaraj and L.J. Thibodeaux, "Interfacial Areas in Packed Cascade Crossflow Distillation Columns," Paper No. 29b, presented at the 1989 Spring National AIChE Meeting in Houston, Texas, April 2-6 (1989).

33. Riojas, A., G. Hopkins, C. Munz and P.V. Roberts, "A Two-Resistance Model for Trace Organic Contaminant Stripping in a Packed Column," Proc. AWWA Ann. Conf., 407 (1983).

34. Ludwig, E., Applied Process Design for Chemical and Petrochemical Plants, Gulf Publishing Co., Vol. 2, Houston, Texas, pages 167-168 (1979).

35. Munz, C., and R.V. Roberts, "Effects of Solute Concentration and Co-Solvents on the Aqueous Activity Coefficient of Halogenated Hydrocarbons," Environ. Sci. Technol., 20, 830 (1986).

36. Ashworth, R.A., G.B. Howe, M.E. Mullins, and T.N. Rogers, "Air-Water Partitioning Coefficients of Organics in Dilute Aqueous Solutions," Jour. Haz. Matls., 18, 25 (1988).

37. Mackay, D., and W.Y. Shiu, "A Critical Review of Henry's Law Constants for Chemicals of Environmental Interest," J. Phys. Chem. Ref. Data, 10, 1175 (1981).

38. Perry, R.H., D.W. Green and J.O. Malone, Perry's Chemical Engineer's Handbook, McGraw Hill Book Company, Sixth Edition, 1984, Section 18, page 33.

39. Leva, M., "Flow Through Irrigated Dumped Packings. Pressure Drop, Loading, Flooding," Chem. Engr. Progs. Symp. Ser., 50, 51 (1954).

40. Ulrich, G.D., A Guide to Chemical Engineering Process Design and Economics, John Wiley and Sons, New York, 1984.

41. Peters, M.S., and K.D. Timmerhaus, Plant Design and Economics for Chemical Engineers, 3rd Edition, McGraw-Hill, New York, 1980.

42. Segesta, R., Standard Operating Procedures for the Analytical Support Laboratory and Associated Project Laboratories of the Hazardous Waste Research Center, LSU-EPA Hazardous Waste Research Center, Louisiana State University, Baton Rouge, Louisiana, February 1985.

43. Supelco GC Bulletin Number 816, Supelco Inc., Bellefonte, Pennsylvania, 1984.

44. Grob, R.L. (editor), Modern Practice of Gas Chromatography, John Wiley & Sons, New York, 1985, pages 412-421.

A P P E N D I X: CHROMATOGRAPH CALIBRATION CURVES

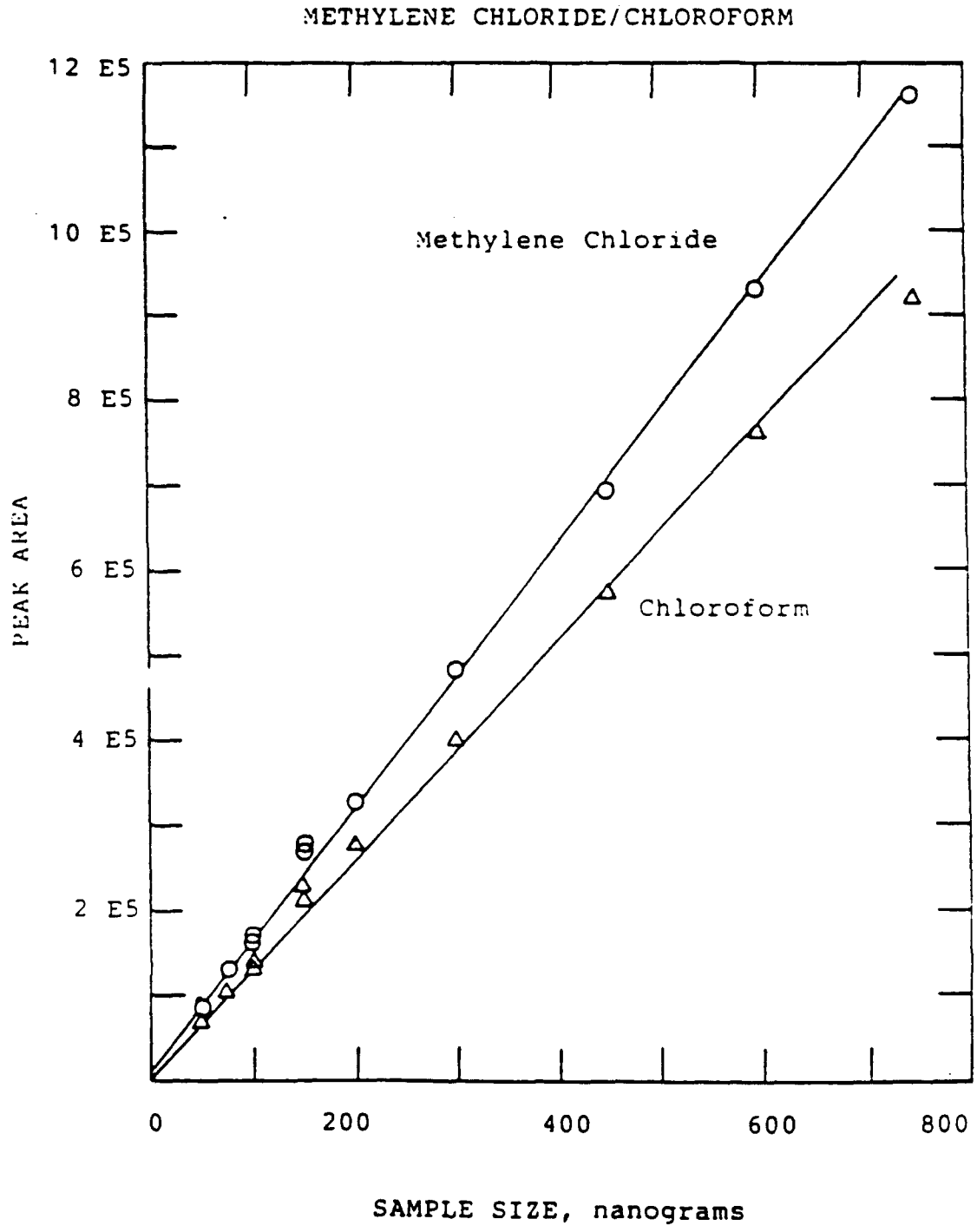

Figure A-1. GC Calibration Curves for Methylene Chloride and Chloroform

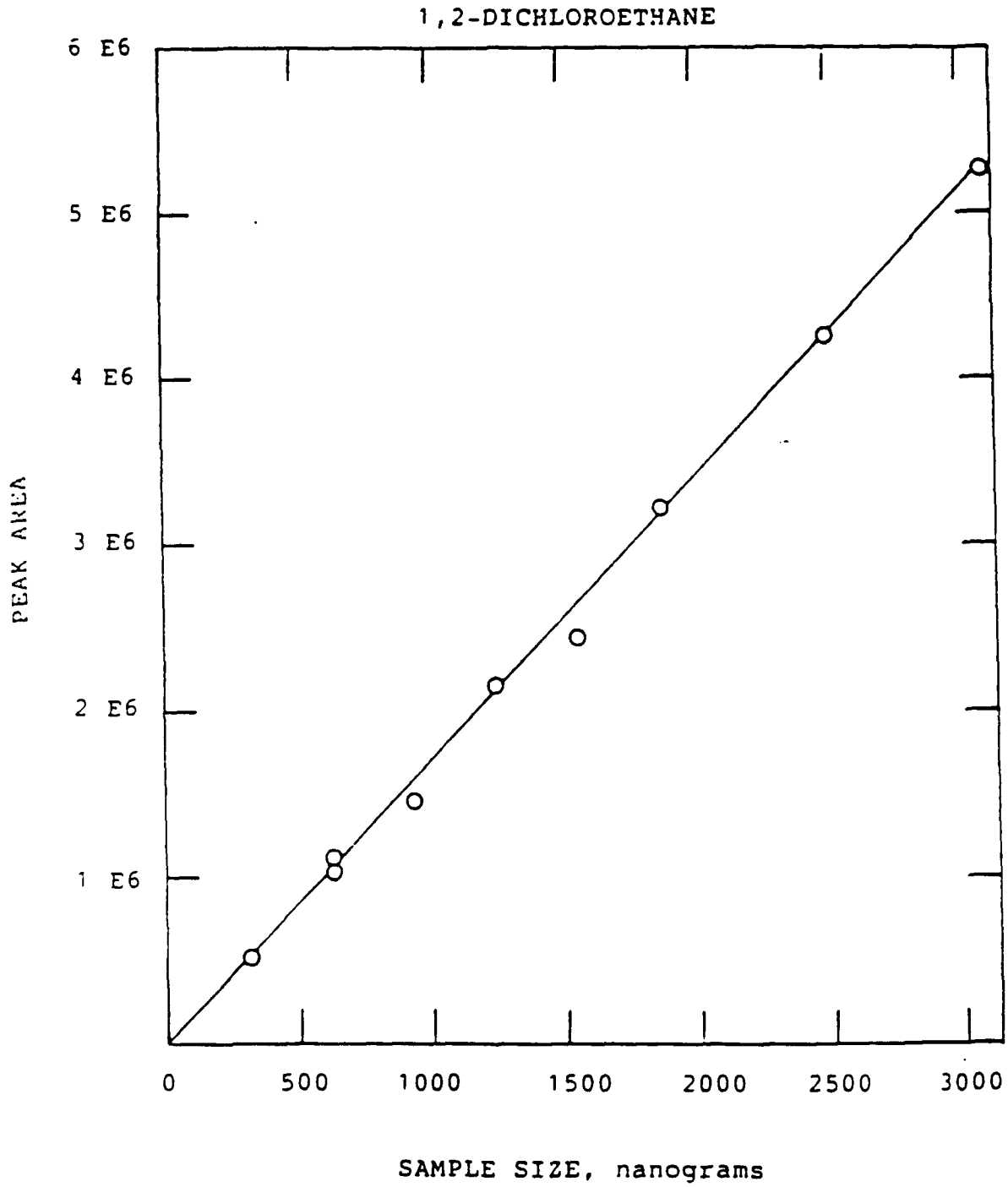

Figure A-2. GC Calibration Curve for 1,2-Dichloroethane

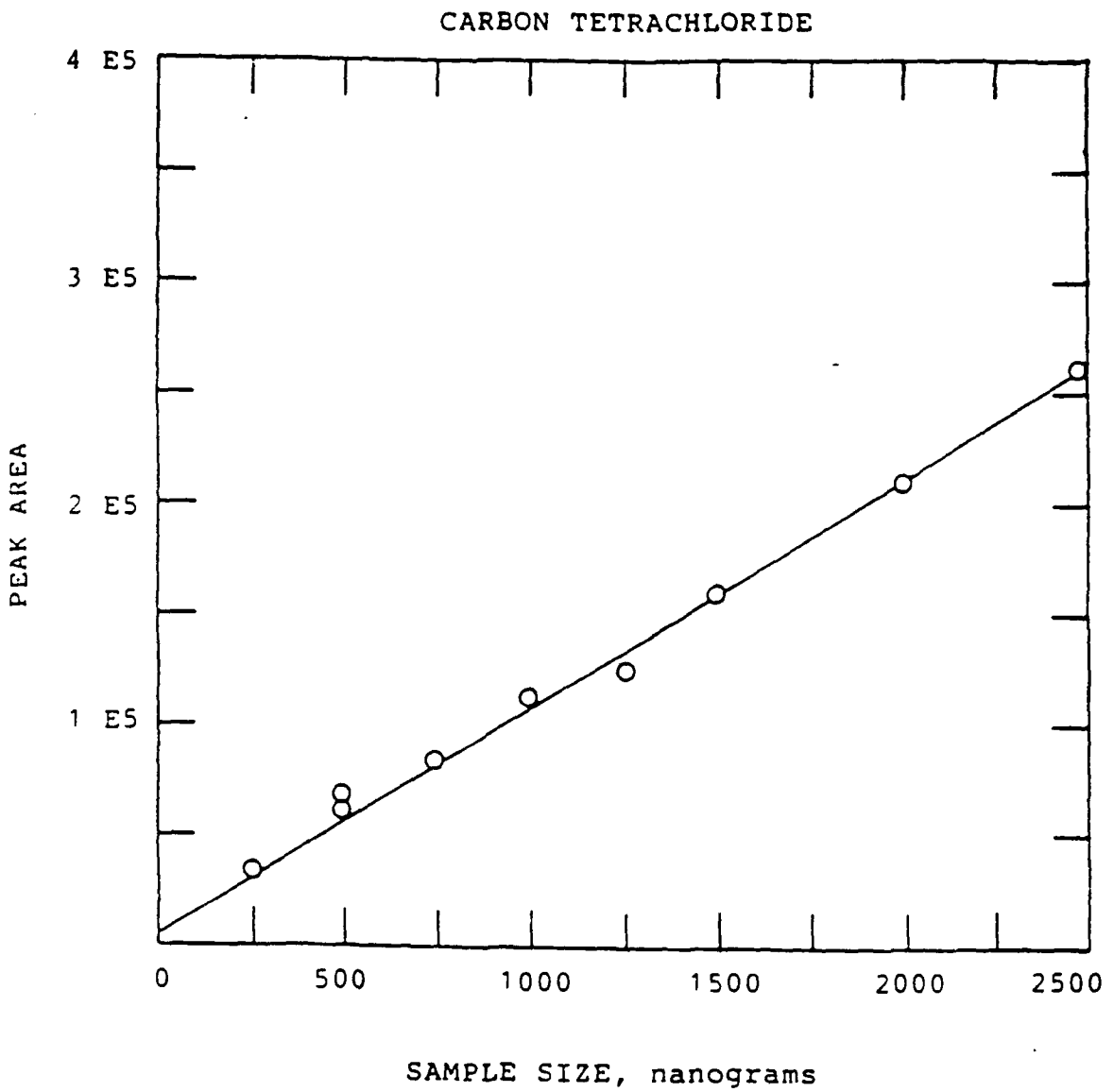

Figure A-3. GC Calibration Curve for Carbon Tetrachloride